5. Adaptation of the Statistical Filter for Statistical Process Control

This section will introduce the adaptation made to the statistical filter to meet Process Control requirements from a theoretical point of view; the practical implementation of the whole theory developed will be described in sections 7 and 8.

5.1 Laboratory analysis of on-line data

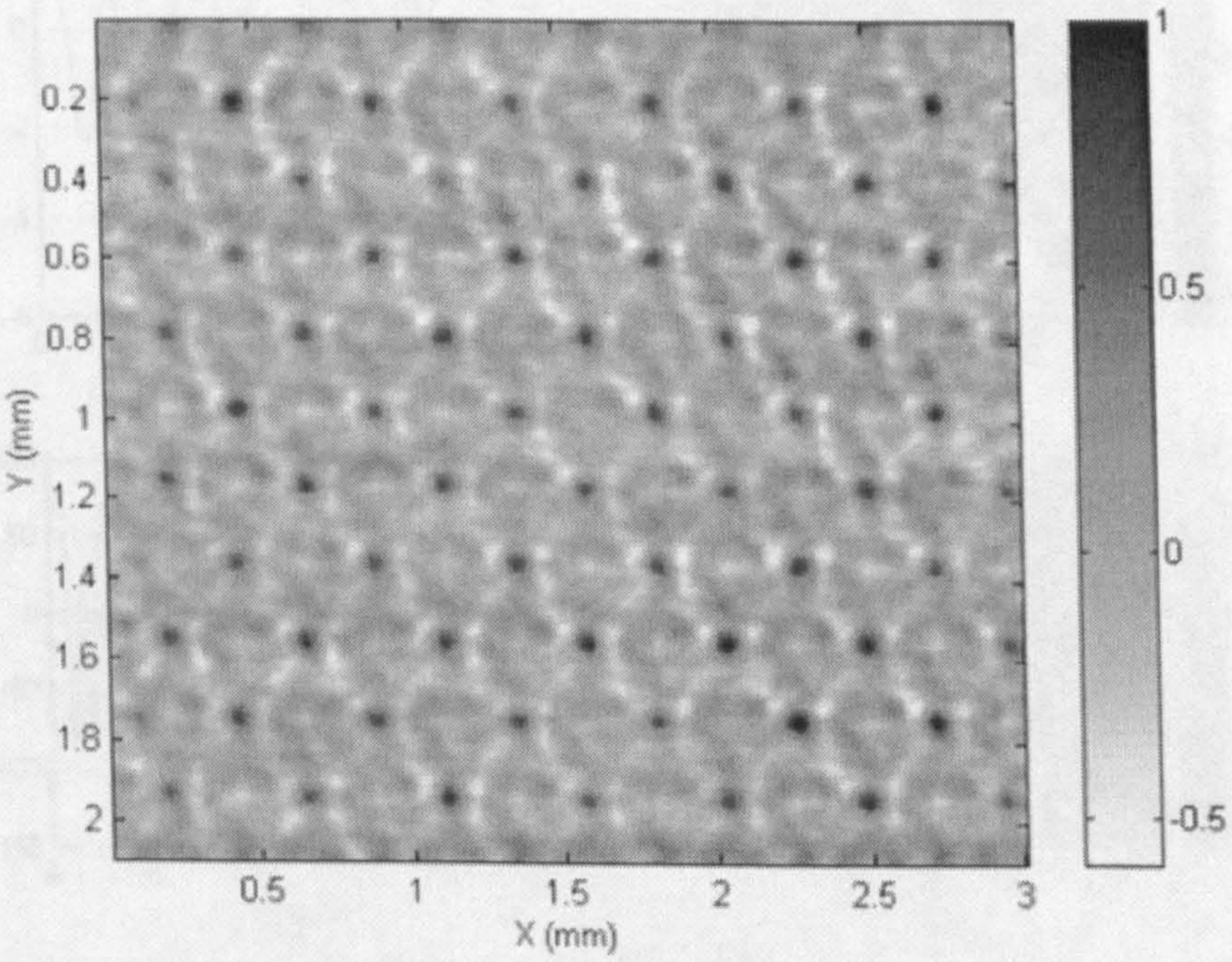

Figure 5-1 – Cross correlation between measurement and greyscale picture

The Cross-correlation function can be applied to greyscale pictures to find where they match laboratory measurements.

It is not necessary to correlate the pictures with a measurement of the same steel sheet they have been taken from. It is sufficient to correlate them with a laboratory sample presenting the same pattern (as for example in Figure 2-25).

The result of such operation for one of the pictures is depicted in Figure 5-1, where a very clear pattern of peaks indicates precise matching.

Figure 5-2 shows a possible application of the cross correlation: an area of the sample measurement corresponding to the greyscale picture can be isolated and compared with it. The red lines on the left hand-side figures indicates the position where the profiles have been extracted.

It is possible to appreciate the precision of the technique in indicating the exact point where the pattern is repeated.

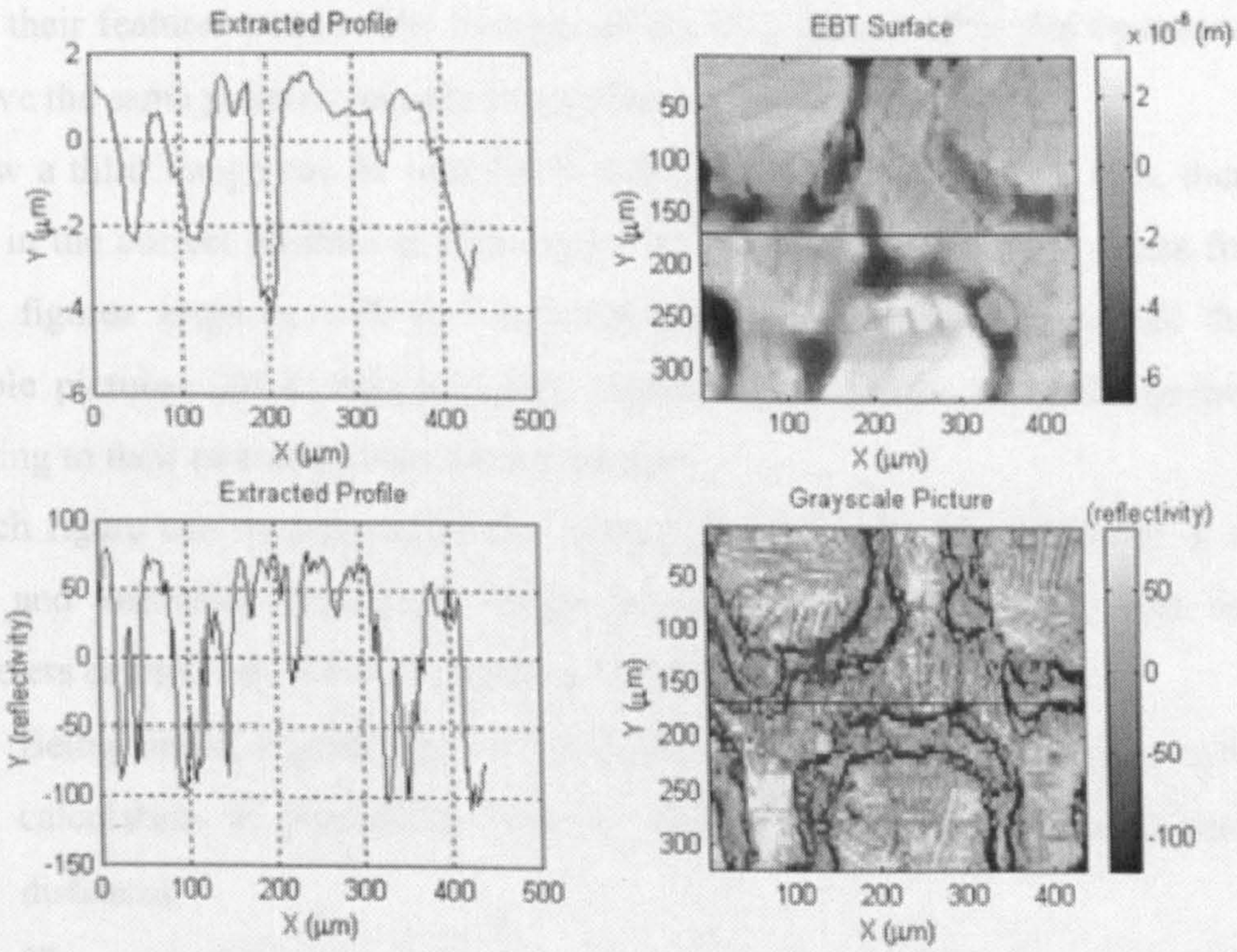

Figure 5-2 – Comparison between highly correlated areas of picture and measurement

Slope values and height values can be associated, even if they do not come from the same sample, to deduce the real shape of the surface depicted in the greyscale image.

The height values of the laboratory sample can be used as "probable values" for the greyscale. The slopes deduced from the greyscale will correct the errors given by the local differences between the two sheets.

5.1.1 Merging

If the cross correlation is applied to two pictures, instead of a picture and a set of height measurements, this will give us indications of the relative position of the two images in the pattern.

The two images can be placed in the correct position suggested by the XCF, so that their features match. The average of the two figures after this operation will have the same pattern characteristics of the previous two.

Now a third image can be correlated with the average of the first two, then placed in the correct position and averaged with them. Iterating this process for all the figures acquired will give a result like in Figure 5-3, where all the available pictures (20 in this particular example) have been merged together according to their position in the general pattern.

Such figure can be considered as a summary of the greyscale pictures; it is larger and smoother than each single image, providing a useful tool for parameters calculation, for the following reasons:

- Being larger, a greater part of the pattern is represented, allowing easier calculation of parameters such as radii of rings and centre-to-centre distances.
- The smoothness of the image is due to the partial elimination of background noise, obtained through averaging.

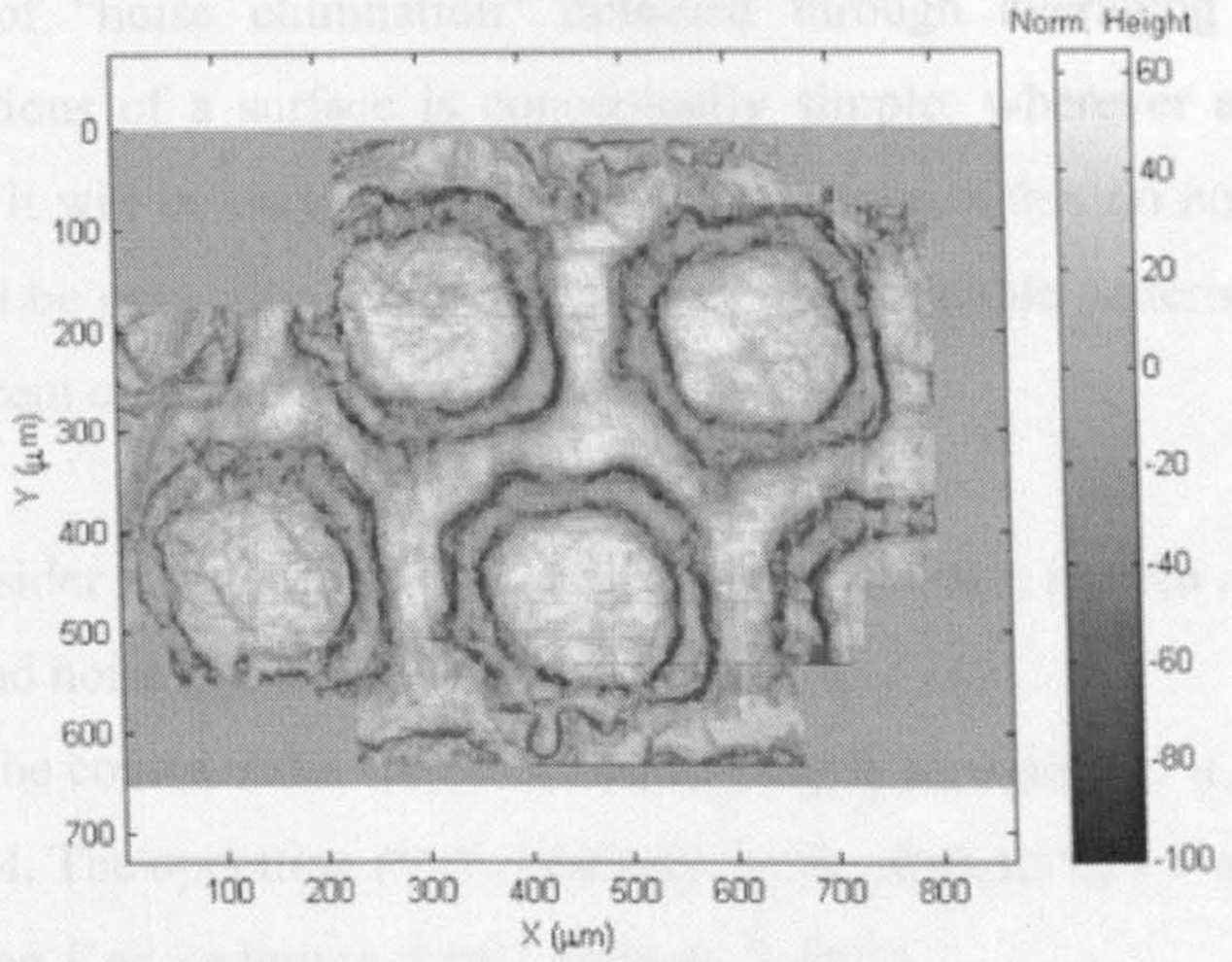

Figure 5-3 – Single patterned pictures merged

In order to visualise how the figures have been merged, Figure 5-4 shows the number of figures that have been averaged for each point. It results clear now why the central part of the image is the clearer and smoother: it is the place where the most pictures are averaged, while towards the borders their number decreases.

The idea of "noise elimination" obtained through averaging of highly correlated portions of a surface is conceptually simple: wherever a feature is often repeated it will be emphasized, vice-versa variations that do not belong to the pattern will be gradually eliminated. In the case of double patterned surfaces the above concept creates complications and differences.

Let us consider a surface X as the sum of three surfaces: pattern A, pattern B and background noise N.

1) B will be considered as noise when filtering X according to A, giving as a result A. The operation $P=X-A$ defines the residual surface P as $B+N$.
2) Filtering P according to B will separate B and N.

Although empirical experimentation seems to confirm the above concepts, there is a logical link that needs further analysis in order to respect a rigorous scientific method.

Point 1) states that B will be considered as noise when filtering X according to A; this is true only if the average of B according to pattern A is null, therefore only if the periodicities of the two patterns are mutually irrational.

In practice this does not represent an impediment, given that the surfaces under analysis are not large enough to experience enough repetitions of the same configuration of features to affect the average.

On the other hand, this represents a conceptual barrier to one of the goals of statistical manipulation: finding the minimum portion of the surface representative of the whole surface (called *base element*). If the two patterns are not correlated, they will never repeat the same relative position of the rings.

In other words, acquiring a portion of surface from a double patterned sample, there will not be another portion where both patterns match: it will only be possible to match either one pattern or the other.

The techniques and methods previously described for correlation with laboratory measurements and merging are thus unsuitable for double patterned surfaces the way they are for single patterns. This is exemplified in Figure 5-5, where a set of double patterned pictures have been merged using the same

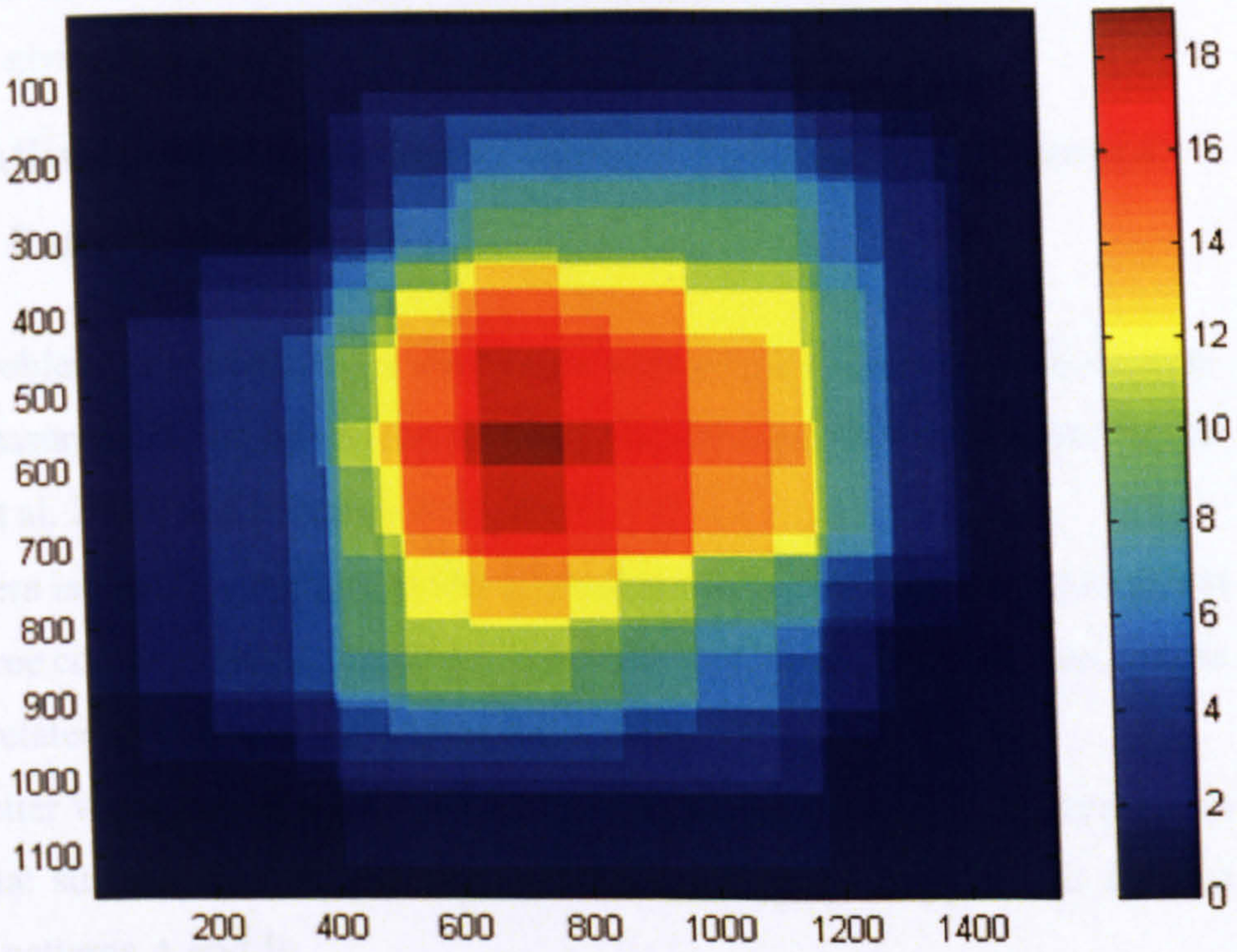

Figure 5-4 - Density of Pictures after Merging

5.1.2 Limitations of Pattern Recognition in Double Pattern Surfaces

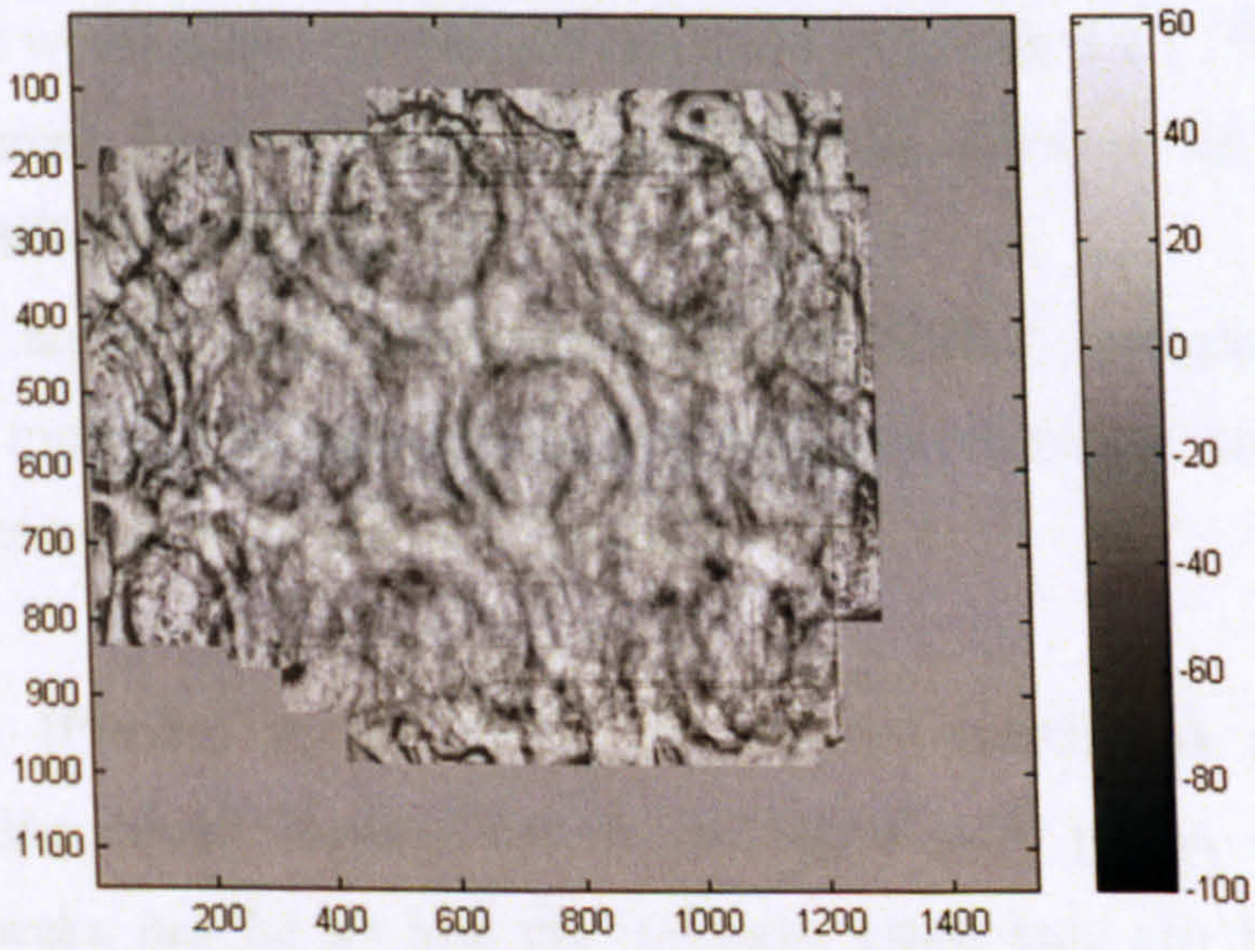

Figure 5-5 – double patterned pictures merged

technique used to obtain Figure 5-3. It is clear that some of the pictures have been placed correctly according to the main pattern, but most of them are misplaced, giving as a result a blurred and indistinct picture.

5.2 Statistical Manipulation of surface features for enhanced Pattern Recognition

The problem of correlating a double-pattern greyscale image with double-pattern measurement can be overcome using the filtering technique described in [Porrino at al. 2000] and [Porrino at al. 2003].

If pattern isolation is applied to the original surfaces, this can be broken down into its three components (*A*, *B* and *N*). Now the on-line acquired pictures can be cross-correlated with one of the patterns at a time.

For better visualisation of the patterns, consider the example of Figure 4-1 as the original surface, and the patterns of Figure 4-3 and Figure 4-8 as the two extracted patterns A and B.

A picture taken from the above mentioned sheet will contain a small portion of both patterns; correlating the picture with pattern A, the features of pattern B present in the picture will be considered as noise and will not find any match. The opposite will happen when correlating the picture with pattern B.

This procedure would allow merging as described in section 5.1.1. The result will be two different figures obtained by merging the same set of pictures according to two different patterns.

If the pictures are in a large enough number, the iterative averaging that is involved in the merging procedure will progressively eliminate noise, and therefore the undesired pattern from each picture.

As stated in [Porrino et al., 2003] one of the patterns is generally predominant having deeper features that create higher ACF peaks, while the other pattern's peaks can be so low that in some cases they can be hardly differentiable from background noise.

The problem becomes even more evident when trying to correlate greyscale camera pictures according to their weaker pattern, due to the very small portion of the surface represented by each one of them.

The following practical example will clarify this concept.

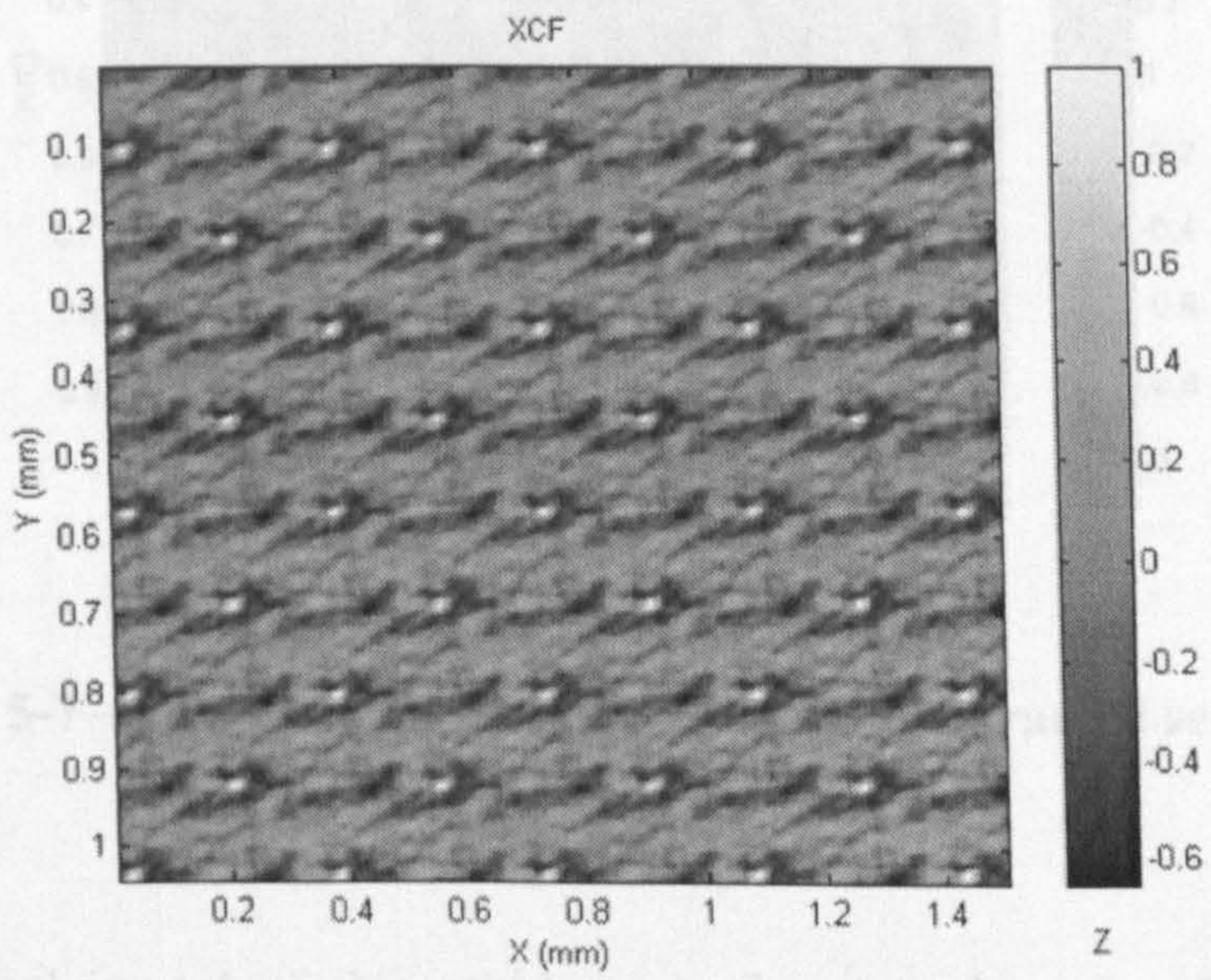

Figure 5-6 – Cross correlation of picture with extracted main pattern

The greyscale pictures of Figure 5-5 can be correlated with their stronger pattern (called *pattern A*), previously obtained from a proper set of height measurements, and give a clear XCF like in Figure 5-6, where only the central portion of the XCF has been considered in order to avoid border effect errors.

The same pictures correlated with their weaker pattern (*pattern B*) are strongly affected by the presence of the deep features of *pattern A* and give a very disturbed XCF like in Figure 5-7, in which isolating the correct positions for peaks becomes impossible.

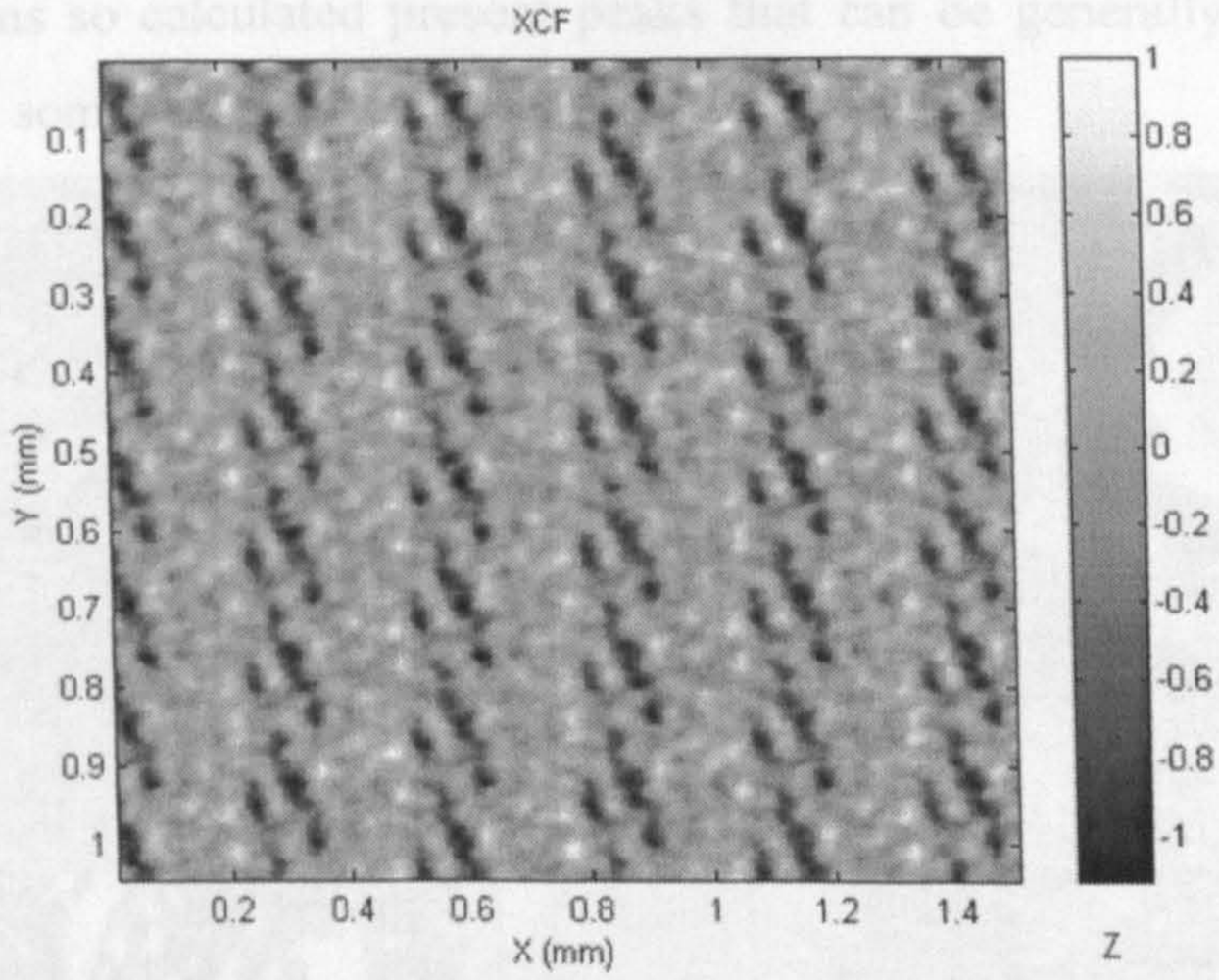

Figure 5-7 – Cross correlation of picture with extracted secondary pattern

The practical impact of this problem can be strongly reduced using once again pattern isolation:

1. The greyscale pictures will be correlated with *pattern A* and merged.
2. The figure obtained through merging can now be filtered using normal GS procedure to reduce noise to the minimum.
3. Now the filtered surfaces can be subtracted from each one of the pictures, removing thus the deterministic part of *pattern A* from them. This is possible because the exact position of each picture with respect to *pattern A* has been established by the XCF for merging.
4. Finally the pictures, "cleaned" from pattern A, can be correlated with pattern B, giving a much clearer ACF that allows the second filtering.

5.3 Greyscale simulation

It has been mentioned in this section that greyscale pictures can be correlated with measurements in order to assign them a specific position in the pattern. It is possible to correlate directly the image and the height measurements, even if this is not conceptually correct because one represents heights, the other slopes. The

cross correlations so calculated present peaks that can be generally identified, sometimes with some difficulty.

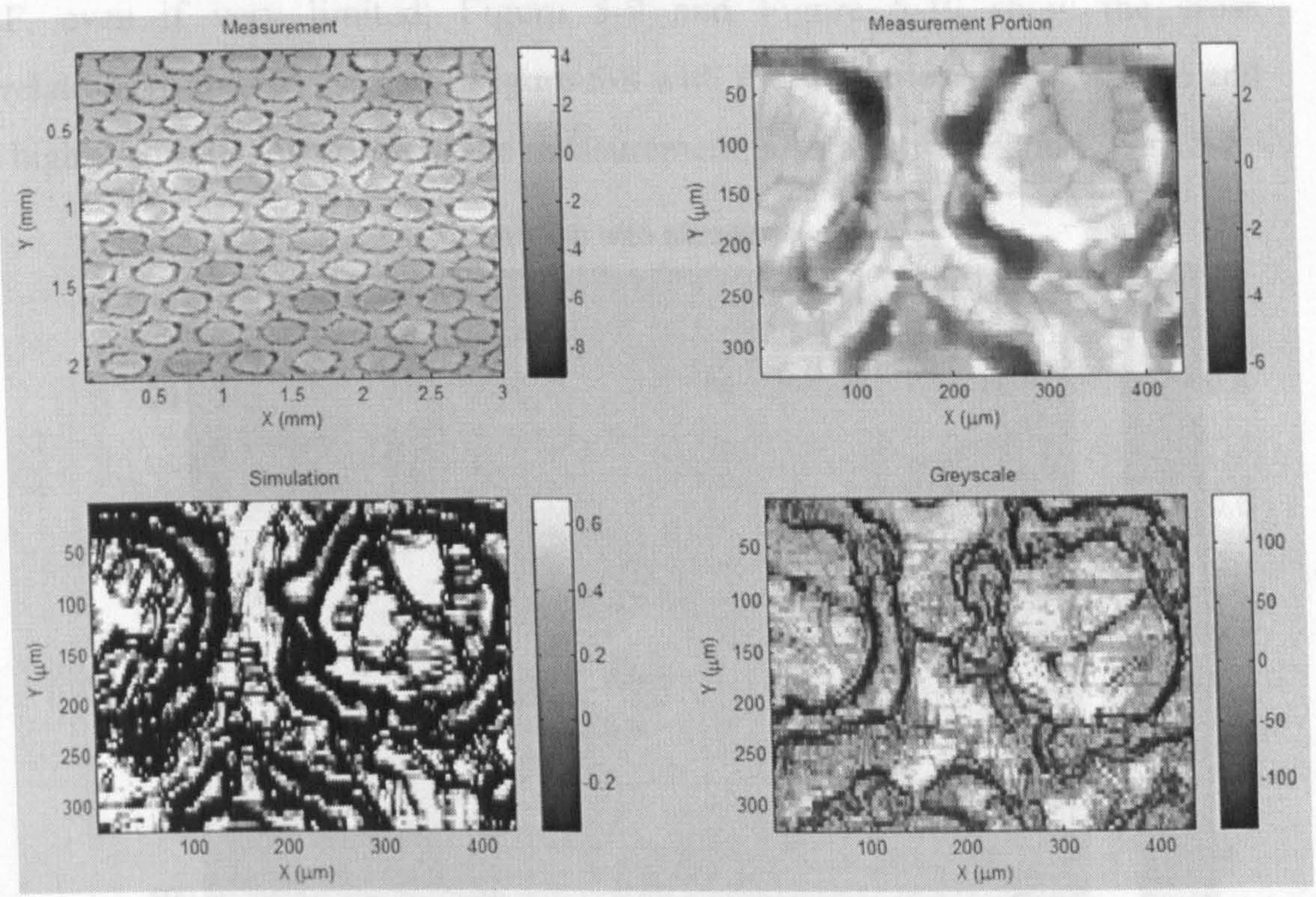

Figure 5-8 - Simulated greyscale

A more conceptually correct way to proceed is to calculate the slope associated to each point of the measurement, creating a simulated greyscale of the measurement. The slope is simply calculated as the gradient of the figure in each point. This has not the pretence to represent a proper simulation of the picturing process, but simply a way to give more physical significance to the operation of cross-correlation, and possibly improve its accuracy.

Figure 5-8 shows an example of greyscale picture (bottom-right) and the measurement it has been correlated with (top-left), which represent the same texture but it is not taken from the same sample.

The most highly correlated portion is extracted and represented on the top-right of the figure, while the remaining figure shows the slopes associated to the portion of measurement. It is possible to notice how the values inside the rings are dark (which means deep) in the measurement, while they are light (which means flat) in both the greyscale and the simulation.

Experiments have shown that there is an improvement in the quality of the XCF, even if very limited; Figure 5-9 and Figure 5-10 show the cross correlations of the Greyscale of Figure 5-8 with the simulated slopes surface and the highly-correlated portion of the measurement, also represented in Figure 5-8.

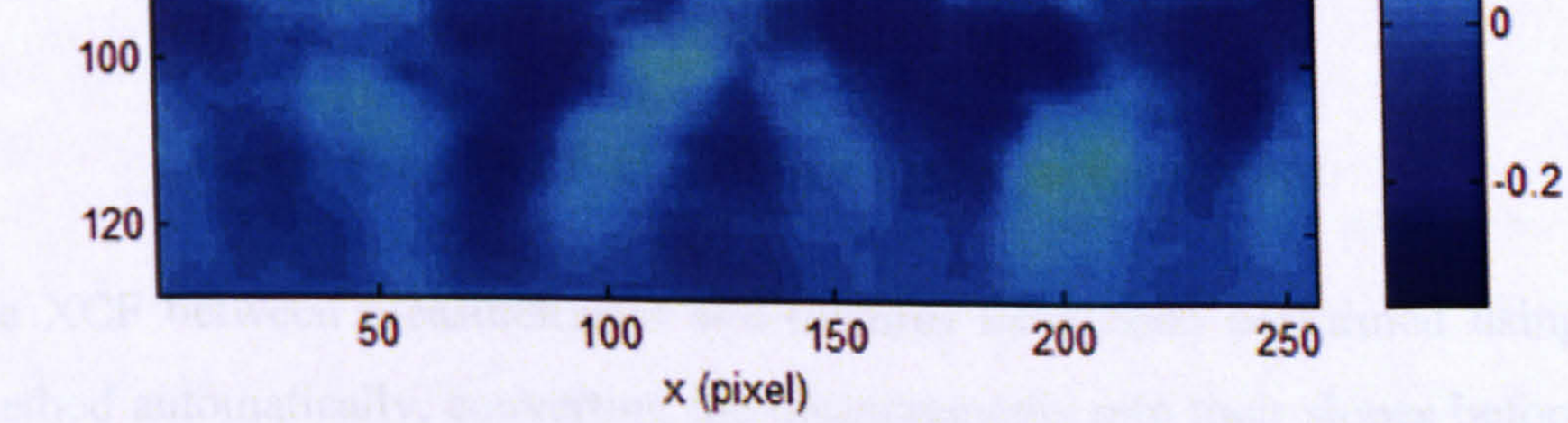

Figure 5-9 - XCF of Greyscale with simulated slopes

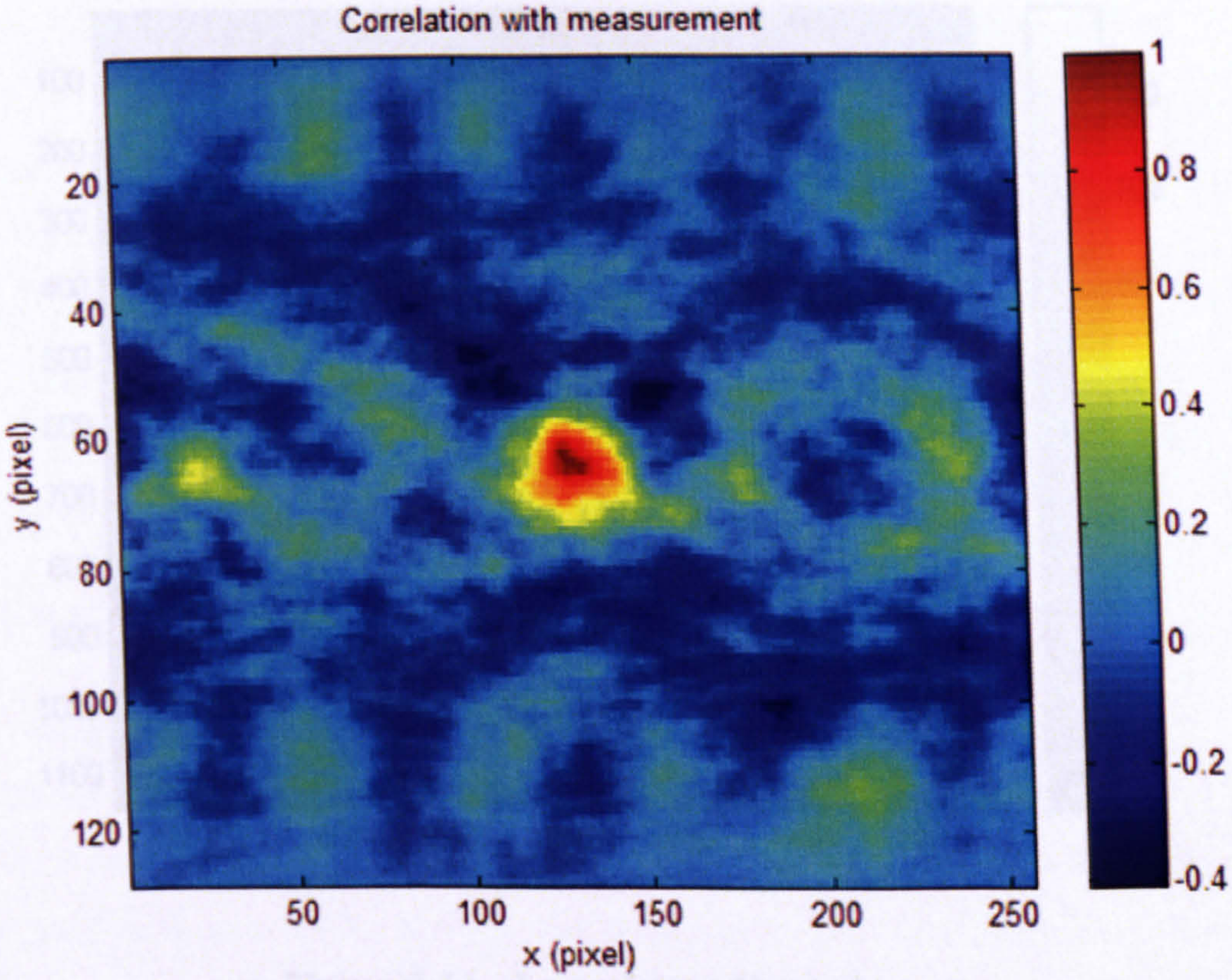

Figure 5-10 - XCF of Greyscale with measurement

The XCF between measurements and pictures have been performed using this method automatically, converting the measurements into their slopes before cross-correlating, in a way completely transparent to the user. For better results the simulation needs to be equalised as well, using gamma correction to try to match the intensity distributions of the two images. This operation also has been made automatic, and uses the histogram equalisation available in the Image Processing Toolbox of Matlab.

5.4 Laser line application

A laser line as described in section 3.2 has been associated with each one of the greyscale pictures; the concept is to use the pictures as a way to identify the relative position of the line with respect to the pattern: if the lines are in a large enough number, and randomly distributed, they should give a measure of the effective heights of the base element of the pattern.

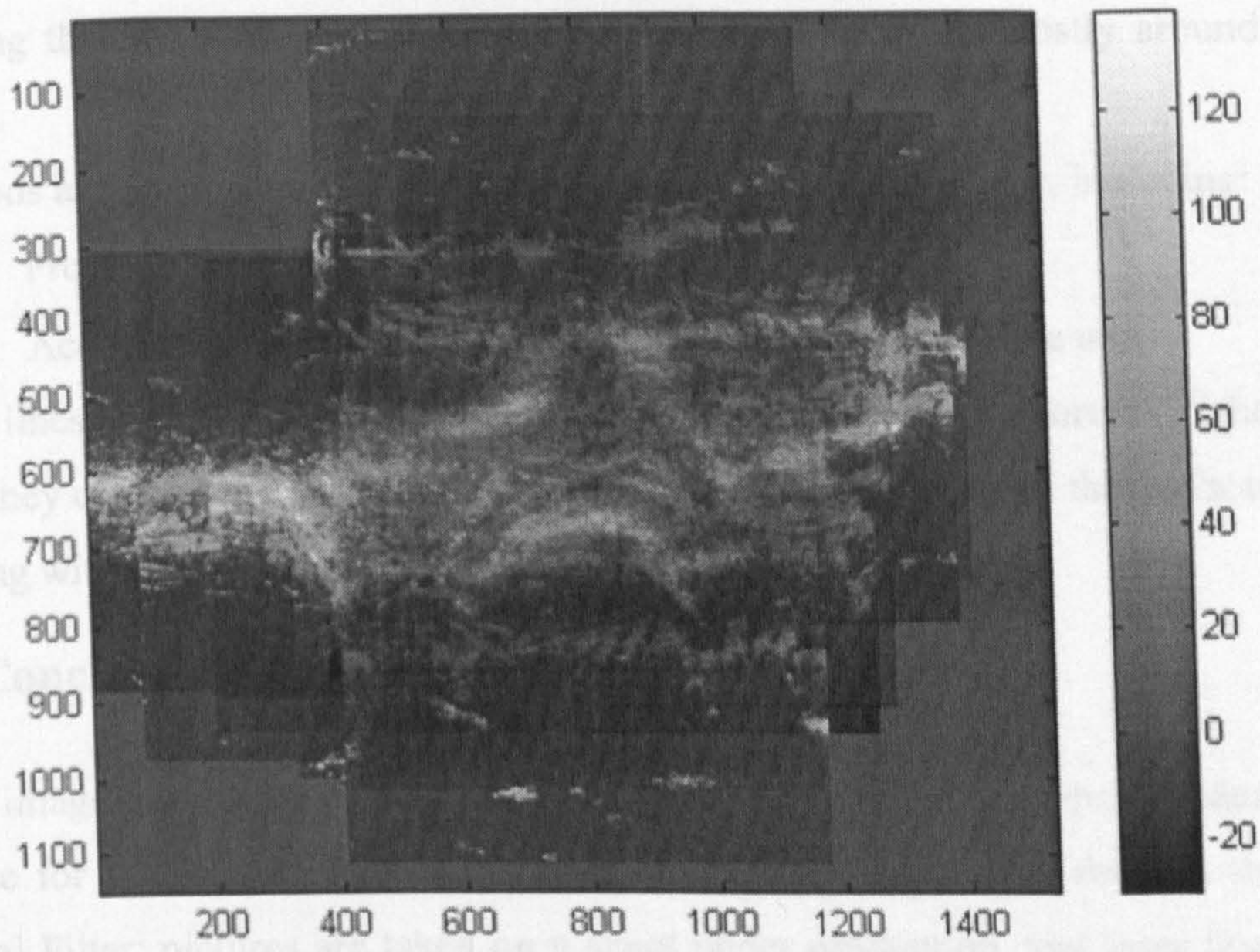

Figure 5-11 - Laser Lines Merged

Figure 5-11 shows the results of the operation of merging on the laser line pictures of Figure 3-4. The figures have been placed in the same relative position of the greyscales merged in Figure 5-3. This figure has the only purpose of showing the differences of intensity around the ring edges, indicative of the correct placement of the images.

This method allows the association of profiles (one per each picture, calculated from the laser lines) to the texture.

The pictures available were in number only twenty per each sample, so that only twenty profiles could be associated to the pictures. The knowledge of such a limited proportion of the surface cannot give valuable information about the amplitude parameters with reasonable accuracy. The scale in Figure 5-11 was left in pixels in order to illustrate this concept: the lateral dimensions of the figure are circa 1100x1400 points, for a total of 1.5 million points; each line is as long as a row in the greyscale picture, circa 800 points, for a total of 16000 points over the surface. The ratio between the size of the surface and the points

whose height is known from the laser lines is too high (~100), particularly considering that the points are distributed non-homogeneously, mostly around the centre.

Methods are under study to increase the number of lines available, including:

- Projecting more than one laser line per each picture.
- Acquiring the highest possible number of pictures per time unit.

If the lines are in a high enough number, covering a reasonable portion of the surface, they can be interpolated in order to deduce the real aspect of the surface, integrating with the information on the slopes given by the greyscale.

5.5 Conclusions

The images produced on-line by the CRM optical system are an ideal candidate for the implementation of an on-line measuring system through the Statistical Filter: pictures are taken on a sheet under production, and laser lines are projected on them in order to allow the estimation of the central profile. The pictures are used to know the relative positions of the profiles with respect to the pattern.

- The operation of merging of the surfaces has been described and inspected, and it has given positive results on single patterned surfaces, while some further considerations are required in order to be adapted to multiple patterns.
- The combined use of the Statistical Filter on measurements and greyscale/laserline pictures provides the tool for pattern separation and features analysis on on-line acquired data.
- The size of the figures available so far is too small compared to the size and the distance between the rings to allow clear separation of patterns; the analysis suggests that images should be taken on a larger area at least for double patterned surfaces, despite the loss of accuracy that would occur.

6. Parameters extraction and validation

The initial use of the Statistical Filter was purely the separation of deterministic patterns from surfaces, seen as a way to estimate stochastic noise and access the average shape of the features. At present the filter is being tested for a variety of other uses, but nevertheless its initial function remains the most important. This section will describe the methods used for the extraction of parameters through the Statistical Filter, as well as their statistical validation.

EBT textured surfaces present a periodic pattern of repeated features, therefore their two main components, apart from noise, are a pattern and a feature. In particular the pattern consists in series of equally spaced points that lay on parallel lines, shifted by a certain constant factor, whilst the feature is the deformation caused on a sheet by the impression of a crater left by a laser beam on a 'Roll'. The analysis of these two components via Statistical Filtering is described in the two following sections.

6.1 Pattern analysis

This section describes the methods used to describe the pattern of surfaces, first considering the geometrical parameters that define it, then studying the general statistics of the surface through the various stages of Statistical Filtering.

6.1.1 Geometrical parameters

The first parameters that can be extracted are relative to the periodicity of the surface, and are calculated directly from the ACF or XCF functions. Considering the filtering process as described in the previous sections, the first steps consist in calculating the correlation function and isolating its peaks. Such operation returns the so called 'Peaks Map' that is a map of the occurrences of the deterministic features; if the function is an auto-correlation, then the distances between the peaks will all be relative to the centre point, whilst the cross-correlation gives the absolute position in the figure where the feature is repeated.

A detailed description of the algorithms and methods for Peaks Map extraction is given in section 8, while here the focus is on the calculation of useful geometrical parameters from the correlation functions.

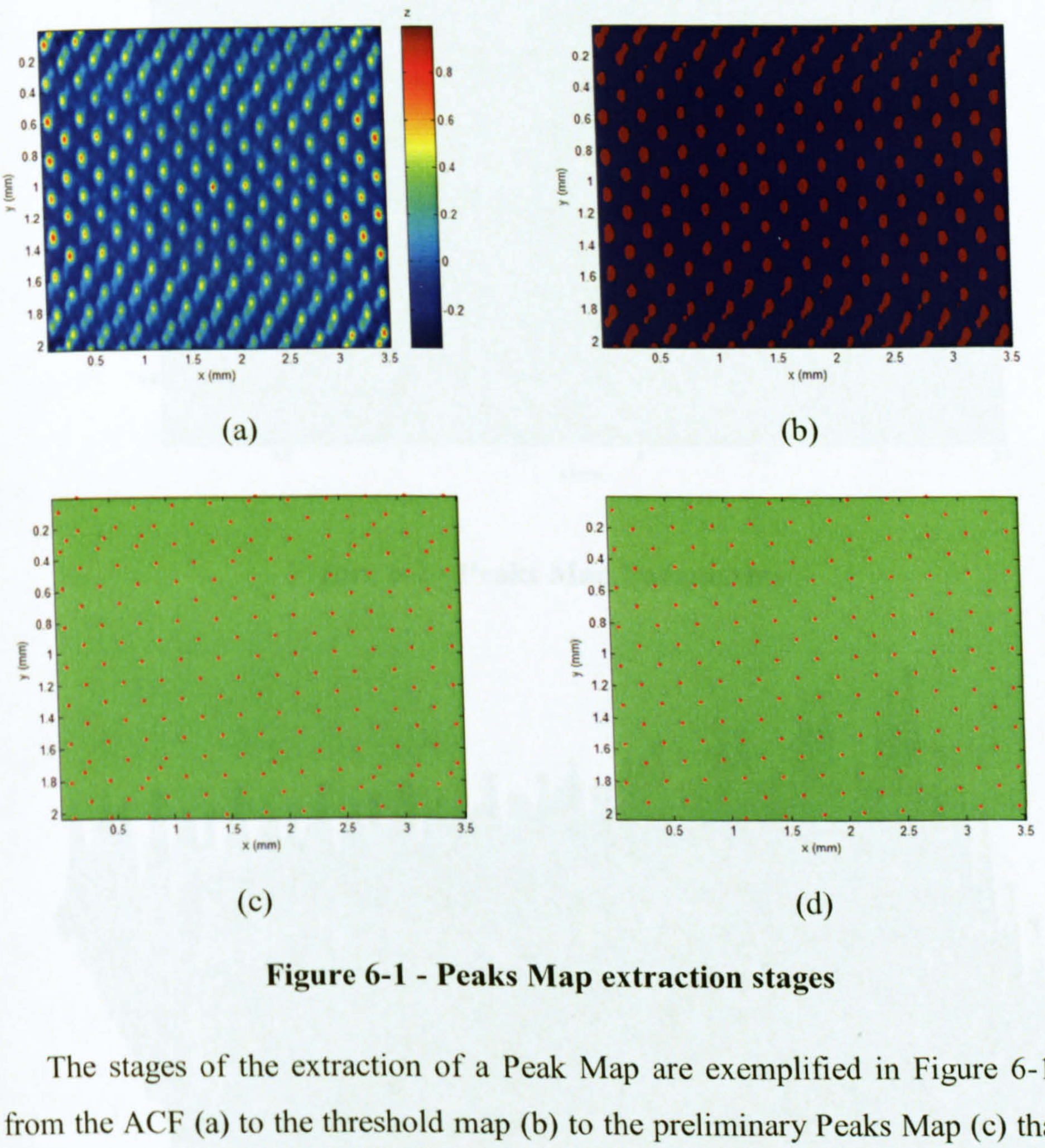

Figure 6-1 - Peaks Map extraction stages

The stages of the extraction of a Peak Map are exemplified in Figure 6-1: from the ACF (a) to the threshold map (b) to the preliminary Peaks Map (c) that is then cleaned from irregularities (d); all these operations are described in detail in sections 7 and 8.

The final Peak Map is reported in a larger scale in Figure 6-2, where are also visualised the basic parameters to identify a pattern: the horizontal and vertical distances between peaks and the rotation angle. The peaks can be also viewed in three-dimensions, as in Figure 6-3 where the peaks, represented by red dots, imposed on the ACF for visual verification of their accuracy.

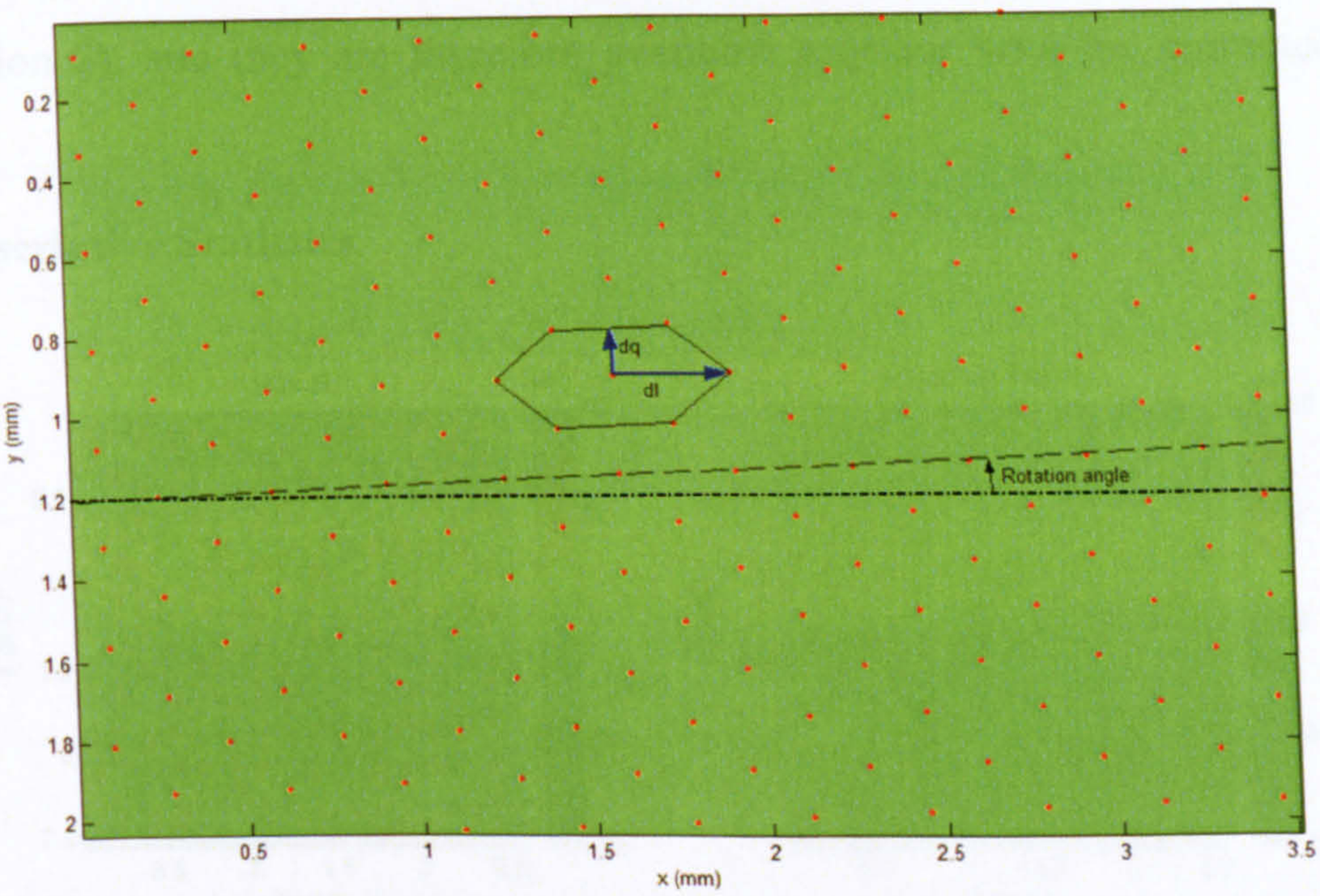

Figure 6-2 - Peaks Map Parameters

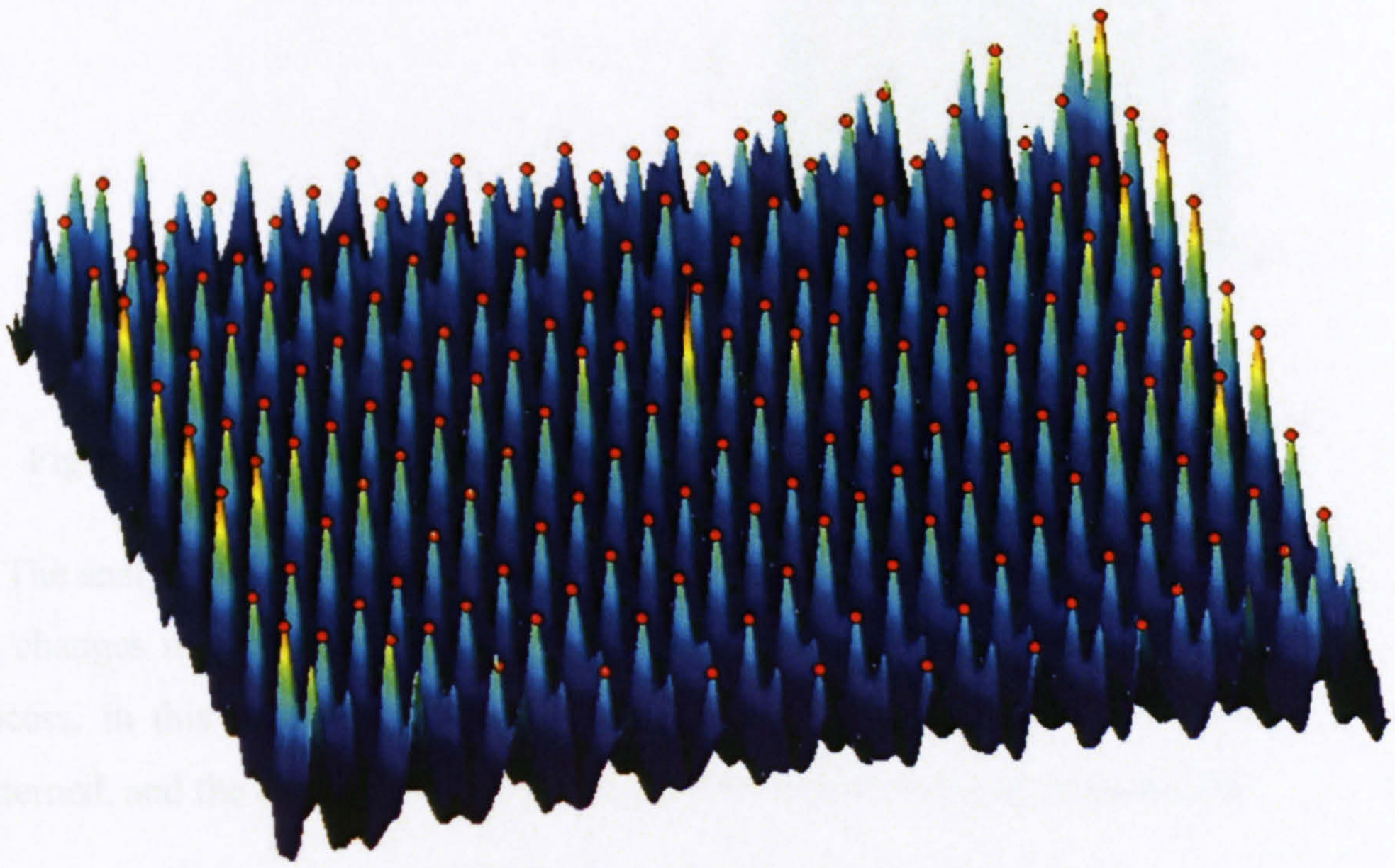

Figure 6-3 - 3D Peaks map

The geometrical parameters shown in Figure 6-2 are easily evaluated from the Peaks Map, but this operation is generally not necessary because the same

parameters are calculated as part of the algorithm for the correction of the Map itself (section 8), and they are therefore available together with the corrected map.

6.1.2 Descriptive Statistics

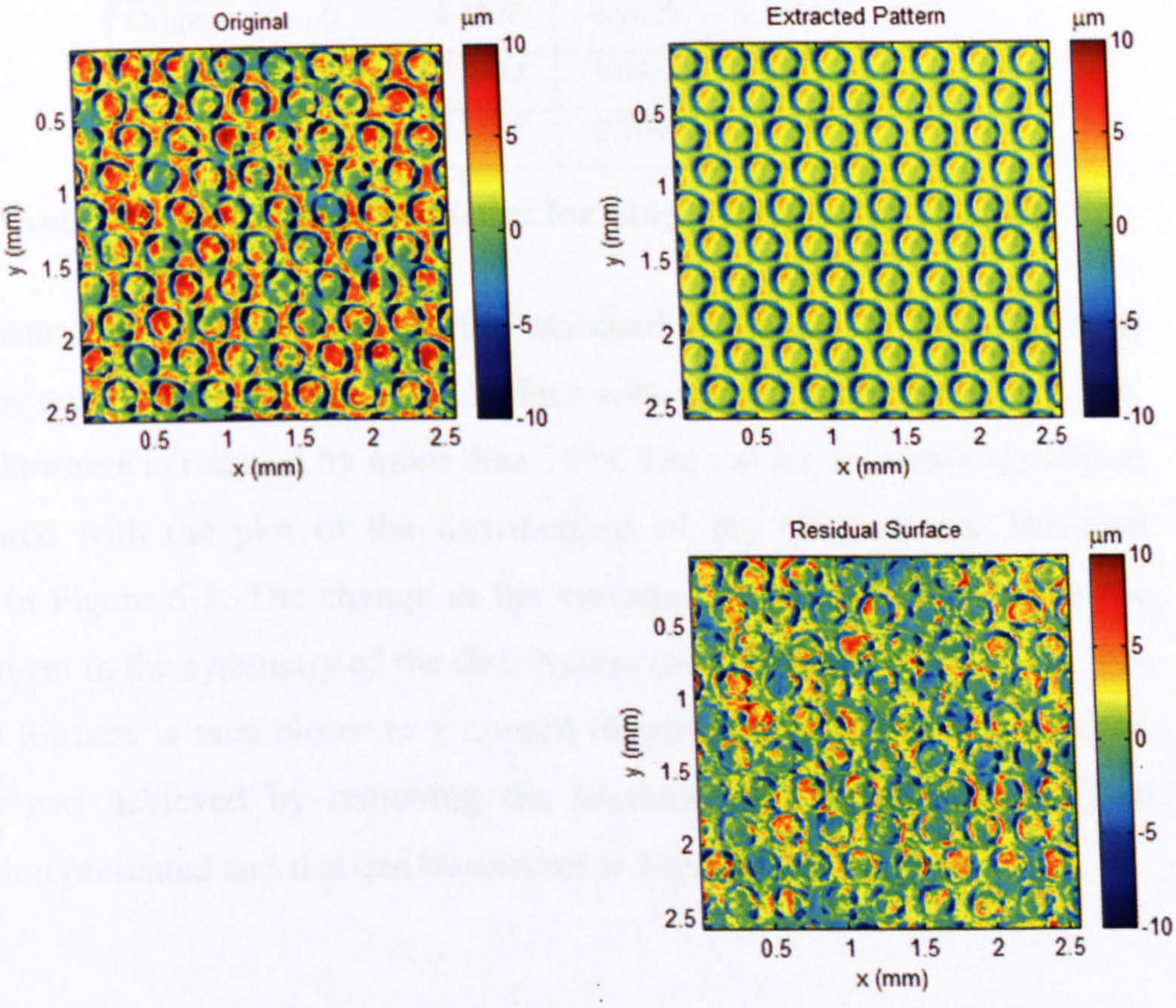

Figure 6-4 - Stages of Statistical Filtering for Single Patterned Surface

The analysis of the distributions of the height values is the best way to follow the changes introduced on a surface by the filter at the different stages of its process. In this section two surfaces are filtered, one Single and one Double Patterned, and the changes of the surface parameters are recorded and studied.

The first surface, Single Patterned, is illustrated in Figure 6-4 in the top left corner; the pattern extracted is depicted on the right, while the residual surface (difference of the two) appears in the bottom. The sample is a 256x256 points matrix that represent a 2.56x2.56mm^2 sheet portion with a spacing of 10µm.

The Original surface has zero mean (first order polynomial form removal is applied to every surface considered in the project) and a standard deviation of the heights ~ 4.5μm. The amplitude parameters Sq Ssk and Sku, and the mean value for the three surfaces (Original, Filtered and Residual) are reported in Table 6-1.

	Mean	Sq	Ssk	Sku
Original	0	4.4938	-0.9029	3.1095
Filtered	-0.0198	2.8858	-1.0958	3.2083
Residual	-0.0198	2.7665	-0.2602	3.4791

Table 6-1 - Descriptive Statistics for Single Patterned Filtering

Parameter Sq, which represents the standard deviation of the points, is reduced by nearly 40% in the residual surface with respect to the Original value, and the skewness is reduced by more than 70%. The values are better visualised if compared with the plot of the distributions of the Original and Residual surfaces in Figure 6-5. The change in the variance results is evident, as is the improvement in the symmetry of the distribution (of which Ssk is an index). The Residual Surface is then closer to a normal distribution than the Original was, and this was achieved by removing the asymmetrical tail that the original distribution presented and that can be noticed in Figure 6-5.

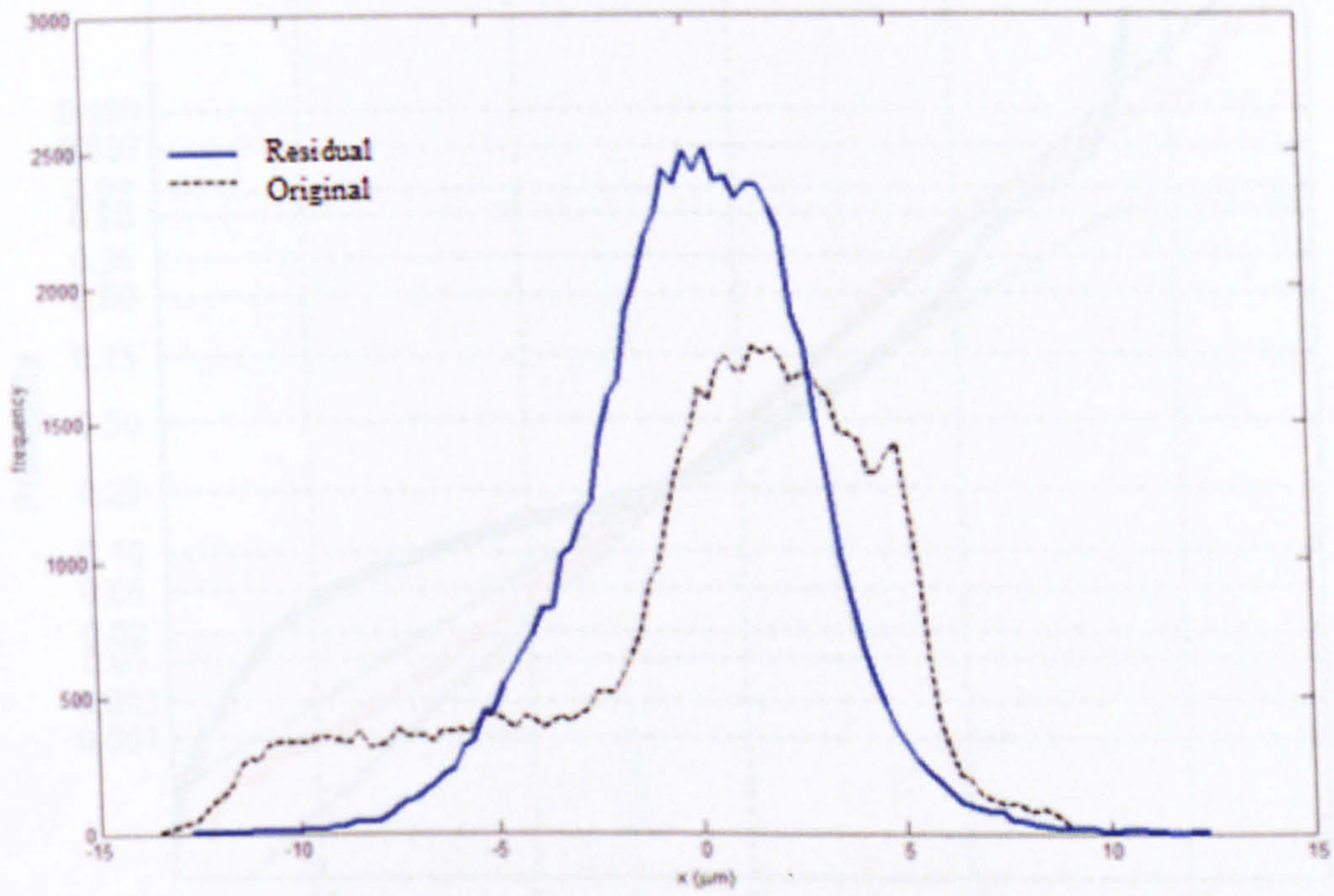

Figure 6-5 - Height Distribution of Statistically Filtered Surface

Another way to verify the validity of the filter in removing the deterministic part of a measurement is to observe the normal probability plots: in Figure 6-6 these plot have been traced for the Original (in blue) and the Residual (in red). It is possible to notice how more linear the latter is with respect to the first, as an index of improved normality of the data.

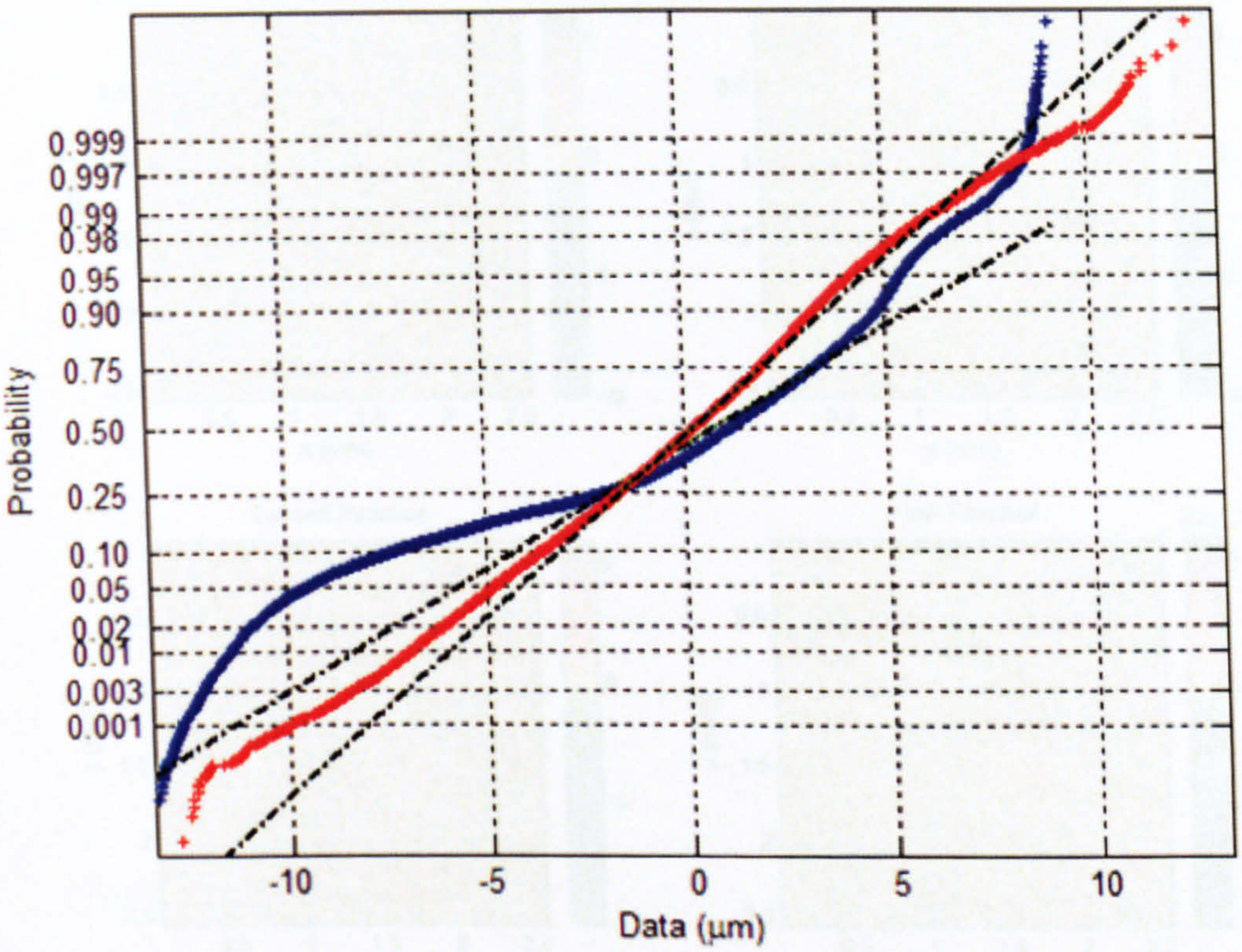

Figure 6-6- Normal Probability Plot for Single Pattern Filtering

Similar considerations can be done on double patterned surfaces, where the filter is applied twice, generating three residual surfaces, according to this scheme: let O indicate the Original, P1 and P2 the Extracted Patterns, R1, R2 and RF the Residual Surfaces (First, Second and Final). Then

O=P1+P2+RF : The Original surface is the sum of the patterns plus noise.

R1=O-P1=P2+RF : The first Residual is the Original minus the first pattern

R2=O-P2=P1+RF : The second Residual is the Original minus the second pattern

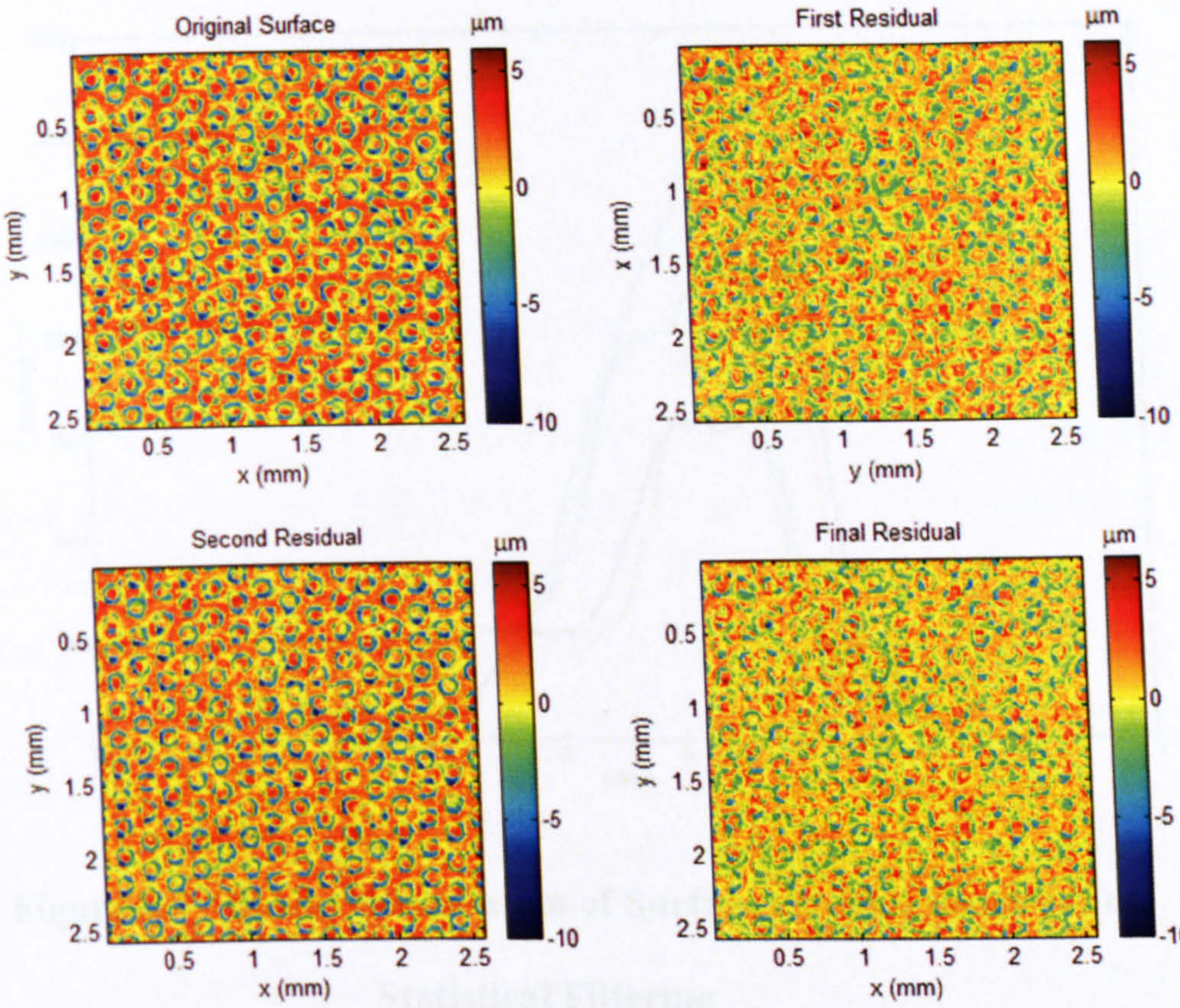

Figure 6-7 – Double Patterned Surface at various stages of Statistical Filtering

Figure 6-7 shows the residual surfaces of a double patterned surface filtered with GS Filter, while Figure 6-8 shows their distributions. Using the colourbars on the side of the figures it is possible to identify the features and the effect they have on the distribution. On the original surface it is possible to consider the following:

- The main plane is orange, therefore just above zero microns height.
- The deeper pattern (smaller rings) is blue, so around -5µm and below
- The shallower pattern (larger rings, hardly visible) is yellow, so around zero microns.

These visual considerations, purely indicative, can find a confirmation on the distribution of the original surface (in black in Figure 6-8), where the main plane and the two patterns can be identified in the positions hypothesised.

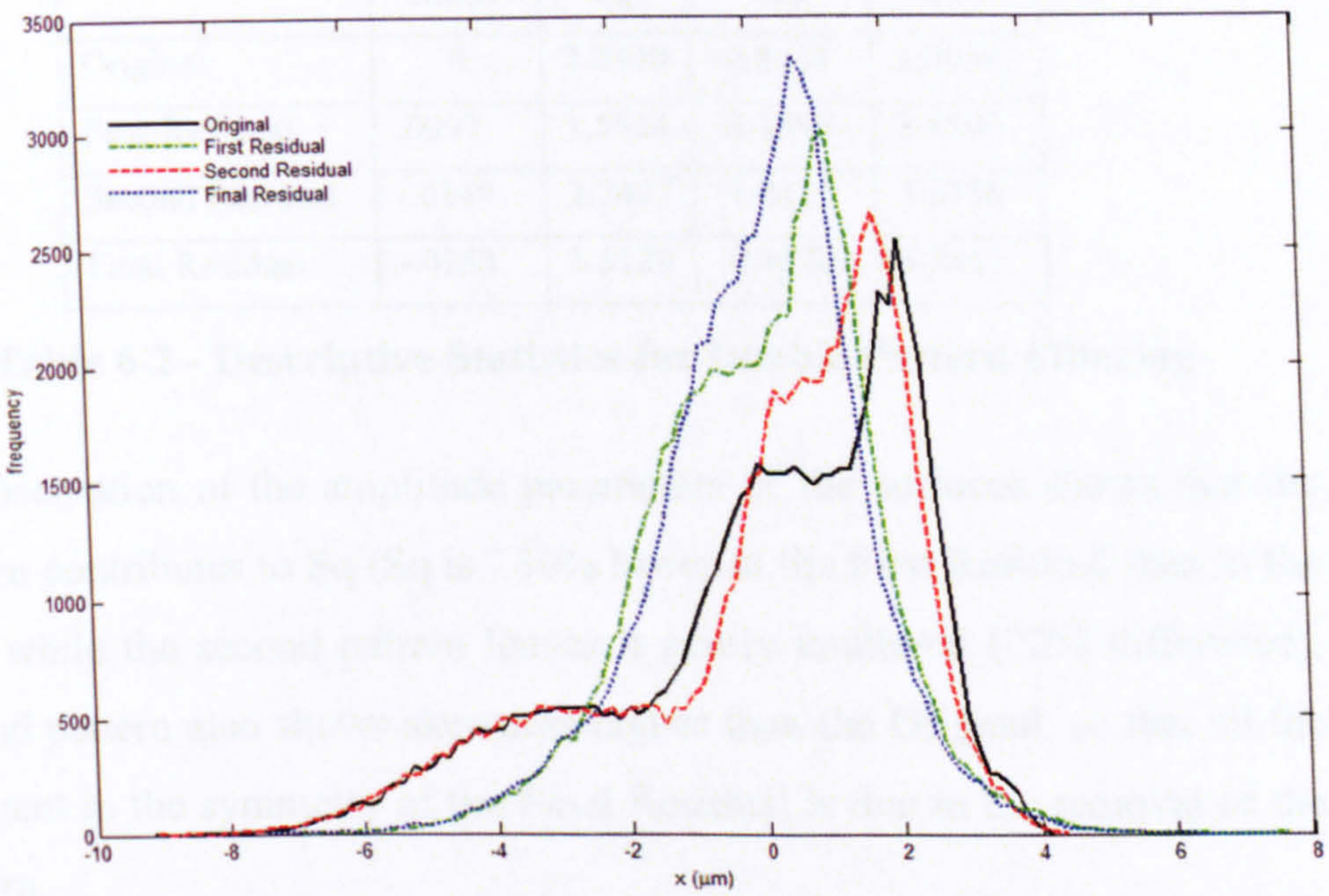

Figure 6-8 - Height Distribution of Surface through the stages of Statistical Filtering

Considering the other distributions, some observations about the filtering process can be made:

- At the first stage the main (deeper) pattern is removed, as it can be seen from the distribution of the First Residual, where the deeper feature is no longer present.
- At the second stage the lighter pattern is removed (from the Original again), and we can notice from the figure that the second pattern is unaltered.
- Finally, with both patterns removed, the distribution of the Residual Surface is depicted in blue: its shape is not symmetrical but there has been a gradual improvement from the Original that has been quantified in Table 6-2.

	Mean	Sq	Ssk	Sku
Original	0	2.2930	-0.8654	3.0054
First Residual	.0097	1.5824	-0.3396	3.3500
Second Residual	-.0149	2.2497	-1.0112	3.2776
Final Residual	-.0153	1.5129	-0.4670	3.8857

Table 6-2 - Descriptive Statistics for Double Pattern Filtering

The observation of the amplitude parameters of the surfaces shows that the first pattern contributes to Sq (Sq is ~30% lower in the First Residual than in the Original) while the second pattern leaves it nearly unaltered (~2% difference). The second pattern also shows skewness higher than the Original, so that all the improvement in the symmetry of the Final Residual is due to the removal of the first pattern.

The above considerations suggest that this approach could be a good answer to the problem of determining the contribution of the two stages of rolling (tandem and temper mill) to the final roughness of the sheets, closely related to Sq.

The normal probability plots also can be studied for the estimation of the contribution of each phase of the texturing process to the final noise. Figure 6-9 shows that the Original surface (black) is strongly not normally distributed, while the first stage of filtering (green) has a much more linear shape; the second stage of filtering (red) is nearly coincident with the Original, while the Final Residual (blue) is nearly coincident with the second stage. It is then evident the very small contribution of the second pattern: removing only the first one or both of them the randomness of the surface heights remains nearly unaltered.

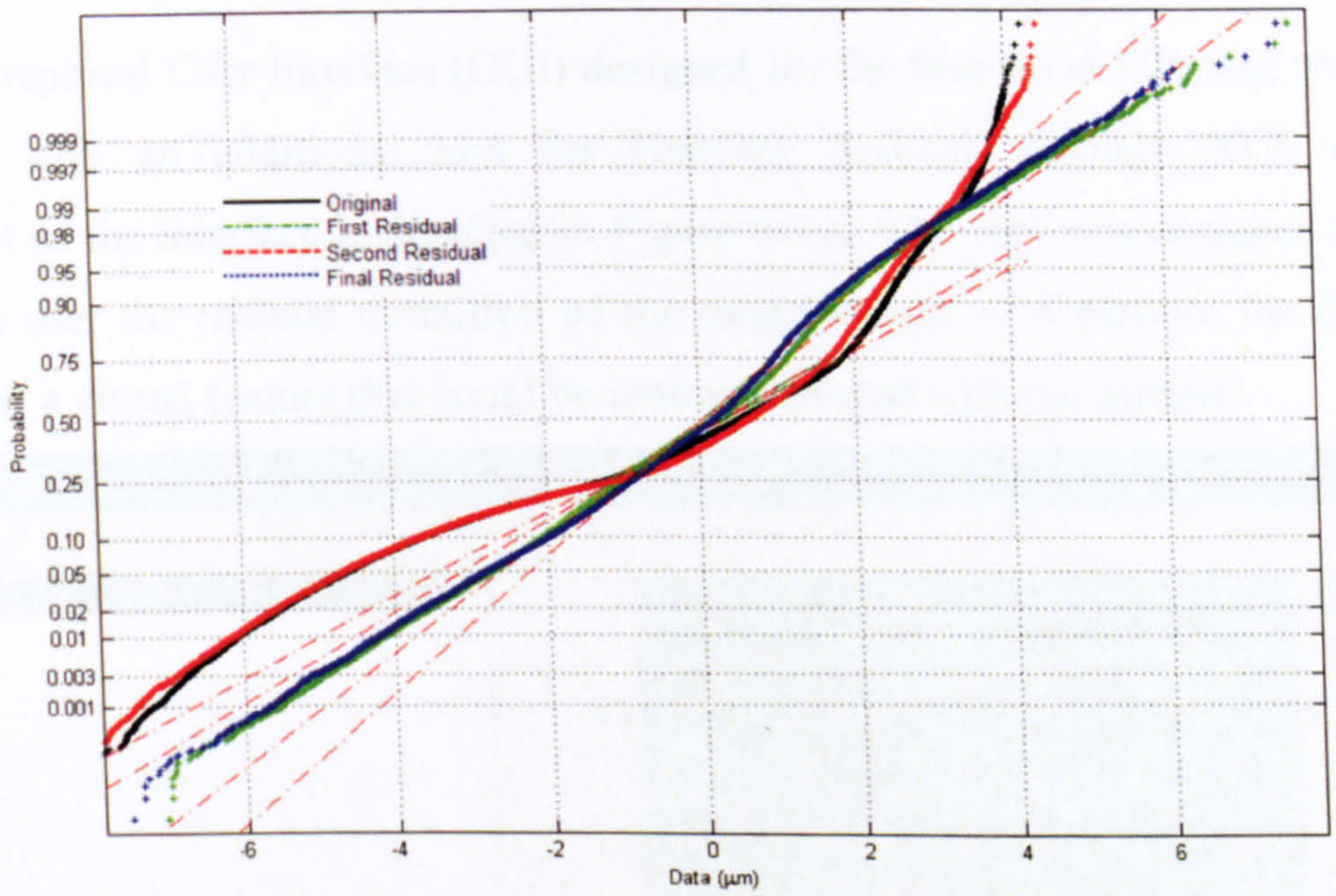

Figure 6-9 - Normal Probability Plot for Double Pattern Filtering

6.2 Features analysis

After describing the methods to access the pattern of a surface, the next natural step consists in the study of its features. The Statistical Filter approach allows the fast calculation of the average of the features, so that the parameters can be calculated only once, and still represent the average value. Alternatively, the calculation of the parameters on each single element allows the study of the distribution of each parameter over the surface, so that it is possible to quantify the number of the features that do not fall within the tolerances and their location.

The next section describes the software interface created to simplify the analysis of features, while the two following sections contain respectively the methods for the analysis of the average feature and the distribution of parameters across the sample.

6.2.1 Feature Analysis Interface

The Graphical User Interface (GUI) designed for the Statistical Filtering was equipped with an additional tool for Features Analysis through XCF (a screenshot of the interface is depicted in Figure 6-10). The tool was designed to allow the user the manual definition of the target values of a pattern, for the creation of a virtual feature that could be cross-correlated with the sample.

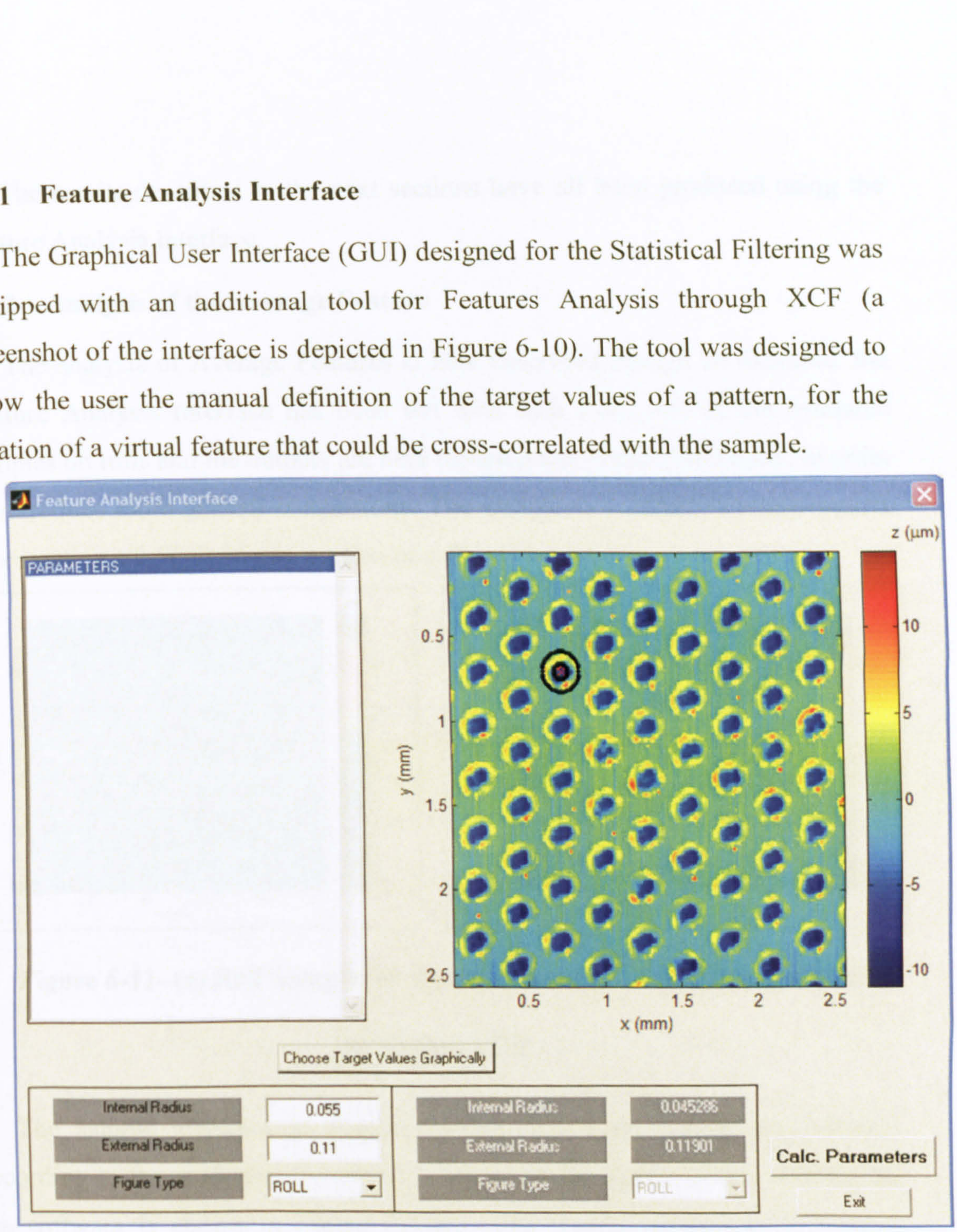

Figure 6-10 - Feature Analysis Interface Matlab Figure

Once the internal and external radii and the type of surface (roll or sheet) have been defined by the user, the software produces a virtual ring made of a parabolic pit and a half-toroidal rim if the type is a roll, vice-versa if it is a sheet. The height of the rim, the depth of the pit and the value of the main plane are all determined automatically according to the parameters of the surface: the averages of the heights of the pit and of the rim are equal respectively to the averages of the negative and positive heights of the surface.

The results described in the next sections have all been produced using the Feature Analysis Interface.

6.2.2 Analysis of the Average Feature

The analysis of Average Features is here described though an example: the Feature Analysis Interface has been fed with data from one of the available samples on rolls and the outputs are here reported and commented upon, in order to introduce more general conclusions. The sample is a 256x256 points matrix representing a 2.56x2.56 mm portion of roll.

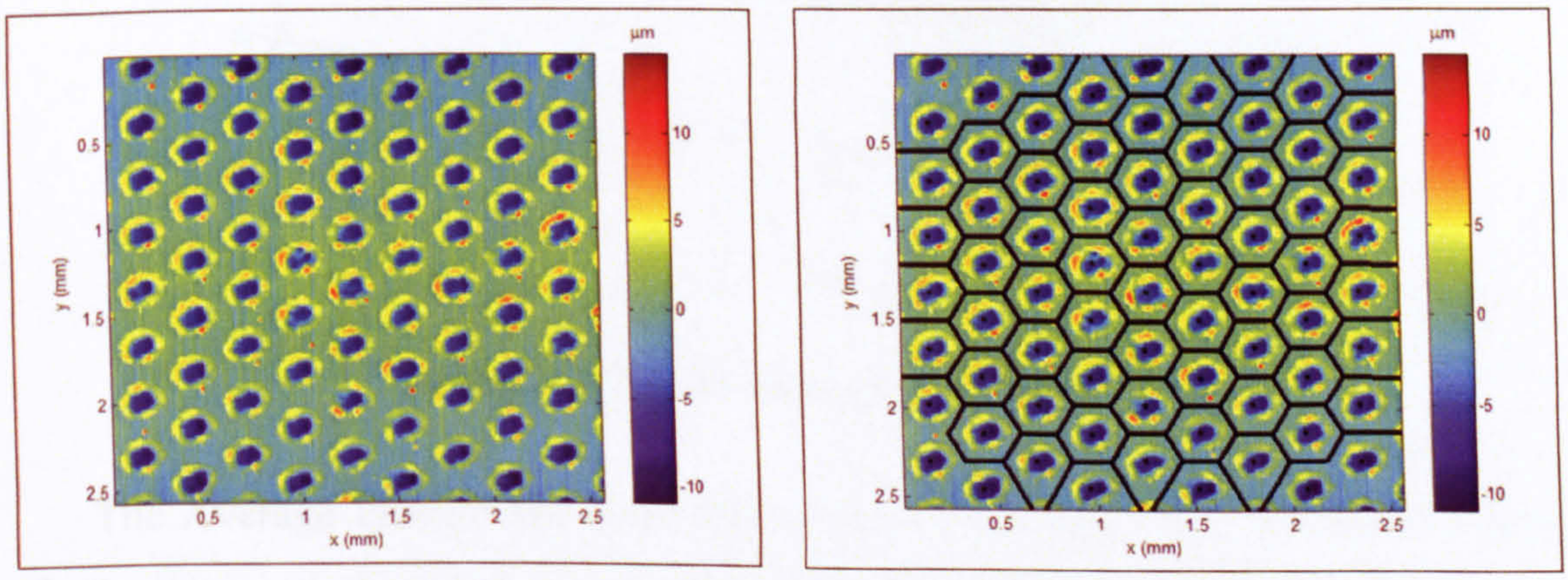

Figure 6-11- (a) Roll Sample for Feature Analysis demonstration and (b) its clusterisation

The sample, depicted in Figure 6-11(a), has been divided into clusters according to the algorithm described in section 8; the clusterisation returned by the software is shown in Figure 6-11(b). The second output of the Feature Analysis Interface is the average of the clusters, rendered as a three-dimensional solid, shown in Figure 6-12, for immediate qualitative evaluation of its shape.

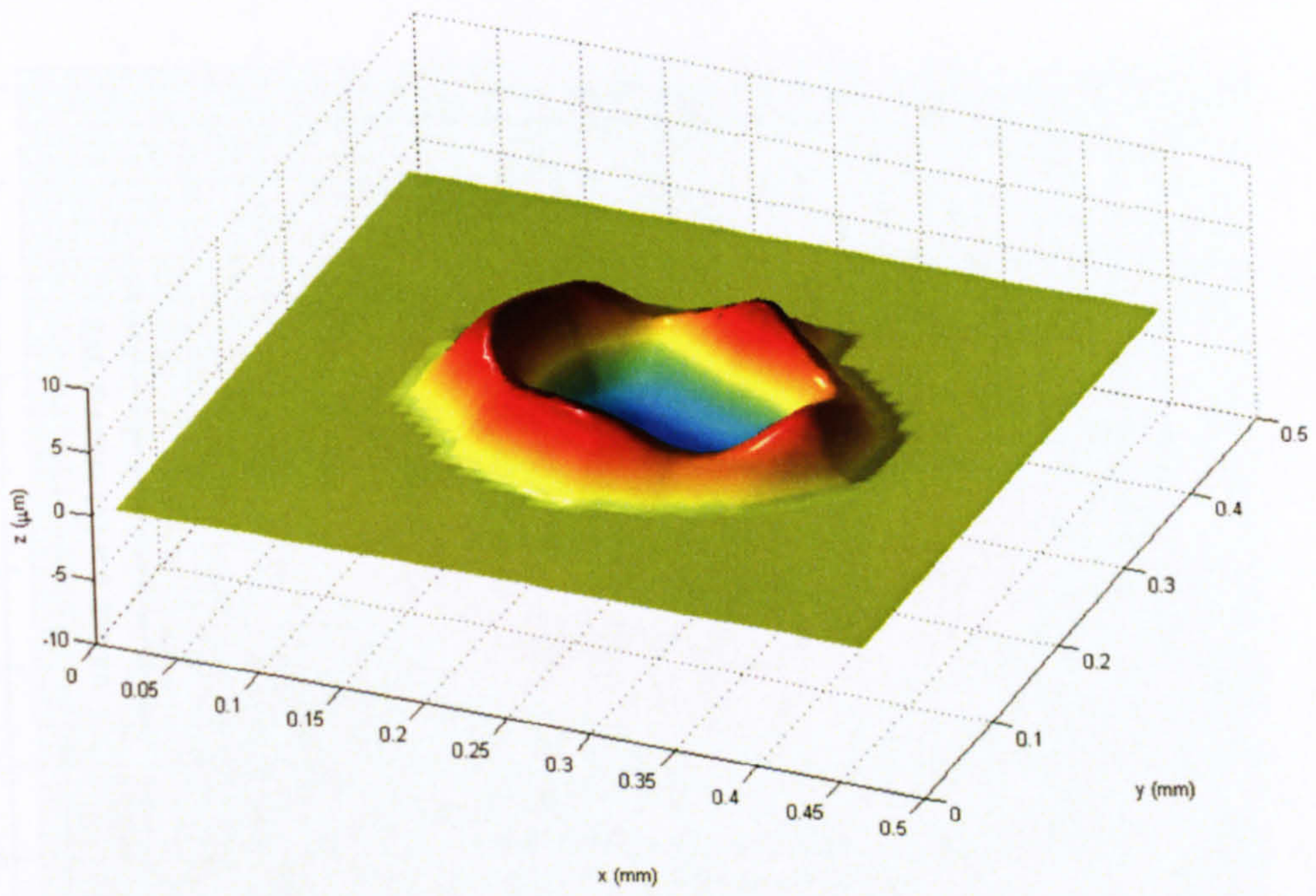

Figure 6-12 - 3D view of Average Feature

The Average Feature has been divided into a pit and a rim and placed on a flat background, for better visualisation and simpler parameters extraction.

At this stage the software has produced a three-dimensional noise-free representation of the feature, so it is in the condition to perform any kind of evaluation about its shape; at the present it returns only the basic set of parameters that are here exposed in order to reduce computational time to the minimum, but it is designed for easy implementation of personalised parameters and functions.

Figure 6-13 shows the colourmap of the Average Features that the software uses to illustrate the shape of the internal and external radii, while Figure 6-14 shows the contours associated to different height values.

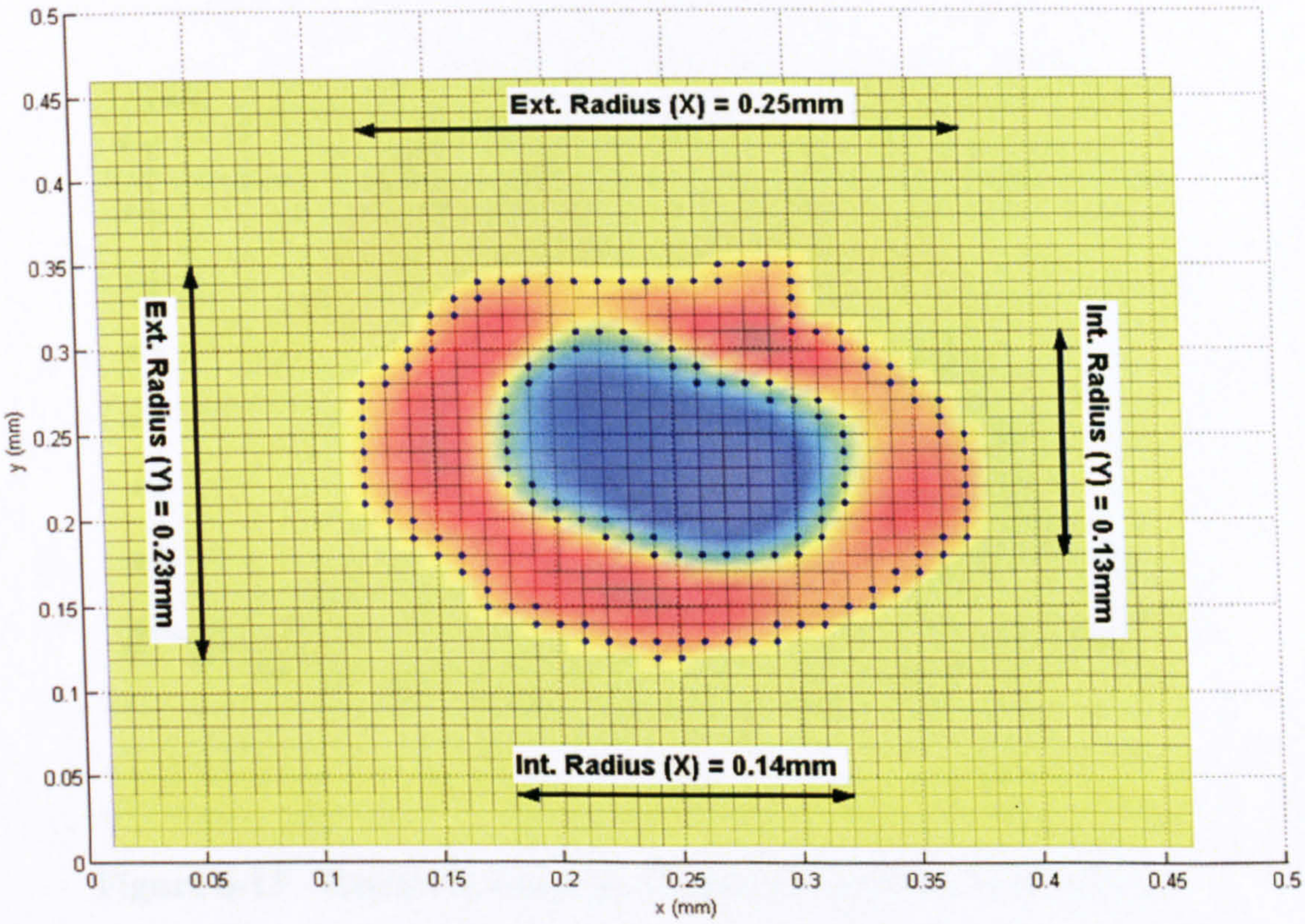

Figure 6-13 - Colourmap of Average Ring for Ring Radii evaluation

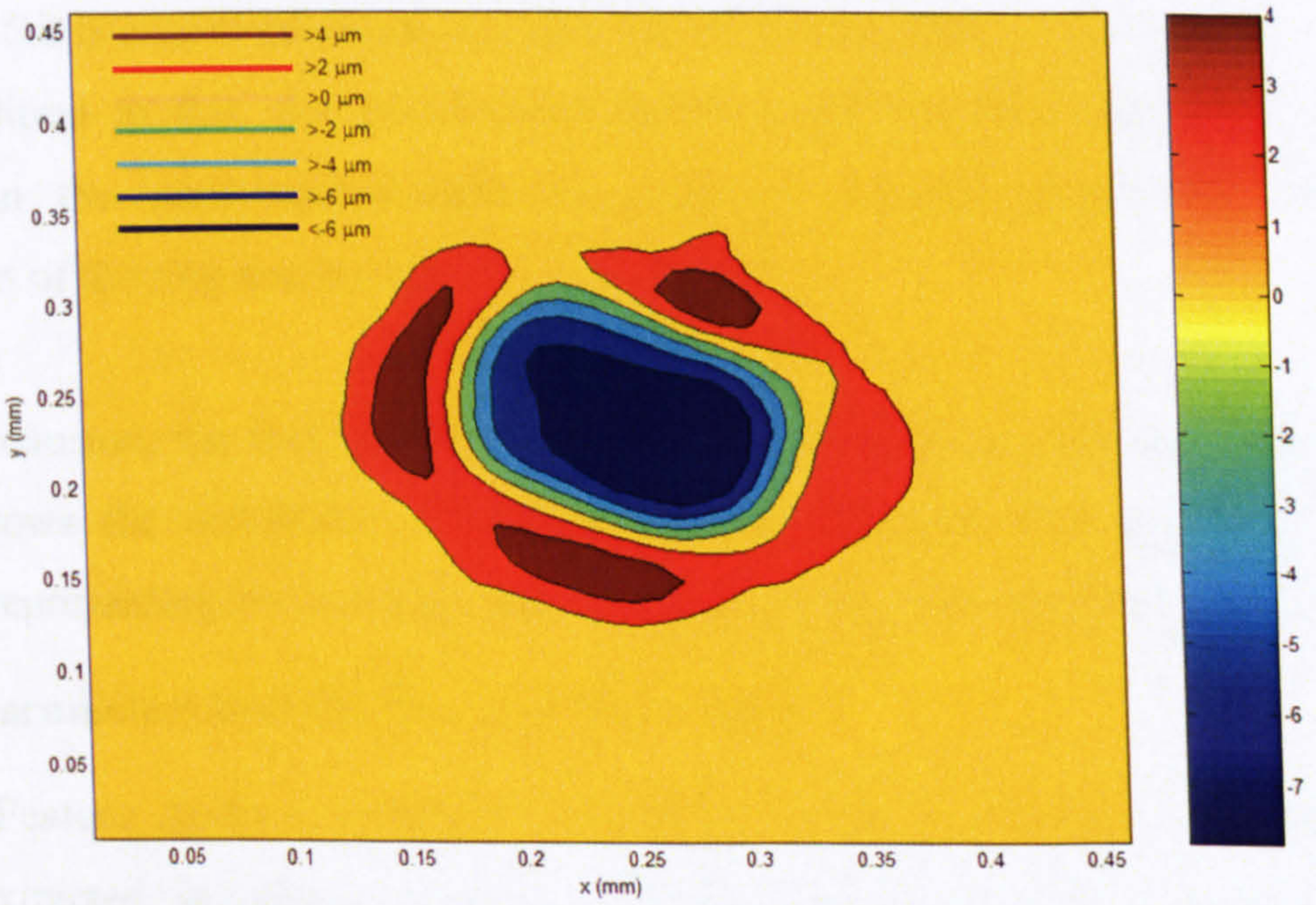

Figure 6-14 - Contour Map of Average Feature

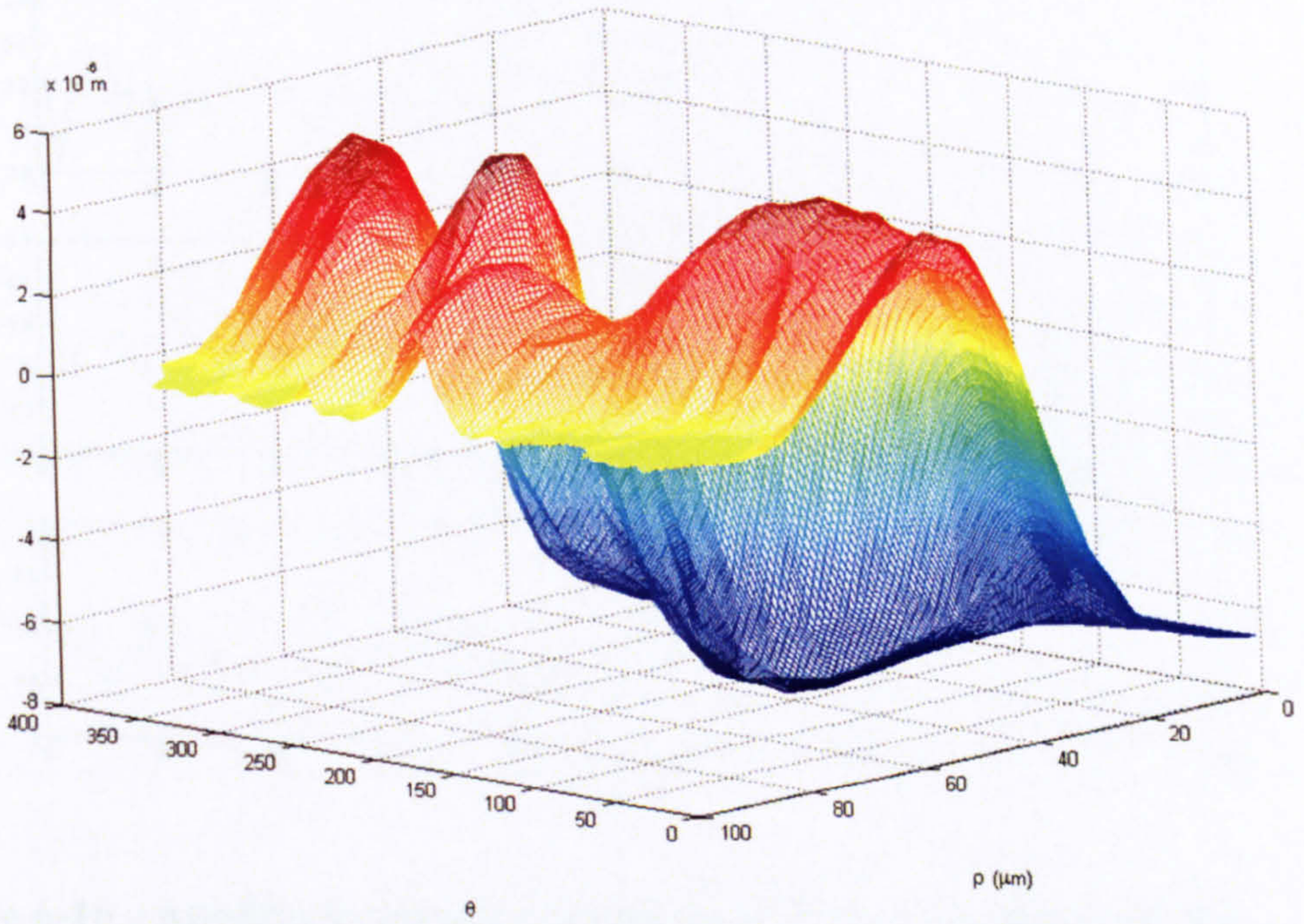

Figure 6-15 - Representation of a feature in Polar Coordinates

The feature is also resampled on a radial grid in order to represent it in polar coordinates, i.e. as a function of angle θ and distance ρ from the origin of axes, which has been placed at the coordinates of the peaks. From the result shown in Figure 6-15 it is easy to calculate the direction of defects and anomalies.

In addition to this, the internal and external profiles have been fitted to ellipses in the mean-square-sense, in order to evaluate eccentricity and orientation of the ring and the pit.

In conclusion, the fact that the average ring has a very simple and smooth shape allows the definition of any geometrical parameter that could be of interest, representing the average value of that parameter over all the clusters.

6.2.3 Parameters Distribution over the sample

The Feature Analysis Interface calculates a series of parameters for each cluster extracted, in order to control the distribution of certain characteristics or defects over the same sample. Also in this case the software has been designed for easy implementation of personalised parameters and functions.

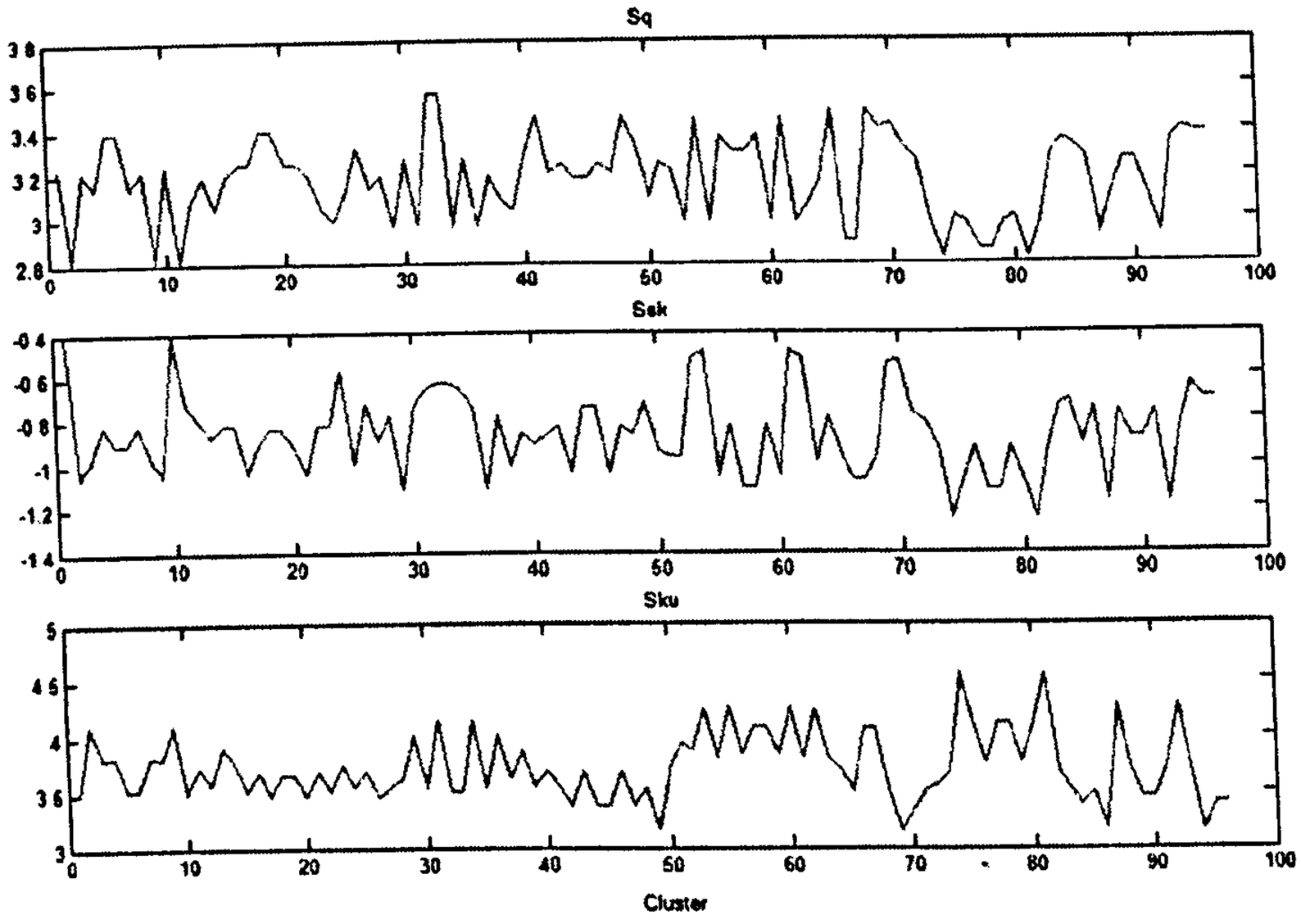

Figure 6-16 - Amplitude parameters calculated for each cluster of the sample

Figure 6-16 shows the values of amplitude parameters Sq, Ssk and Sku for each one of the clusters extracted from the data. The sample is the same one analysed in the previous section.

Each value can be associated with the position of the cluster it refers to, creating a map of the parameter over the surface; standard parameters are not suitable for this particular analysis, which has to be focused on the shape of the feature.

Knowing the value of parameters for each feature of a surface will be useful for the validation of specific parameters that define defects in the shape of the ring, like incomplete rims and asymmetric pits, which are closely related to the production process. In this case the distribution would tell how scattered a parameter is and identify those features that do not fall within the tolerance.

At the present the software has not been equipped with other parameters than the standard amplitude and descriptive statistical ones. Defining parameters for the defects of the features is considered one of the inputs of the software: any

combination of ready-made or user-defined parameters can be linked to the software in order to be calculated on each cluster.

6.3 Batch analysis

The data set described in section 3 has been used for testing the capability of the filter to perform automatic analysis of a large number of samples. The Statistical Filter software can be executed through the Graphical User Interface to study one sample at a time, but can also be launched from the prompt line requiring as only argument the path of the folder containing the samples; in this case the program automatically performs the filtering on each surface, using the algorithms described in chapters 7 and 8, recording the values of the desired parameters for each surface. The parameters to be calculated can vary and they can be user-defined.

Unfortunately the set of data available throughout the project does not have the necessary characteristics for the validation of the parameters extracted with the Statistical Filtering, as discussed in section 3; moreover, the Statistical Filter has been designed to access particular surface features, while the existing standardised parameters are not feature-oriented and not specifically dedicated to one production process.

This section presents the results of the filtering of the homogeneous set of 2x2mm samples described in section 3, and the conclusions that can be drawn from them.

The software performed one operation of pattern removal on each surface, based on ACF, with the threshold defined by the bearing area parameters as described in section 8. The total number of surfaces was 220, extracted on 21 different samples of rolls, sheets and rolls replicas. The same parameters have been extracted for the Original, Filtered and Residual Surface of each sample.

6.3.1 Considerations on the parameters distributions

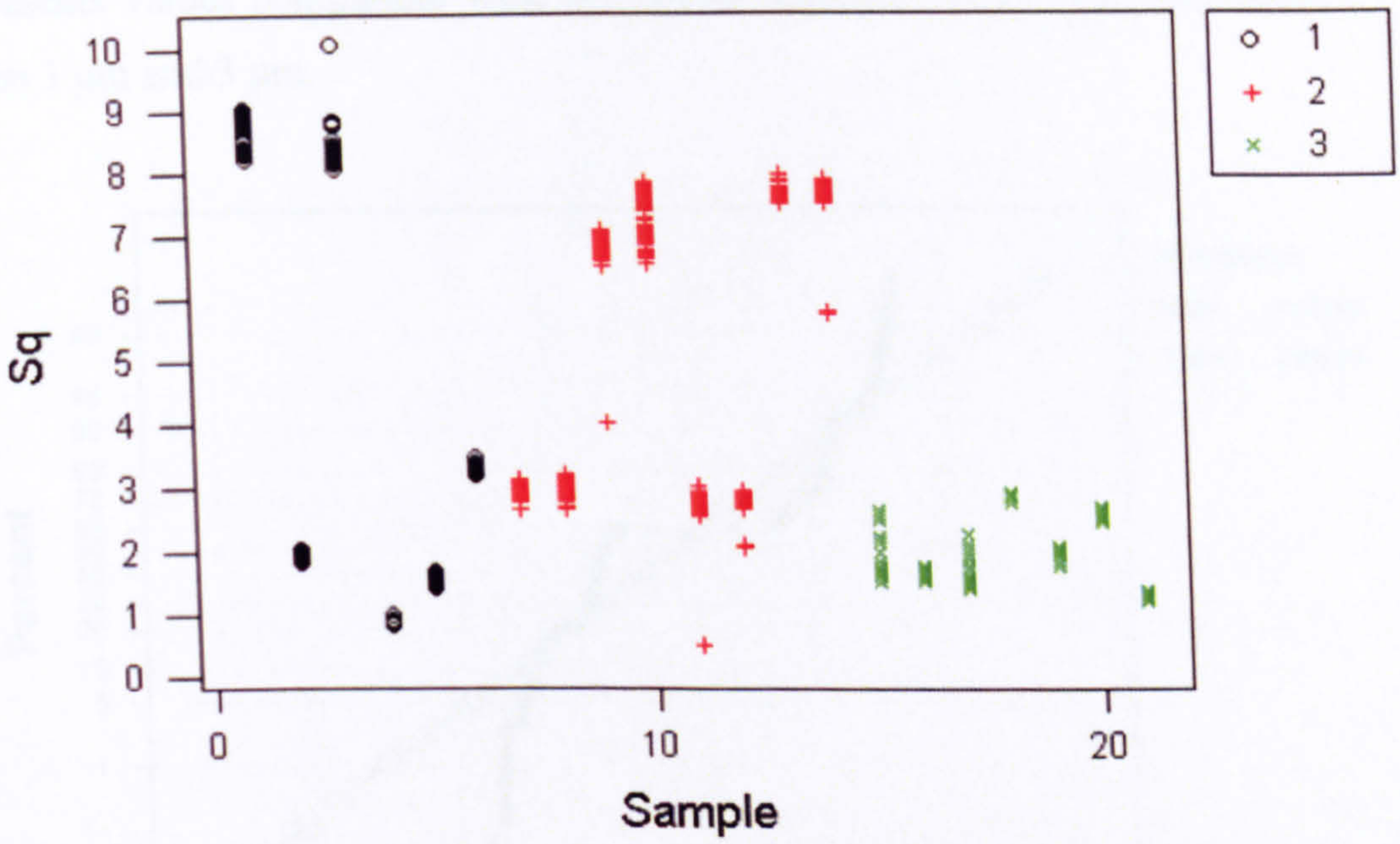

Figure 6-17 - Values of Sq by Sample (on original surfaces)

The parameters returned by the batch filtering operation can be plotted versus the sample ordinal number: the plot returned for parameter Sq is shown in Figure 6-17. The colours are associated with different values of parameter 'Type', which assumes values of:

1) Represented with black circles (o) the Roll Samples
2) Represented with red plus (+) the Replica Samples
3) Represented with green cross (x) the Sheet Samples

It is clear that the rolls and the replicas are divided into two well defined groups: one group presents Sq values between 6 μm and 9 μm, while the other one presents values compatible with the sheets samples, which are distributed between 1 μm and 3 μm.

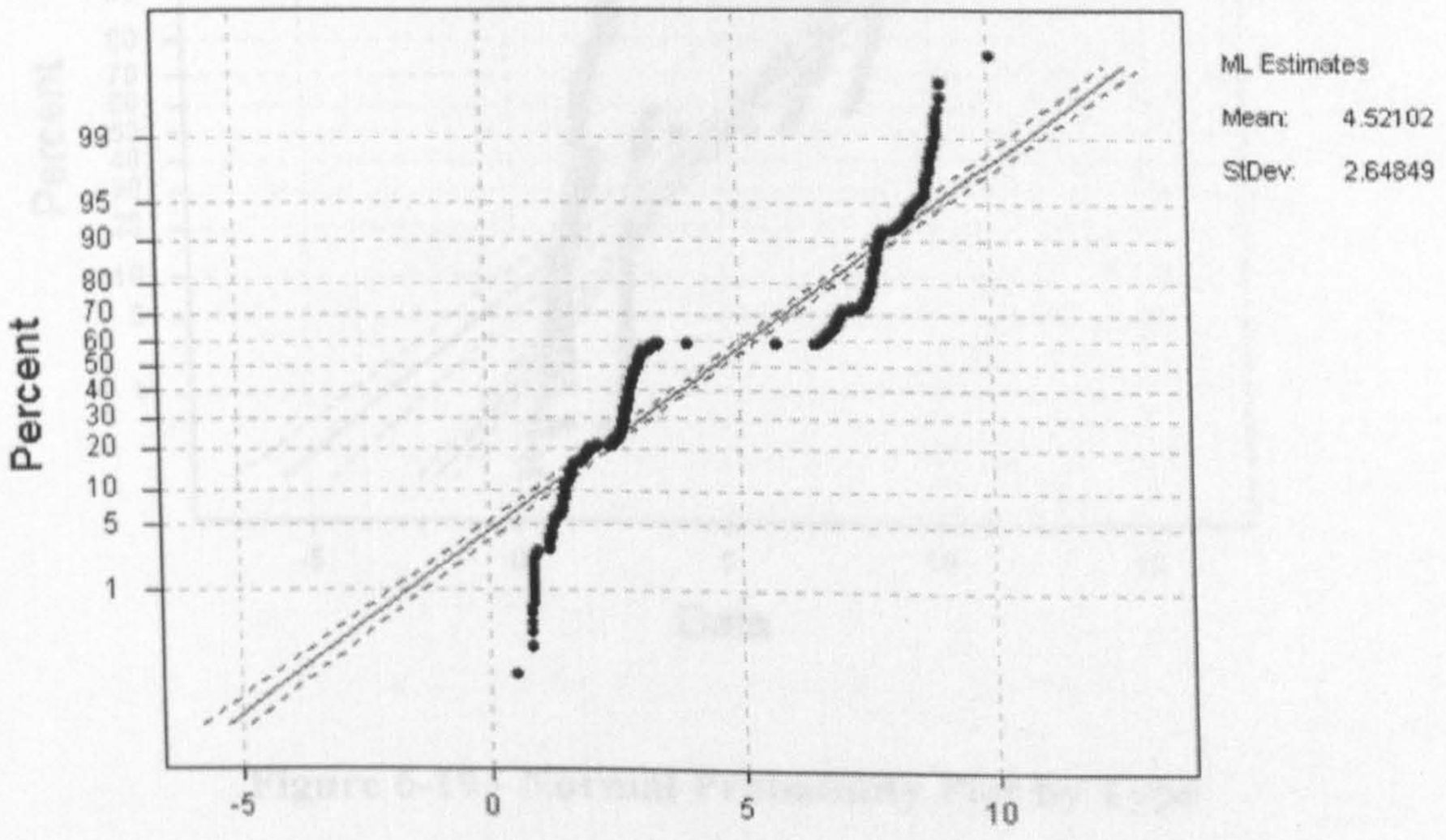

Figure 6-18 - Normal Probability Plot for Sq

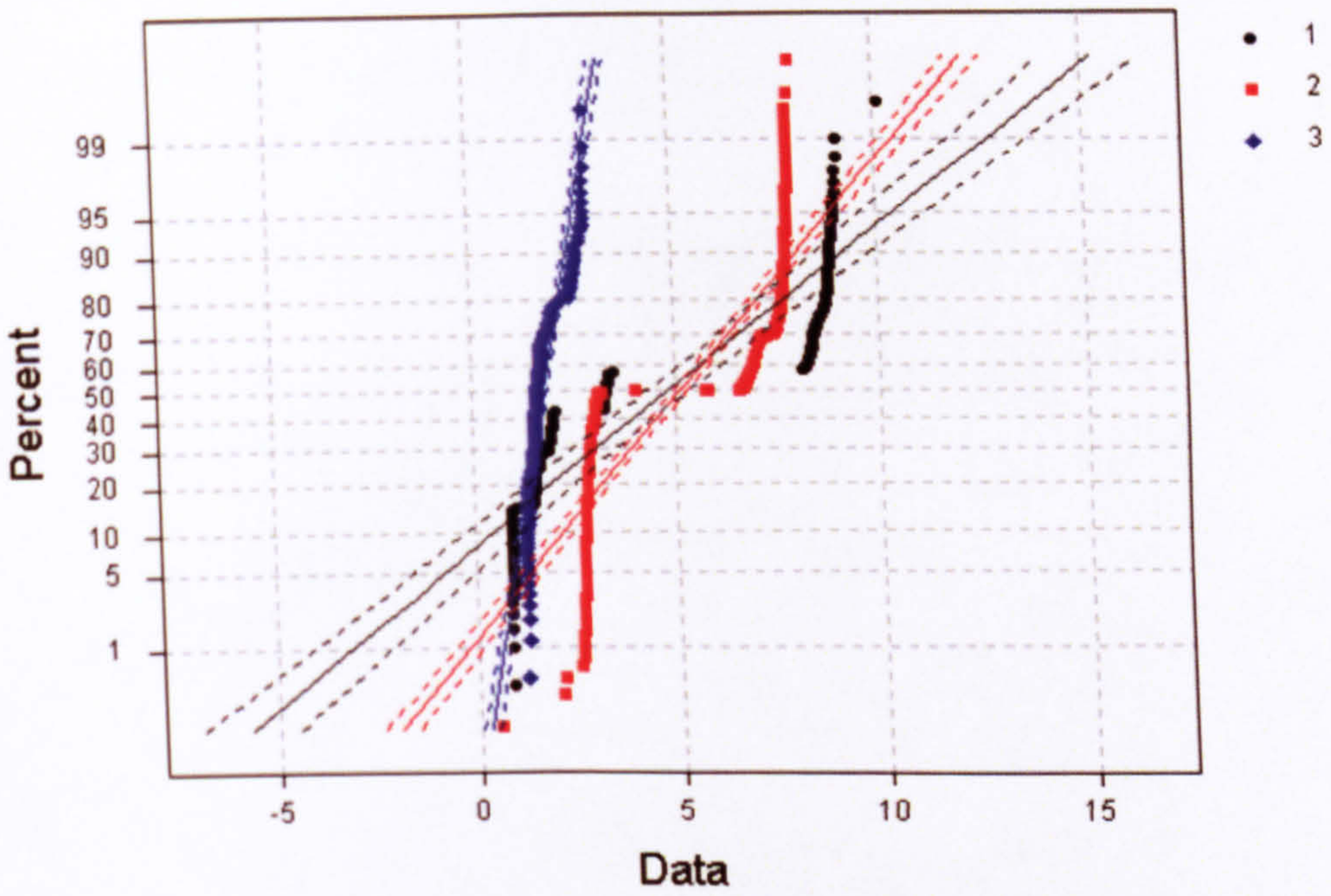

Figure 6-19 - Normal Probability Plot by Type

Analogue considerations can be done observing the normal probability of Sq in **Error! Reference source not found.**, which clearly presents two distinct sets of values. In the normal probability by type, shown in **Error! Reference source not found.**, the sheet samples (in blue) show a normal distribution, while rolls (in black) and replicas (in red) present the expected division into two groups. Within the groups, the samples seem to present linear distributions, particularly within the same sample's repetitions, which would confirm the validity of the resampling operation performed on the surfaces, at least for parameter Sq.

6.3.2 Correlations between parameters

The results have also been inspected for correlations between the values in the Original, Filtered and Residual Surfaces. **Error! Reference source not found.** and **Error! Reference source not found.** show respectively the regression plots of Sq_filt vs. Sq and Ssk_filt vs. Ssk, where Sq_filt and Ssk_filt represent parameters Sq and Ssk calculated on the filtered surface.

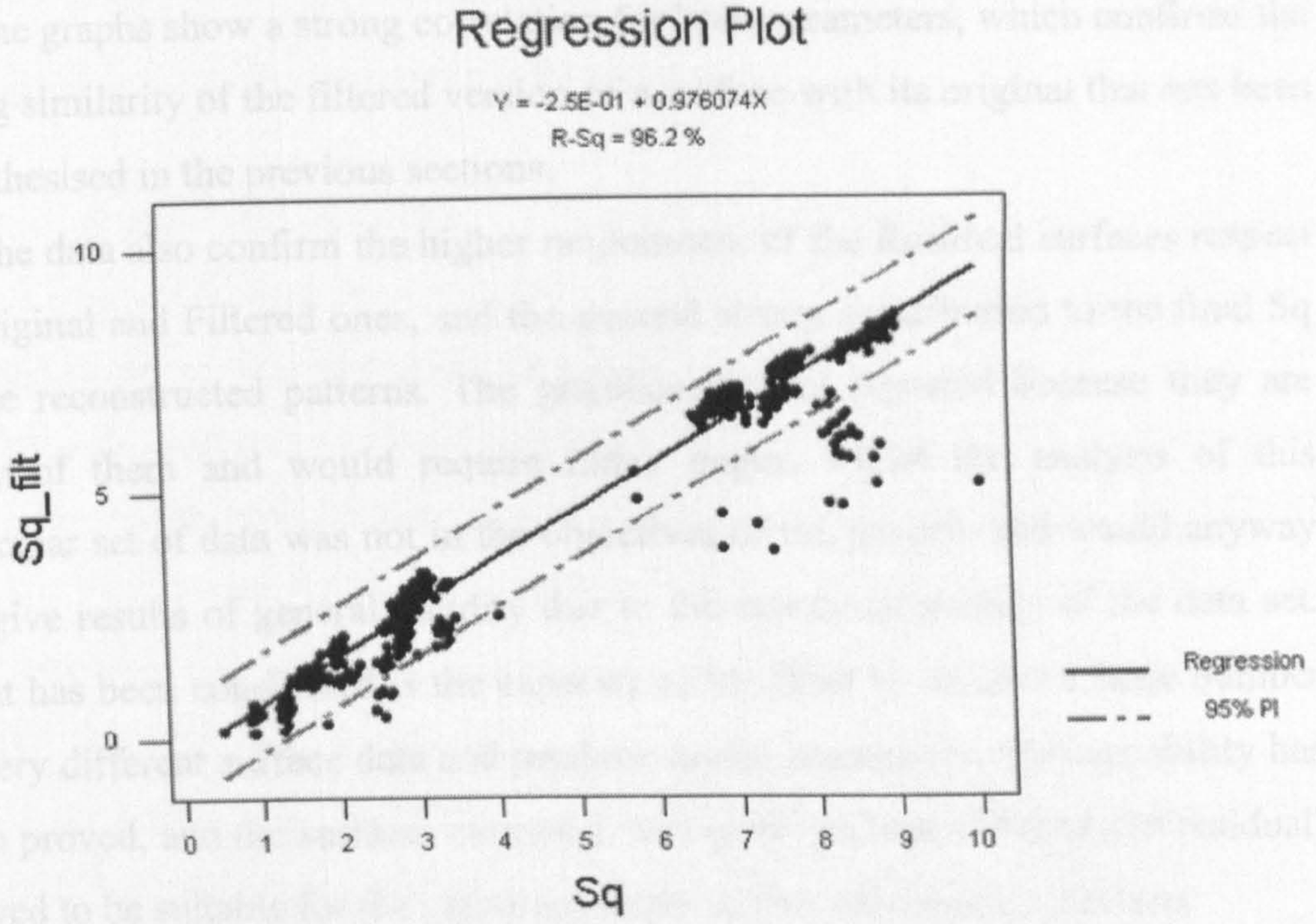

Figure 6-20 - Regression Plot of Sq_filt vs. Sq

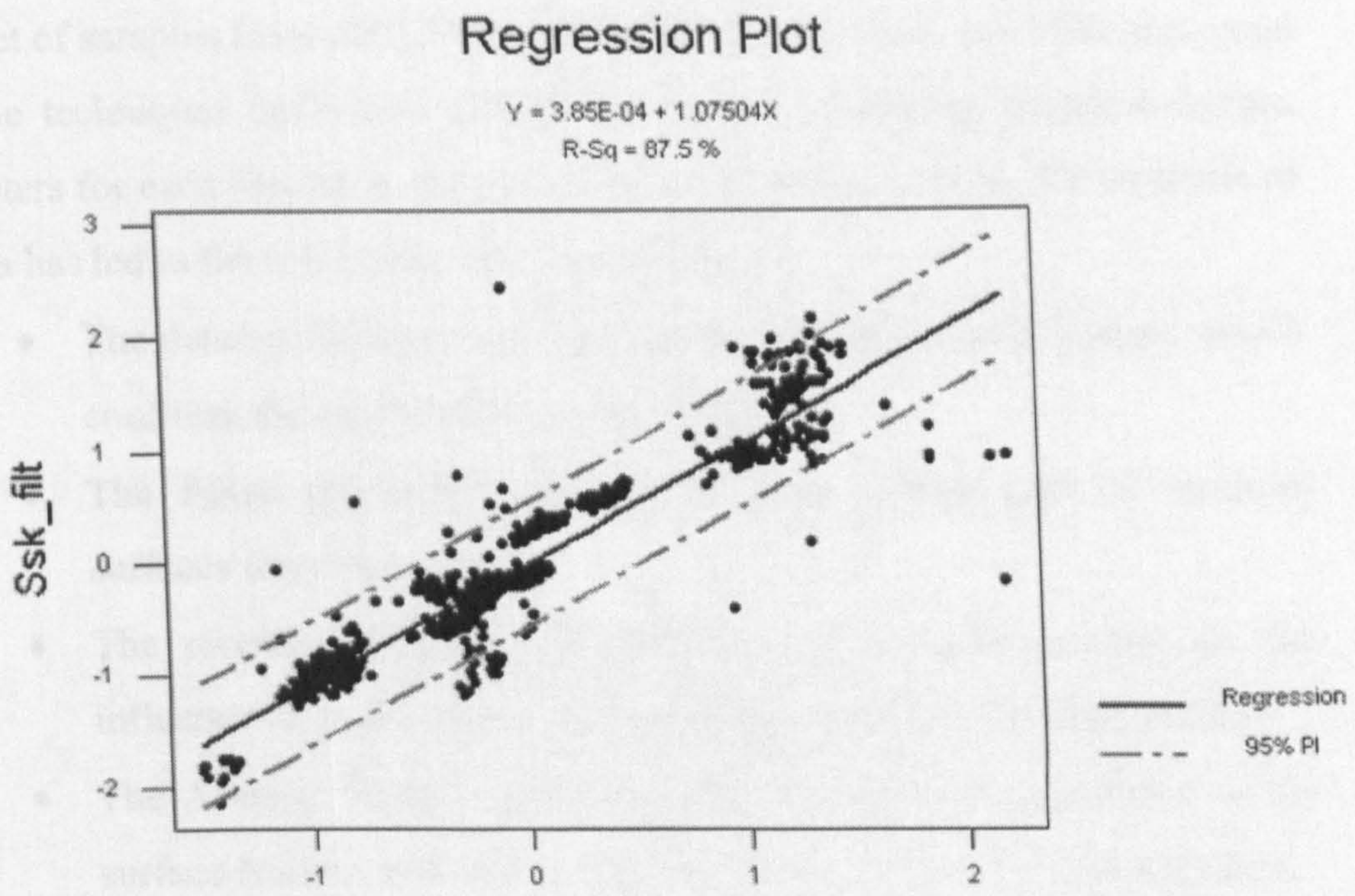

Figure 6-21 - Regression Plot of Ssk_filt vs. Ssk

The graphs show a strong correlation for both parameters, which confirms the strong similarity of the filtered version of a surface with its original that has been hypothesised in the previous sections.

The data also confirm the higher randomness of the Residual surfaces respect to Original and Filtered ones, and the general strong contribution to the final Sq of the reconstructed patterns. The graphics are not reported because they are many of them and would require many pages, whilst the analysis of this particular set of data was not in the objectives of the project, and would anyway not give results of general validity due to the non-homogeneity of the data set. What has been considered is the capacity of the filter to process a large number of very different surface data and produce useful parameters. This capability has been proved, and the surfaces extracted during the process (filtered and residual) proved to be suitable for the characterisation of the deterministic patterns.

6.4 Conclusions

A set of samples from EBT Textured Surfaces production has been processed with the techniques developed during the project, recording standard surface parameters for each sample at each stage of the filtering process. The analysis of the data has led to the following main considerations:

- The deterministic pattern has been recognised in each sample, which confirms the repeatability of the technique
- The Filter effectively isolates the deterministic part of textured surfaces from the noise
- The reconstructions of the patterns can be used to estimate the influence of each stage of the texturing process on the final product
- The Average Feature extracted with the Filter is a synthesis of the surface features and can be used for the analysis of recurring defects

7. Software Implementation

This chapter will consider the logistical, mathematical and algorithmic aspects of the practical implementation of the theoretical work, rather than an analysis of the pure programming aspect of the project.

The entire research has been conducted analysing surface data by calculation using the Matlab programming environment. The main advantage of the Matlab platform is a simple syntax derived from BASIC and very quick deployment of the procedures for testing (as opposed to C++ where coding time is generally of greater magnitude than testing time).

Another advantage of using Matlab is the way functions are organised: once a function is created and saved it becomes another Matlab command just like any other, and it can be used in new programs or functions or directly from the command prompt in the Matlab command window.

Instead of a single program, many functions have been created and collected in a library: this approach introduces extreme modularity in the organisation of the project. Additionally, the SCOUT software (described in the next section) was created with the same kind of philosophy; therefore the whole new library created for this research can be included into the SCOUT software as another one of its set of modules.

7.1 SCOUT

SCOUT (Surface Characterisation Open-source Universal Toolbox) (see section 1.1) consists of a set of Matlab modules (exemplified in Figure 7-1) and since its first version, grew steadily in size and complexity as the time passed, thanks also to the open-source philosophy that characterises it [Sacerdotti et al. 2002].

The modules are organised in various groups as detailed in the next sections.

```
SCOUT
  Surface Characterisation Open-Source Universal Toolbox

                        Developed by AUTOSURF consortium


  I/O
    readsdf      - Reads  a surface in SDF Format
    writesdf     - Writes a surface in SDF Format
    readsurf     - Reads 3D surface data in any format
    readprf      - Reads a profile in PRF Format
    writeprf     - Writes a profile in PRF Format
    drawsurf     - Draws a properly scaled surface/profile
    surfconv     - General Conversion program from any to any surface format

  Euclidean Transformations
    isometry     - flips/Rotates a surface

Form Removal
    linfrm       - Removes the regression plane from surface data
    sqrfrm       - Removes the regression 2nd order polynomial from surface data
    islevel      - Checks if the surface is levelled

Filtering

    gau_filt     - Gaussian Filtering
    rob_filt     - 3D Robust Filtering ( Courtesy of Hannover University )
    robfil2d     - 2D Robust Filtering ( Courtesy of Hannover University )

 Parameters

    condsurf     - Applies form removal to Surfaces (To use BEFORE
                   calculating parameters)
    dis_pars     - Height Distribution Parameters
    bea_pars     - Calculates Bearing Area (Firestone-Abbott) Parameters
    amp_pars     - Calculates Amplitude Parameters
    cla_pars     - Closed Areas Parameters
    acf_pars     - Autocorrelation Function Parameters
    wcindex      - Wihlborg-Crafoord Index
    pervsa       - Perimeters calculated with fractals

 Miscellanous

    scoutgi      - Scout Graphical Interface
    slicesur     - Graphically Slices a surface
    scoutver     - Gives the current version of scout
    cstfrm       - Removes the regr. plane calculated from a selected poligonal zone
    clareas      - Lists all closed areas above zero in a surface
    clacurve     - Plots the distribution of closed areas vs. height
    acorr2       - Auto Correlation Function (No Signal Processing Toolbox Required)
```

Figure 7-1 - SCOUT Matlab help

7.1.1 Input / Output

This group of procedures is mainly concerned with reading and writing the raw surface data from disk. The adopted file format is the Surface Data Format (SDF) defined by the Surfstand [SurfStand website] Group. Every other format can be read, written or converted into any other by the SURFCONV module (see section 3.4).

7.1.2 Form Removal & Filtering

This group of procedures is concerned with the conditioning of surfaces detailed in section 2.3.

Linear and polynomial form removal algorithms handle most of the possible measuring conditions. Filtering algorithms are then used to separate roughness and waviness components.

7.1.3 Parameters

These procedures are concerned with the parameter calculation and include both new parameters developed within the Autosurf Project and old standard parameters. The modules were used for all the parameter calculations in the previous chapters.

7.1.4 Miscellaneous

The procedures that do not fall into previous sections are grouped here. Amongst those, particular effort was dedicated to a user-friendly graphical interface.

7.2 The Statistical Filter – Supporting Functions

Basic functions were created before the actual development of the Statistical Filter, in order to have the most commonly used routines ready to use in any other function or program later developed.

A brief qualitative description of the most important of them is given in the next sections.

7.2.1 The auto and cross-correlation functions

The correlation functions are at the base of nearly every application and method described in this document, deserving therefore particular care in the development and optimisation.

Matlab contains a function for performing bi-dimensional cross-correlation functions, but it is a very time-consuming version implemented using the cross-correlation definition [Definition 2-1].

A new version of the function was implemented using a different definition of the correlation functions that derives from Fourier analysis [Proakis et al. 1996]

$$R = F^{-1}\left\{\left[F(\eta_1)\cdot F(\eta_2)^*\right]\right\} \qquad \text{[Equation 7-1]}$$

According to this definition the XCF can be calculated performing two Fourier transforms and one inverse transform. The great advantage in this approach is the use of FFT algorithm (Fast Fourier Transform), which allows very fast calculations of Fourier transforms, as the name suggests.

The performances of the two definitions applied are evident in Figure 7-2, where the timings for calculation of XCF using the two algorithms are compared calculating the XCF of random square matrices of different dimensions.

The Matlab function, that applies the classic definition ([Equation 2-2]), assumes a characteristic parabolic aspect, in accordance with the linearity of the equation and the quadratic increase in the number of elements in the matrix with its lateral dimension.

The FFT based XCF algorithm is strongly affected by a characteristic of the FFT algorithm: it can only be calculated for sequences of data whose length is a power of two [Orfanidis 1996].

Matlab uses a high-speed radix-2 algorithm if the input sequence is a power of two, giving a computational complexity of *N*log(N)*; when the sequence length is not an exact power of two, a separate algorithm computes a mixed-radix discrete Fourier transform whose timings vary according to the number of prime factors in the sequence length.

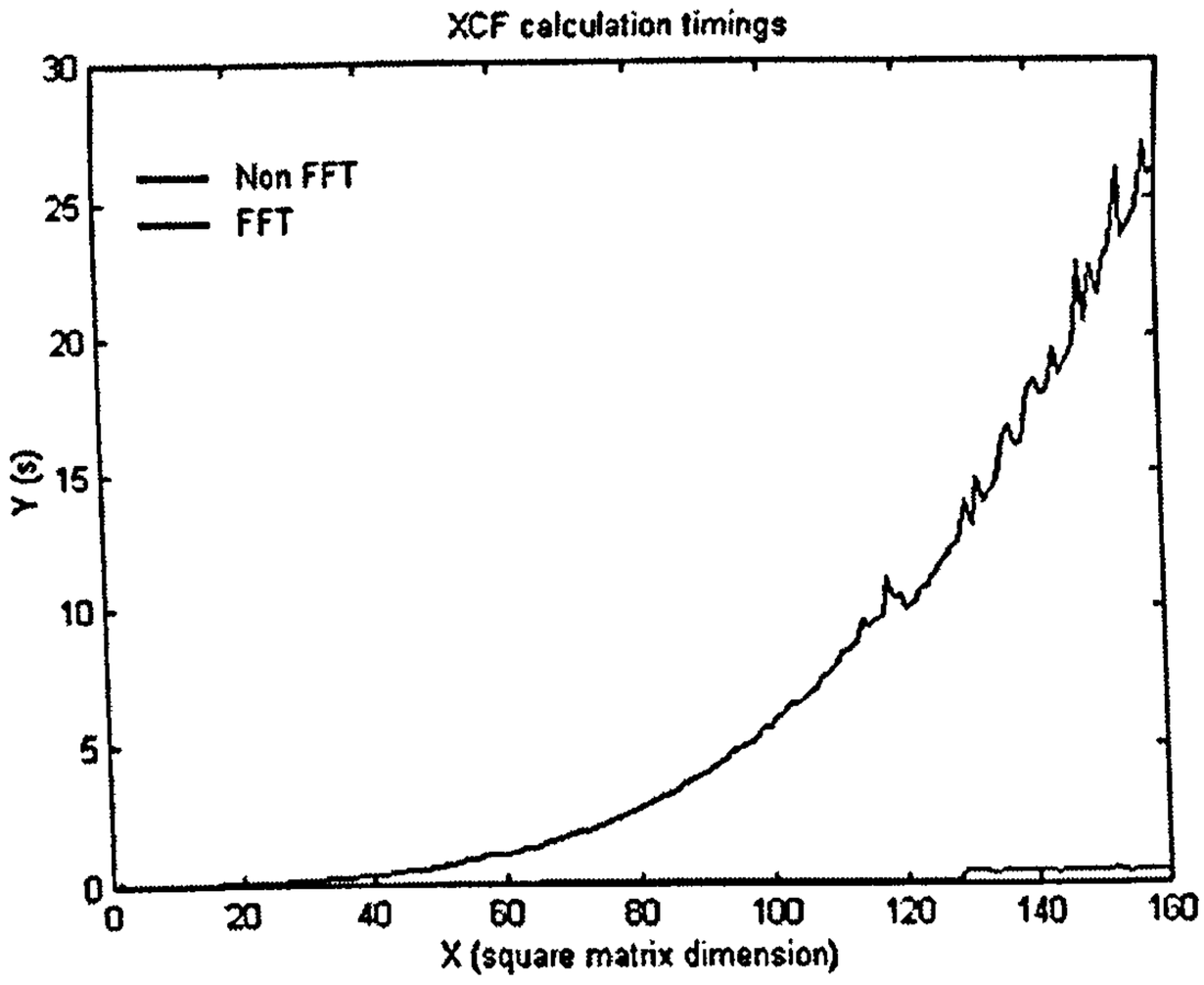

Figure 7-2 - Timings for calculation of XCF using FFT and non-FFT based methods – linear scale

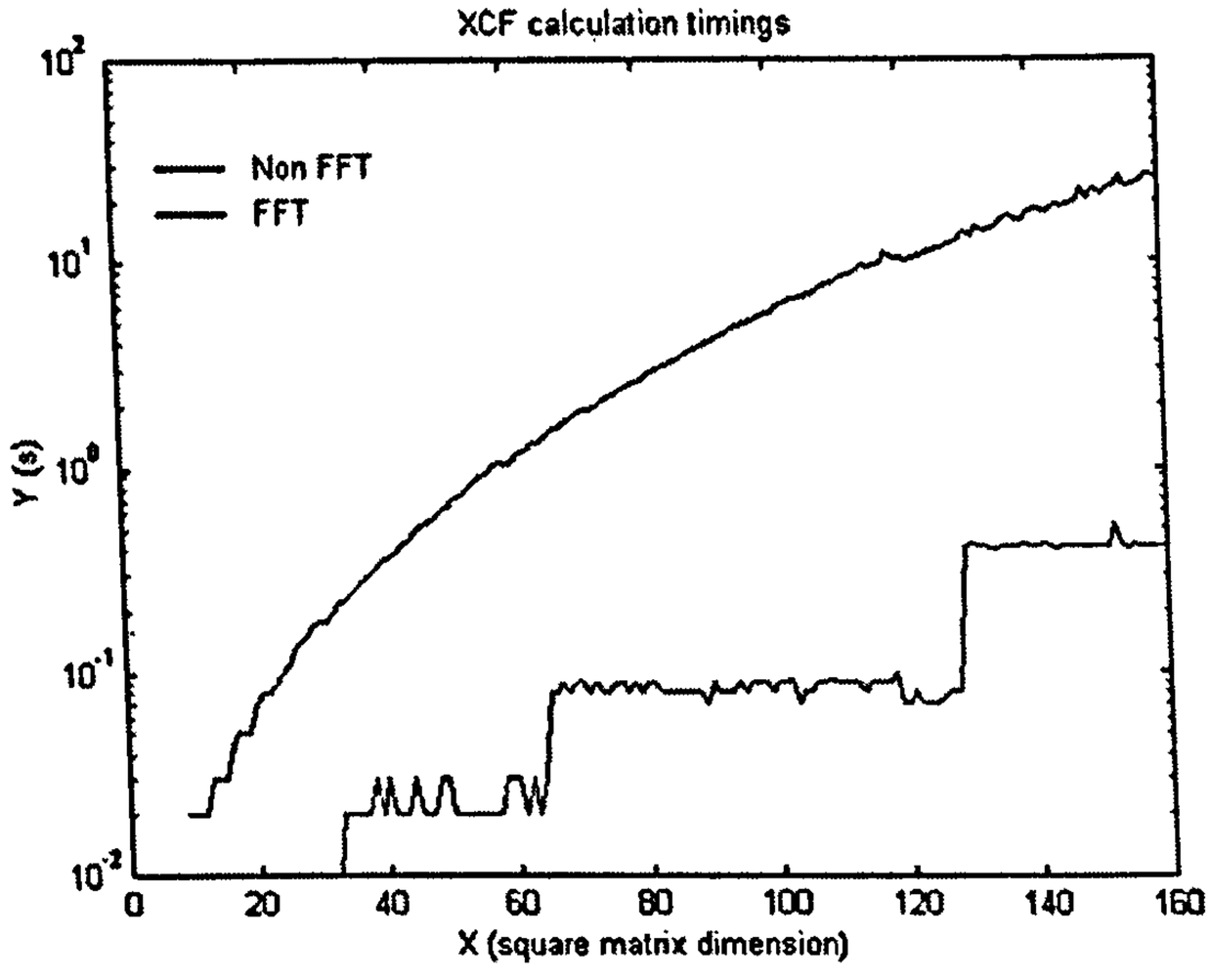

Figure 7-3 - Timings for calculation of XCF using FFT and non-FFT based methods – logarithmic scale

To perform autocorrelations using only powers of two as input dimensions the technique used was called "zero padding" [Meyers 1990], consisting in adding null values at the end of the sequence to be transformed. Using this

technique, only the fastest FFT algorithm is used, and the precision of the calculation results improved (the longest is the sequence to transform, the higher becomes the definition of the FFT sequence [Proakis 1995]).

The graph in Figure 7-3 in logarithmic scale shows how the FFT based algorithm changes radically in correspondence of the powers of two, due to the zero padding that makes every 2^n+1 be zero padded to 2^{n+1} (32, 64 and 128 are clearly visible in the graph) but always representing a great advantage in time consumption respect to the classic algorithm.

Being the XCF at the very base of the Statistical Filter Project, an elevate execution speed represents an indispensable pre-requisite for on-line industrial applications.

7.2.2 Peaks determination

As previously described, auto and cross-correlation functions are calculated to obtain the coordinates of their peaks, which represent the points where a surface matches itself (ACF) or another surface (XCF).

The first implementation of the function for peaks isolation required as arguments the auto-correlation function and the threshold that defines a peak (section 4.1.1). The threshold has been initially found empirically through a process of trials and errors. Its definition is one of the delicate points of the process, because the on-line version of the program needs to be fully automated and self-tuning. Solutions to this problem are introduced in section 8.1.

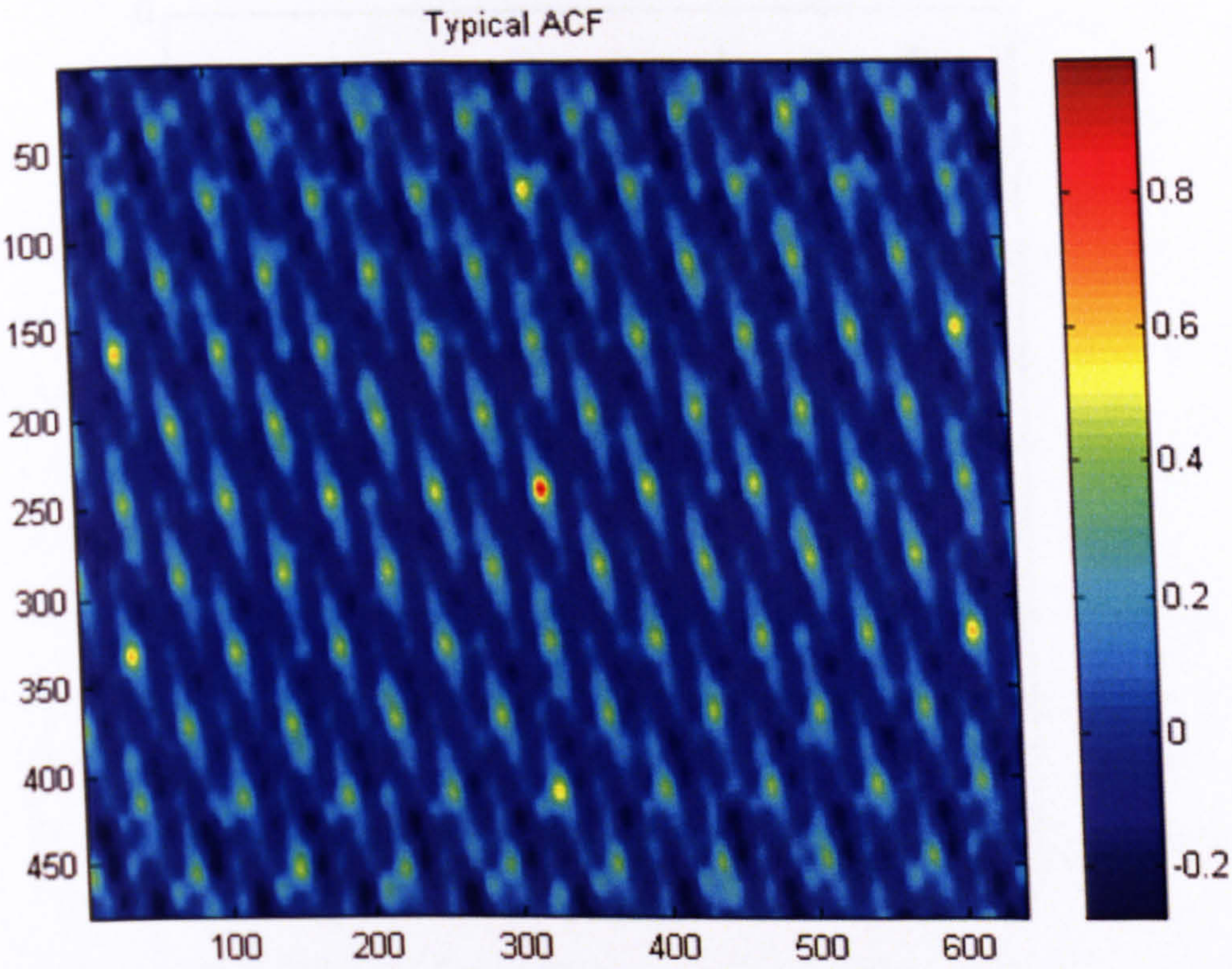

Figure 7-4 - Typical ACF

Let $R(\tau_i, \tau_j)$ be an auto-correlation function, represented by Matlab as a matrix of double-precision elements, normalised to 1 (so that $|R(\tau_i, \tau_j)| \leq 1$). An example of ACF is depicted in Figure 7-4; the axes represent the elements of the matrix.

Once the threshold ε has been established, or given, the peaks map $P(\tau_1, \tau_2)$ is created as a matrix of boolean values

$$P(\tau_i, \tau_j) = \begin{cases} 1 & R(\tau_i, \tau_j) > \varepsilon \\ 0 & R(\tau_i, \tau_j) \leq \varepsilon \end{cases} \qquad \text{[Equation 7-2]}$$

An example of threshold map calculated on the ACF of Figure 7-4 using an $\varepsilon=0.29$ is depicted in Figure 7-5 ("nz" indicates the number of non-zero elements).

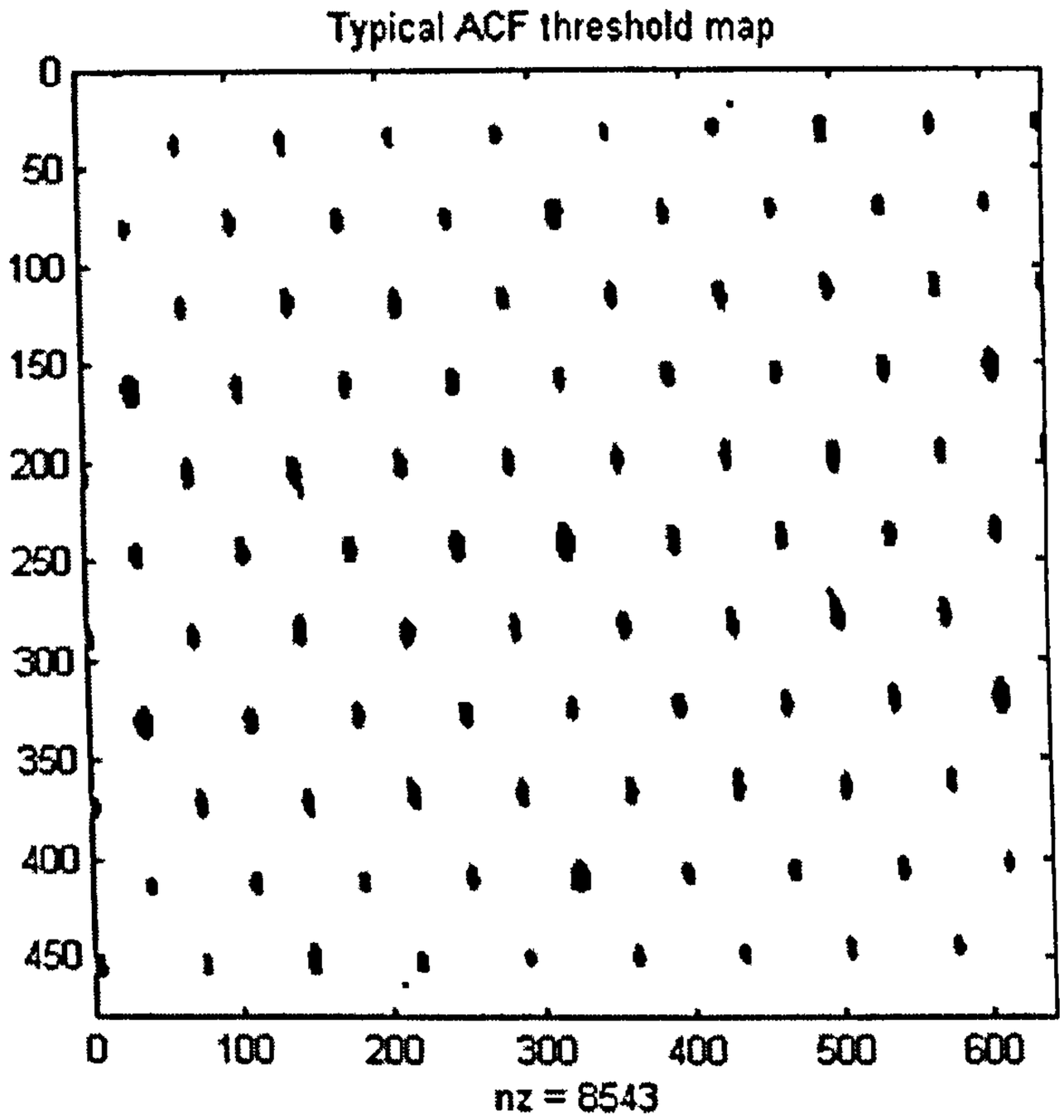

Figure 7-5 - Threshold image of a typical ACF

The map as it is cannot be used yet, because instead of high-correlation "areas" the program needs the exact coordinates of the peaks. In this situation a small but useful function included in SCOUT, `clareas`, has been used which finds every closed region [Pferstof at al. 1998] in a surface and assigns the same unique number to each one of its elements. $P(\tau_i, \tau_j)$ is not anymore a boolean matrix but a matrix of integers between *1* and *K*, if *K* is the number of closed areas A_n in the threshold map.

The *n-th* peak *?*$_n$ can be now defined as the highest point of the *n-th* area, in formulae:

$$\gamma_n = \max_{(i,j)\in A_n} \left| R(\tau_i, \tau_j) \right| \qquad \text{[Equation 7-3]}$$

with $n=1...K$.

7.2.3 Other functions

A small library of common-use modules was created in order to simplify and accelerate all the programming done during the course of the project.

Their main purposes are:

- Extracting parts of surfaces or inserting parts of surfaces into others in specified positions, using re-scaling where needed.
- Converting the matrices dimensions into physical dimensions using the header files contained in the .SDF format.
- Batch routines for automatic reading/writing/executing of large amounts of files, with optional statistical representation of the outputs.
- Statistical analysis and representation of parameters.

7.3 The Statistical Filter - Basic implementation

The first version of the Statistical Filter as described in section 2.5 was based on the Gram-Schmidt decomposition of vectors. The statistical decomposition of the clusters seen as vectors, together with the correlation coefficients, was meant to give a way of reconstructing a surface considering only the most relevant terms in the decomposition of each cluster C_s. The results were in accordance with the theory, but the filter has been developed differently; the matrix of the coefficients showed clearly that the average cluster, chosen as starting vector of the decomposition, contained enough information to represent the deterministic part of the surfaces. Moreover, the reconstruction of surfaces with adjustable level of correlation with the original is an interesting academic result, but a single surface containing the most needed information is of more industrial use.

The Gram-Schmidt decomposition has been abandoned in the following versions of the Filter, where the base cluster is the only one used to reproduce the surface features.

In this section will be described the initial implementation of the filter as introduced in section 2.5.

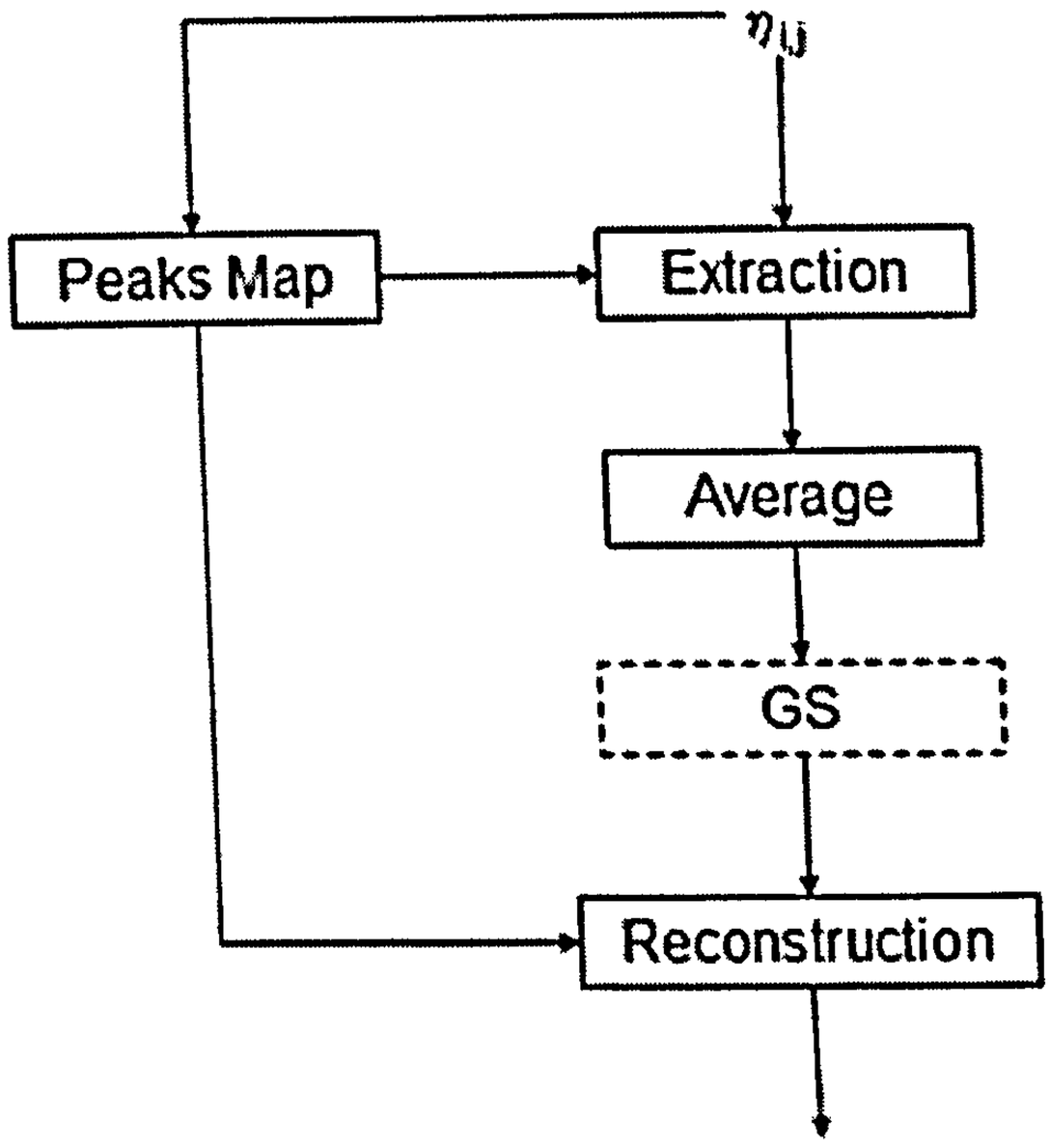

Figure 7-6 – GS Filter scheme

Figure 7-6 illustrates the organisation of the GS Filter software; the next sections explain the various modules that compose it.

7.3.1 The 'Peaks Map'Block

This module receives as input the surface and the threshold, calculates the XCF and its peaks map $P(\tau_1, \tau_2)$, returning finally the coordinates of the peaks $?_n$. The technique has been described in sections 7.2.1 and 7.2.2.

7.3.2 The 'Extraction' block

This module creates the clusters, isolating circular parts of the surface centred on each peak. It needs to be remembered here that the ACF function has double the dimensions with respect to the surface, according to Definition 2-1. When the autocorrelation is calculated using [Equation 7-1] though, its dimensions will be the smallest powers of two larger than the surface dimensions (section 7.2.1).

Let $\eta(x_k,y_l)$, with $k=0,..,M-1$, $l=0,..,N-1$ be a surface and $R(\tau_i, \tau_j)$ its autocorrelation function calculated with FFT using zero padding.

Then the dimensions of the autocorrelation function will be

$$i \in \left[0,2^{M_R}-1\right]$$
$$j \in \left[0,2^{N_R}-1\right]$$

where

$$\mathrm{M_R} = \min(x)\big|_{2^x>M}$$
$$\mathrm{N_R} = \min(x)\big|_{2^x>N}$$

The peaks coordinates do not have to be rescaled to fit the surface, since the ACF preserves the same spacing between points (Δ_x, Δ_y) as the surface; a portion of the peaks map of the same dimensions of the surface has to be considered, and the best position is the centre of the ACF, the least affected by border errors.

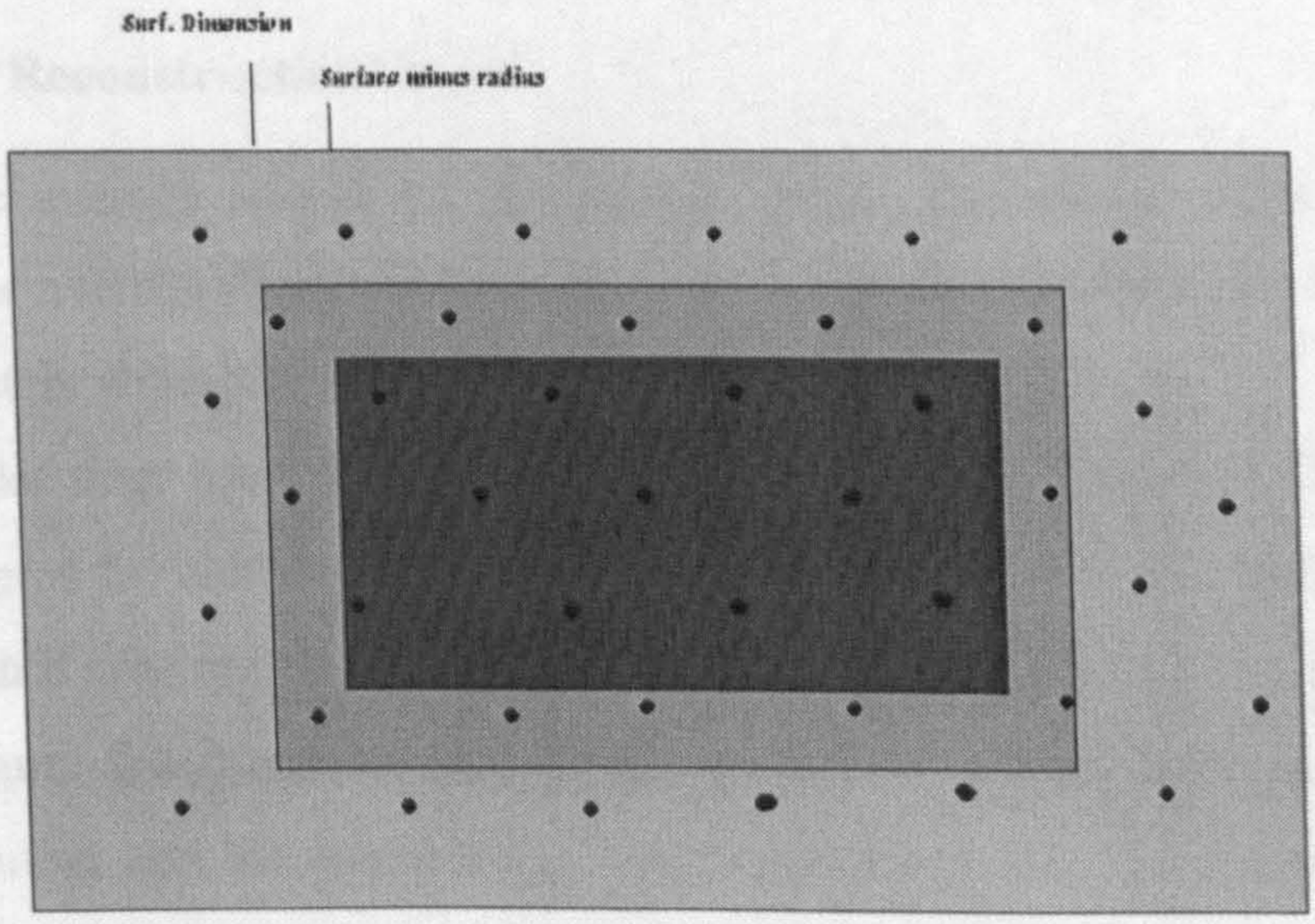

Figure 7-7 - Peaks map's areas

The clusters need to fall entirely into the surface to be extracted, therefore the portion considered for clusters extraction has to be further reduced by the length of a cluster diameter in both dimensions.

Figure 7-7 can clarify the concept: the yellow area represents the ACF area, the orange area has the same size of the surface, then reduced of a cluster diameter and represented in red. The orange area contains some peaks, but the

clusters extracted with centre on them would fall partly out of the surface's area; those that fall into the red zone are the only ones chosen for clusters extraction. The entire map will not be discarded, for reasons that will be clarified in section 7.3.4.

The clusters are extracted using the general purpose modules discussed in section 7.2.3, according to [Equation 2-3].

7.3.3 The 'Average' block

The creation of the average cluster C_0 is done through normal averaging of the elements of the other clusters:

$$C_0(i,j) = \frac{\sum_{k=1}^{W} C_k(i,j)}{W} \qquad \text{[Equation 7-4]}$$

The aspect of an example average cluster is shown in Figure 2-27.

7.3.4 The 'Reconstruction' block

Once the average cluster C_0 has been created, the filtered surface can be produced; the average cluster is repeated with centre on every peak, replacing the original clusters with their average.

The peaks map used for reconstruction is the entire map, not the central portion adopted for clusters extraction in section 7.3.2. If only the peaks that fall into the central area are considered, the average cluster will not cover part of the borders. Figure 7-8 illustrates the concept, referring to Figure 7-7: if only the peaks contained into the red area are used (diagonal lines filled cluster) part of the orange area will not be covered; also the rings contained in the orange area (vertical lines filled cluster) might not be enough to cover the whole surface. All of the peaks have to be used to ensure a complete result, covering an area larger than the one needed to overlap the original surface.

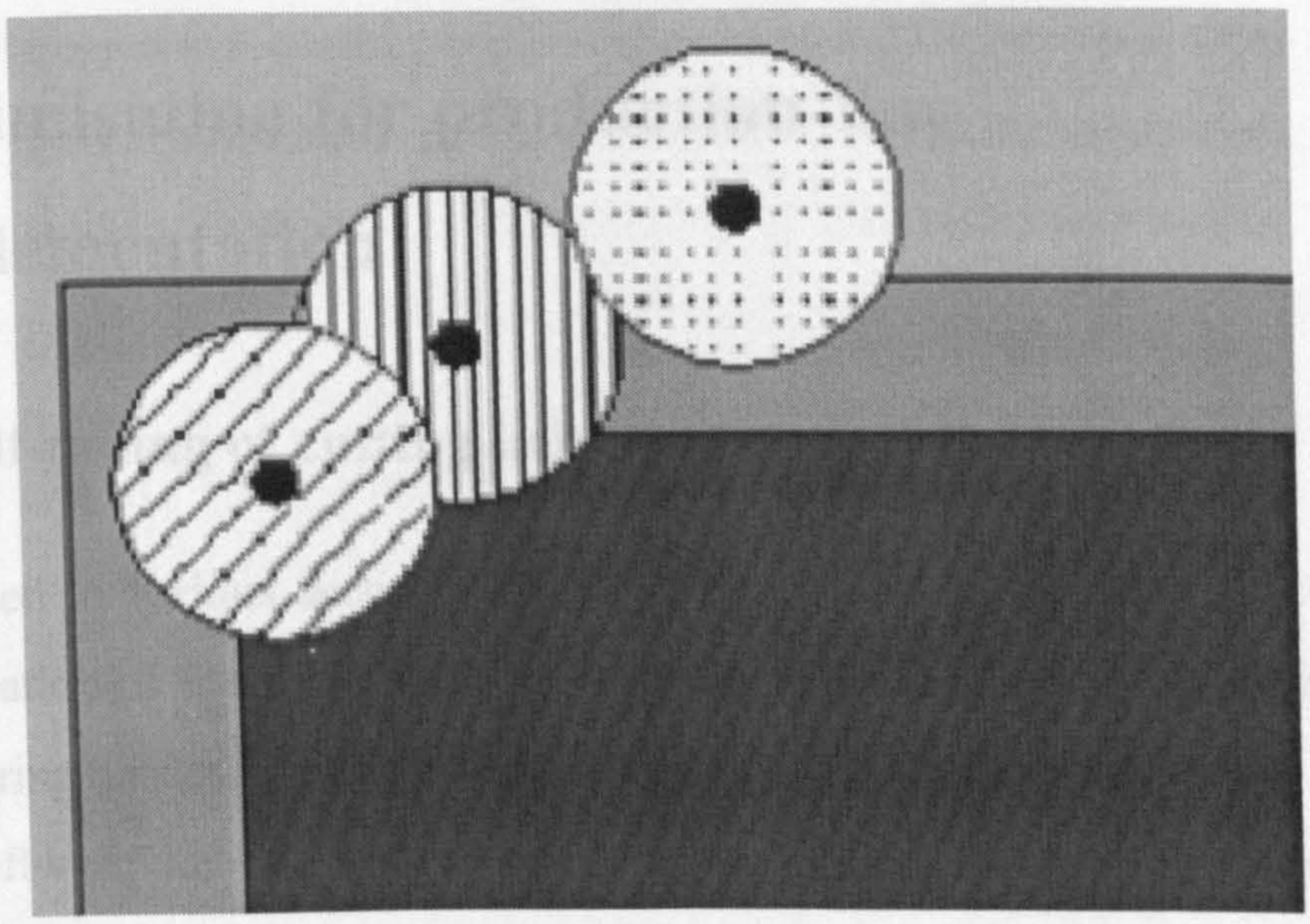

Figure 7-8 – Peaks map areas for reconstruction

The production of a filtered version of the surface does not add information to what can be deduced from the average cluster: C_0 is the average of highly correlated deterministic features of the surface, and repeating it to cover the whole area of the surface does not constitute added information. The reconstructed surface has a purely practical use: it allows easy calculation of the residual surfaces, useful for statistics on the surface noise and indispensable for double patterned surfaces filtering.

7.3.5 The GS block

The Gram-Schmidt decomposition was implemented according to its definition, just adapting it to the bi-dimensional nature of the data ([Equation 2-4] and [Equation 2-5]).

The coefficients of the decomposition are stored in a lower triangular matrix (Figure 2-28) and returned as output, as well as all of the C_s clusters generated during the decomposition process.

8. Optimisation for production-line implementation

8.1 Self-tuning of cutting height.

As stated in various sections of this thesis, the cutting height, or threshold, for the creation of the peaks map from the ACF is the most delicate step of the entire filtering process.

The software that isolates the peaks has to be as general as possible and be able to deal with:

- Unknown orientation of the surface
- Unknown shape of the pattern
- Highly variable density of peaks from case to case
- Unknown amount of background noise
- Possible presence of other patterns

All of the above requirements become even harder to meet considering that the algorithm has to be very fast not to represent a bottleneck in the process.

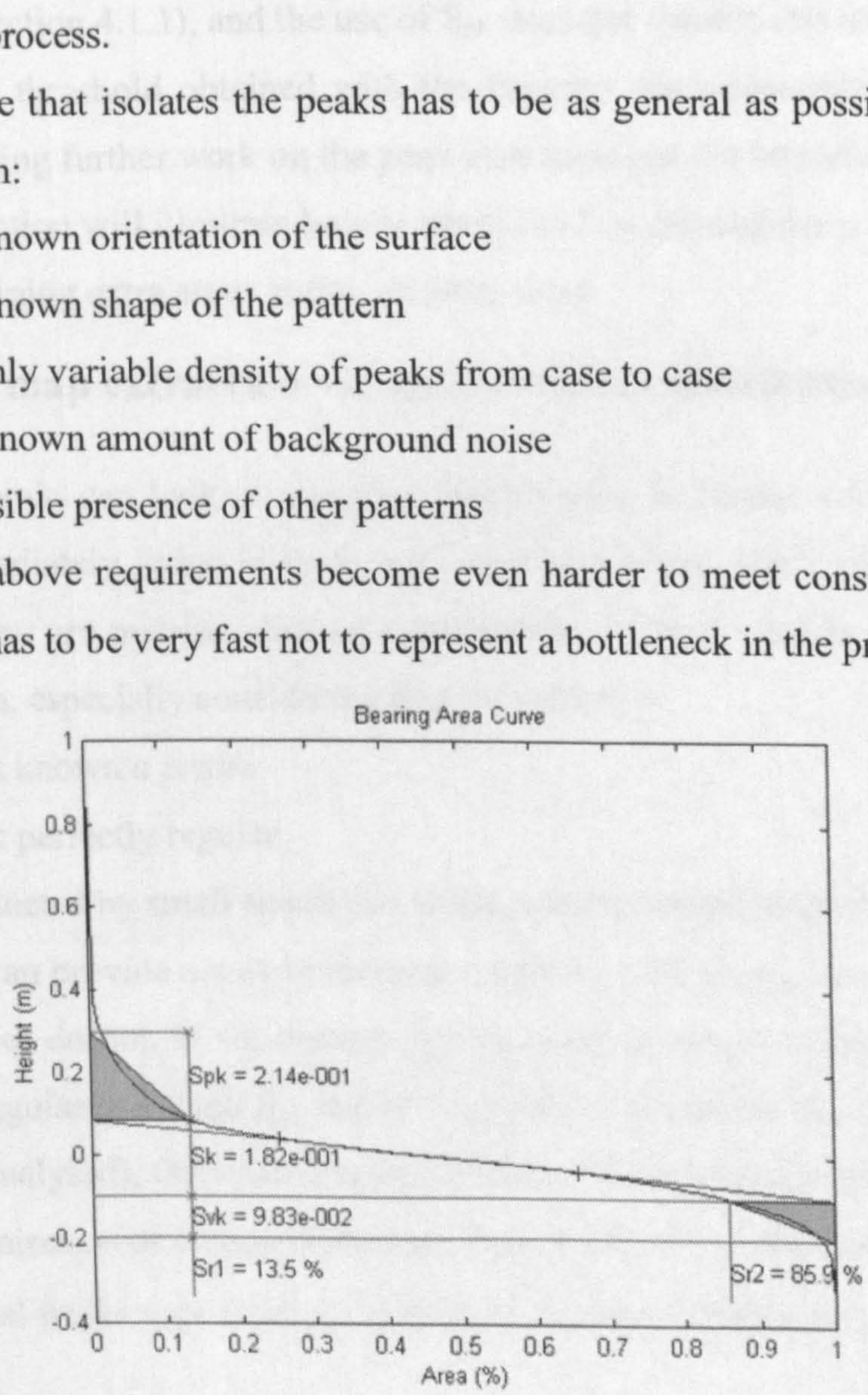

Figure 8-1 - Bearing area curve for an example ACF

A solution can be found in the Bearing Area (Firestone-Abbott) parameters calculated once again using the SCOUT software. The parameter S_{pk}, called "reduced peak height", gives an indication on the height of the peaks present in a surface, and is thus the best candidate for the peaks isolation threshold. Statistical work on a large amount of samples has shown that sectioning the ACF at half of the height of S_{pk} most of the peaks are intersected and most of the noise is not.

Unfortunately there is often no way to isolate all of the peaks avoiding all of the noise (see section 4.1.1), and the use of S_{pk} does not resolve this issue. On the other hand, the threshold obtained with the Bearing Area parameter is fast to calculate, allowing further work on the peak map to adjust the imperfections.

The next section will illustrate how to obtain a clear and regular peak map from one containing extra areas and/or missing ones.

8.2 Peaks map extraction via peaks vectors distribution

A human brain can look at a regular pattern (like in Figure 4-6 and Figure 4-7) and immediately judge if there are extra points that don't belong to the pattern or if any are missing. Not so immediately a calculator can perform the same operation, especially considering that the pattern is

- Not known *a priori*
- Not perfectly regular
- Affected by small errors due to the discrete nature of the data

Statistics can provide a way to recognise which peaks belong to a regular grid and which ones do not. If we assume that most of the peaks isolated using S_{pk} belong to a regular grid (and S_{pk} has proven able to guarantee this condition for the surfaces analysed), the vectors defining their relative distances should show a strong predominance of certain directions. Figure 8-2 shows the distance vectors of hypothetical peaks γ_1, γ_2 from γ_3, expressed in polar coordinates as module ρ_{ij} and angle α_{ij}.

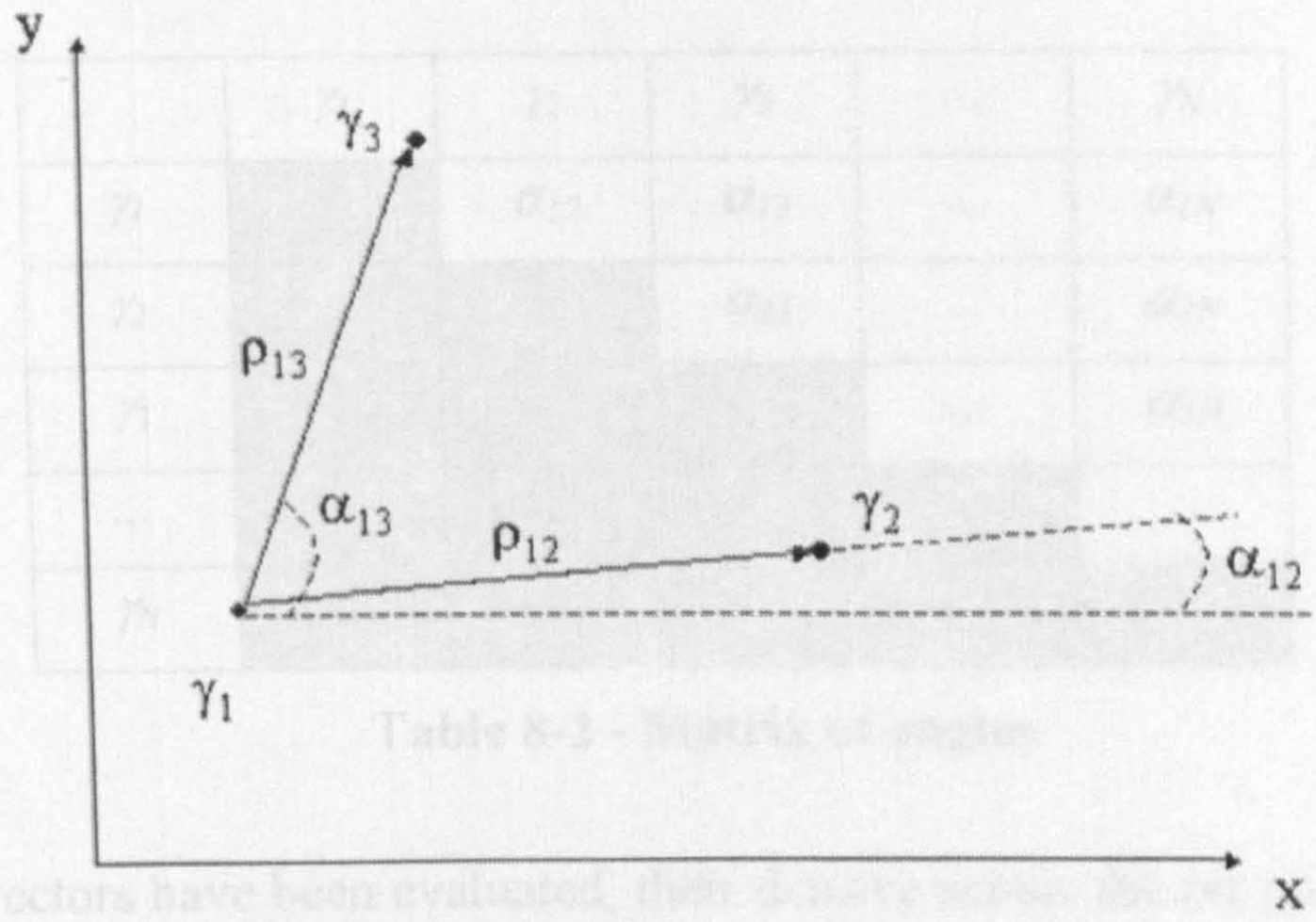

Figure 8-2 - Peaks distance vectors

All the combinations of two peaks can be considered and their relative distance evaluated, generating two triangular matrices as shown in Table 8-1 and Table 8-2:

	γ_1	γ_2	γ_3	...	γ_N
γ_1		ρ_{12}	ρ_{13}	...	ρ_{1N}
γ_2			ρ_{23}	...	ρ_{2N}
γ_3				...	ρ_{3N}
...					...
γ_N					

Table 8-1 – Matrix of modules

	γ_1	γ_2	γ_3	…	γ_N
γ_1		α_{12}	α_{13}	…	α_{1N}
γ_2			α_{23}	…	α_{2N}
γ_3				…	α_{3N}
…					…
γ_N					

Table 8-2 - Matrix of angles

Once vectors have been evaluated, their density across the $\rho\alpha$ plane is easily plotted, considering that the discrete nature of the data will make many of them fall on the same points (or *pixels* in a graphical representation). Figure 8-3 shows the density plot for an example EBT auto-correlation.

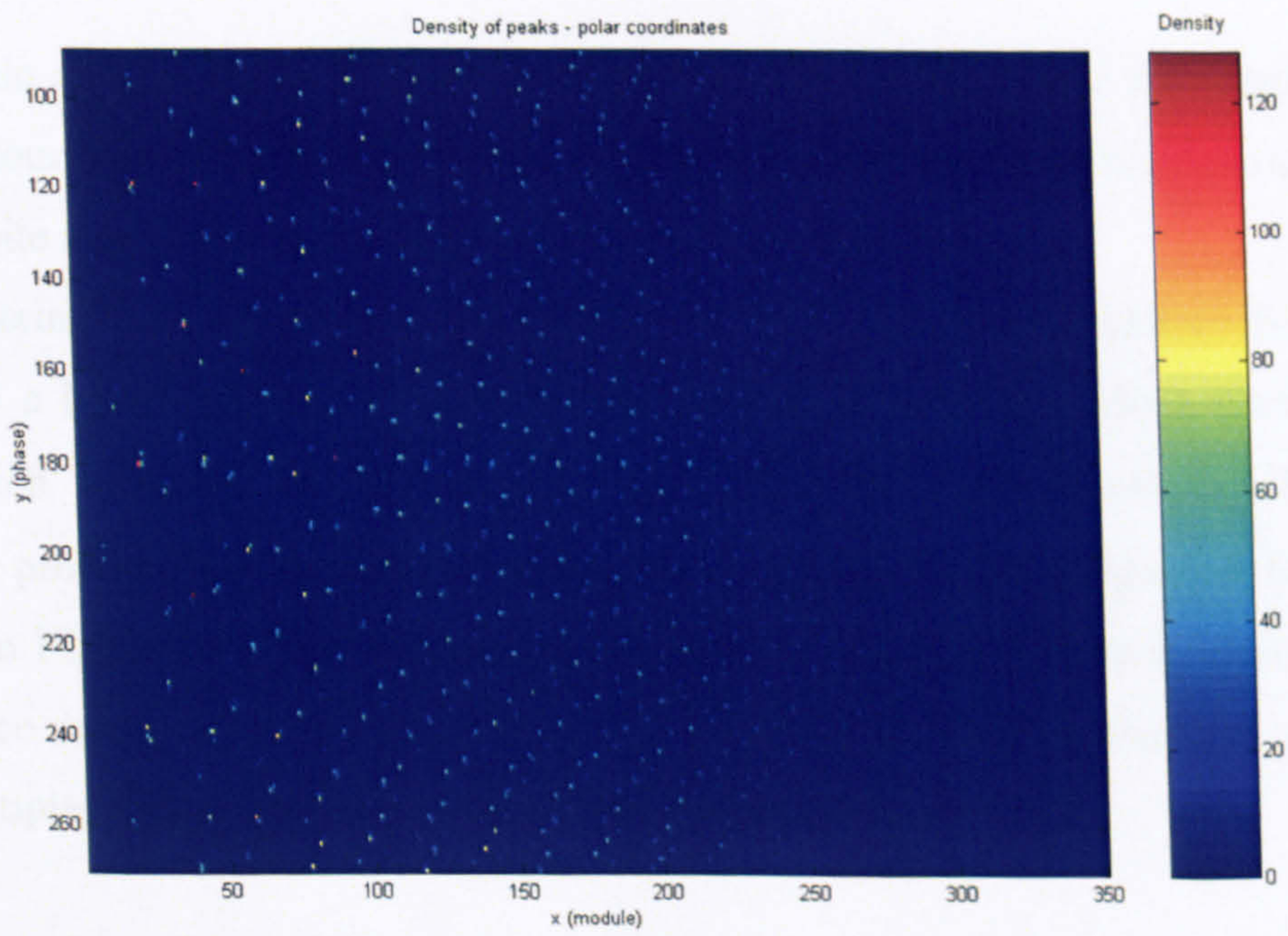

Figure 8-3 - Peaks population in polar coordinates

The graph shows that some vectors are exactly repeated more than 120 times, and this occurs mainly for small modules as it could be expected given the limited dimensions of the ACF under analysis.

The main directions can be found plotting the distribution of peaks according to the sole angle (equivalent to the sum of the columns of the matrix represented in Figure 8-3). The result is depicted in Figure 8-4.

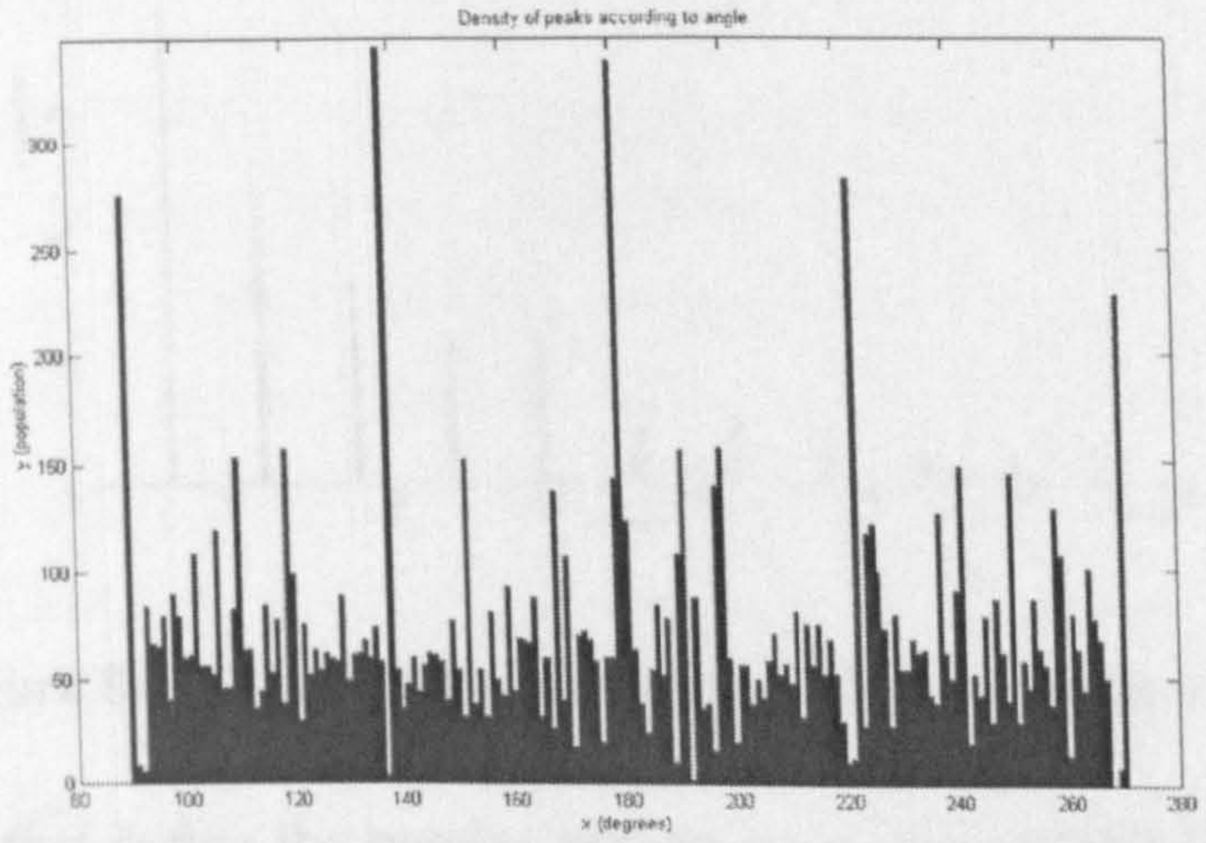

Figure 8-4 - Peaks population vs. angle

The main directions can be easily deduced from the graph, where five angles (or better four, considering that 90 and 270 degrees indicate the same direction with opposite sign) show a clear predominance over all others.

Considering one of the directions at a time, it is possible to extract from Figure 8-3 a horizontal line in correspondence with each angle, which should show which modules are predominant according to each direction. The horizontal profile obtained for α=138 degrees (highest peak in Figure 8-4) is depicted in Figure 8-5. The regularity of the plot indicates the main module of the distance according to the given angle (first and higher peak on the left), and all its multiples that necessarily belong to the same direction.

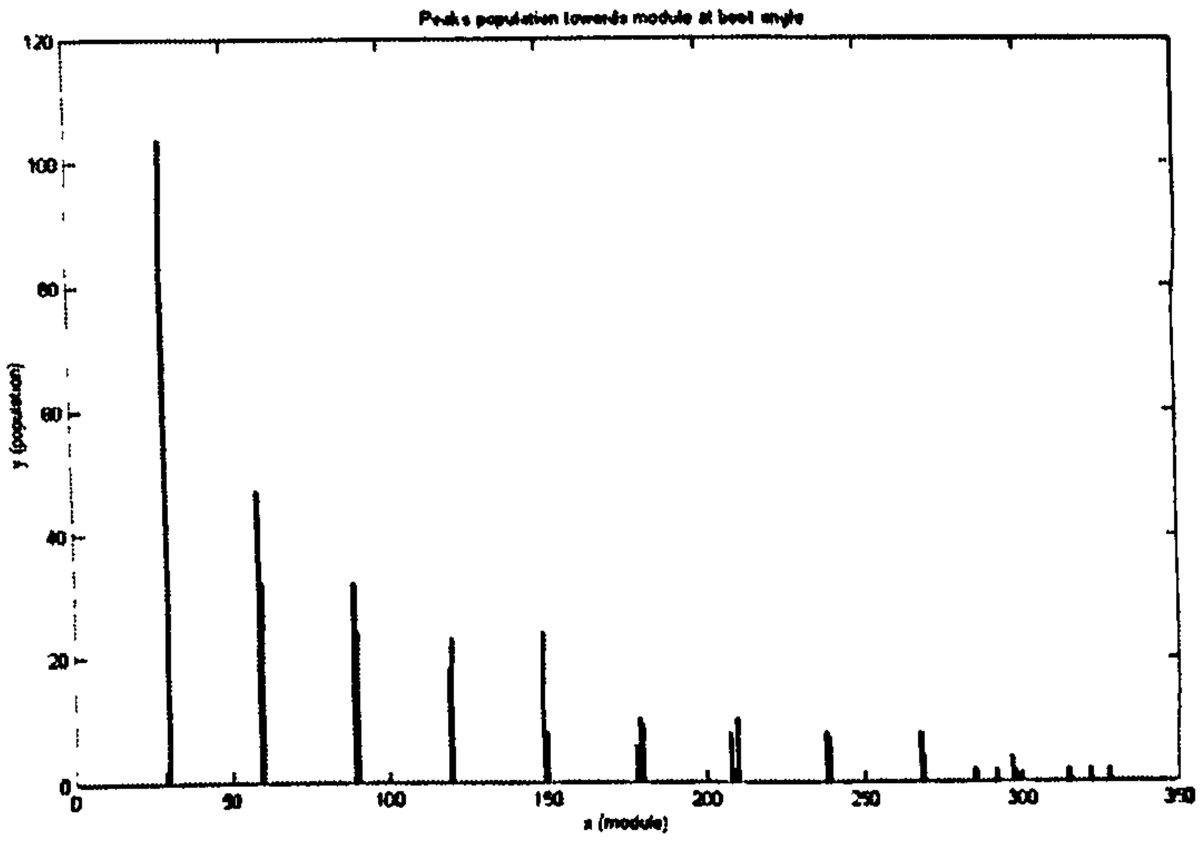

Figure 8-5 - Peaks population vs. module at given angle

The vectors that define the regular pattern have been established in module and angle, so the peaks map generated by S_{pk} can be corrected according to them.

8.2.1 Peaks map correction

The pattern of peaks can be corrected in several ways once the vectors that define the positions of the points have been calculated:

- **Eliminating extra points directly from Table 8-1 and Table 8-2.** It is possible to choose which peaks belong to the grid checking that they present one or more couples (ρ, α) with the correct values. Unfortunately two points that do not belong to the pattern might present the same distance vector of the regular points. To solve the problem it could be considered a peak only that point that presents two or more correct vectors, but this might incorrectly eliminate some point on the borders that have only one neighbour. Moreover, points could only be eliminated and not added where they are missing.
- **Building the whole grid from the directions.** Given the vectors of the peak distances a calculator can generate an ideal map of peaks with the correct distances. The problem is, the distances are relative, so the map will be correct apart from a translation factor. In order to

correct the misplacement it would be sufficient to know the position of one peak and refer the whole map to it; but a point can not be chosen as reference when the aim is exactly to find and eliminate the extra points.

- **With a recursive algorithm.** An algorithm implemented with a simple recursive function can explore the grid of points moving along the given directions and modules. A *counter* for each peak (or empty position) is increased for each visit coming from a different direction. At the end of the process the peaks with high counters will be kept, those with low counters will be verified (if they are close to the border, if there is another point very close with a lower counter too, etc.), those with null counters will be removed and the empty spaces with high counters will be assigned a peak. This technique involves an algorithm for decision-making to be repeated at every step that can represent a serious problem in computing time consumption; furthermore, recursive algorithms are notoriously to be avoided for their computational complexity and memory use wherever the number of recursions can be large. In the case of typical stylus measurement the number of features to analyse is not always negligible, and some worst-case-scenario examples have proven to represent a computational problem.

8.2.2 Timings and computational complexity

The number of non empty elements in Table 8-1 and Table 8-2 is $\frac{K \cdot (K-1)}{2}$

and represents the number of times that a couple (ρ_{ij}, α_{ij}) is evaluated.

The operations for determining each couple are very basic and involve integer numbers, as shown in the following formulas.

$$\rho_{ij} = \sqrt{dx^2 + dy^2}$$

$$\alpha_{ij} = \tan^{-1}\left(\frac{dy}{dx} \cdot \frac{180}{\pi}\right)$$

where dx and dy are the horizontal and vertical displacements between peaks γ_i and γ_j.

It is possible to reduce the number of operations by avoiding consideration of every peak that presents a module higher than a certain value (value that can be estimated from the density of peaks). The calculation of α_{ij} would be avoided for most of the pairs of peaks, and the creation and manipulation of the density charts would be accelerated. The disadvantage would be lower density where isolating the main directions and modules would result in more difficulty.

The number of peaks in a map is of an order of magnitude small enough in all common applications, that the density evaluation does not constitute a problem of computational complexity. For the same reason also the recursive algorithm used for peaks map correction is not above the timings tolerance.

8.3 Peaks map extraction via Voronoi diagram

The final solution to the Peaks Map extraction came from the **Voronoi Polygons** [Barber et al. 1996] [Aurenhammer 1991], which are strongly related to the **Delaunay triangulation**. Here are reported the definitions of the two concepts as given by the Matlab Help Documentation [Matlab website (a)]:

- Consider a set of coplanar points. For each point in the set, you can draw a boundary enclosing all the intermediate points lying closer to than to other points in the set. Such a boundary is called a Voronoi polygon, and the set of all Voronoi polygons for a given point set is called a Voronoi diagram.
- Given a set of data points, the Delaunay triangulation is a set of lines connecting each point to its natural neighbours. The Delaunay triangulation is related to the Voronoi diagram: the circle circumscribed about a Delaunay triangle has its centre at the vertex of a Voronoi polygon.

These definitions have been considered ideal for the problem of determining which peaks belong to a regular grid. One way is to use the peaks vectors

distribution as described in the previous section, but using only the Delaunay triangles' sides as vectors.

Alternatively, a simple routine could inspect the Voronoi polygons in order to find those with a similar shape, which then identify a regular pattern; non-regular polygons are either made of regular ones (where points are missing) or vice versa (regular polygons are made of irregular ones where points are in excess).

This is the solution implemented at present, primarily because of its extreme immediateness and computational simplicity, but also because of the geometrical meaning of the set of Voronoi polygons, which clearly match the concept of 'cluster' formulated in section 2.

A visual example of clusterisation of a surface through Voronoi diagram is illustrated in Figure 6-11.

8.4 Peaks map evaluation for industrial application

The creation of the peaks map that allows pattern reconstruction can be approached from a very different point of view respect to the solution proposed in section 8.2, where the problem is considered to be the as general as possible, reducing the initial assumptions to the minimum. It represents indeed a more valuable academic achievement, but not necessarily the most convenient industrial solution.

The main assumption that can be made about industrial production is that the steel sheets being produced belong to a well defined finite set of surfaces, therefore there is no need for absolute generality of the algorithms. The peaks map extracted from the ACF of a surface is a set of coordinates that define the peaks positions, and the same map can be used on different surfaces that present the same pattern, if their orientation is the same. So, if the aspect of the pattern being produced is known (and it generally is), then the whole peaks map evaluation could be skipped, and the software could be fed directly with the coordinates of the peaks and the filtering performed.

In practice things cannot be made so easy: the regularity of the pattern and its orientation are quality related characteristics that cannot be assumed to be correct, even if they rarely are not.

What it can be done is to simplify the process using the added information available on the production site, like the expected geometrical parameters (ring radii, *dq*, *dl*, etc.) of the surface being textured.

Figure 8-6 illustrates the structure of the Statistical filter as described so far: the original surface generates the ACF that generates the peaks map, which is used to filter the surface.

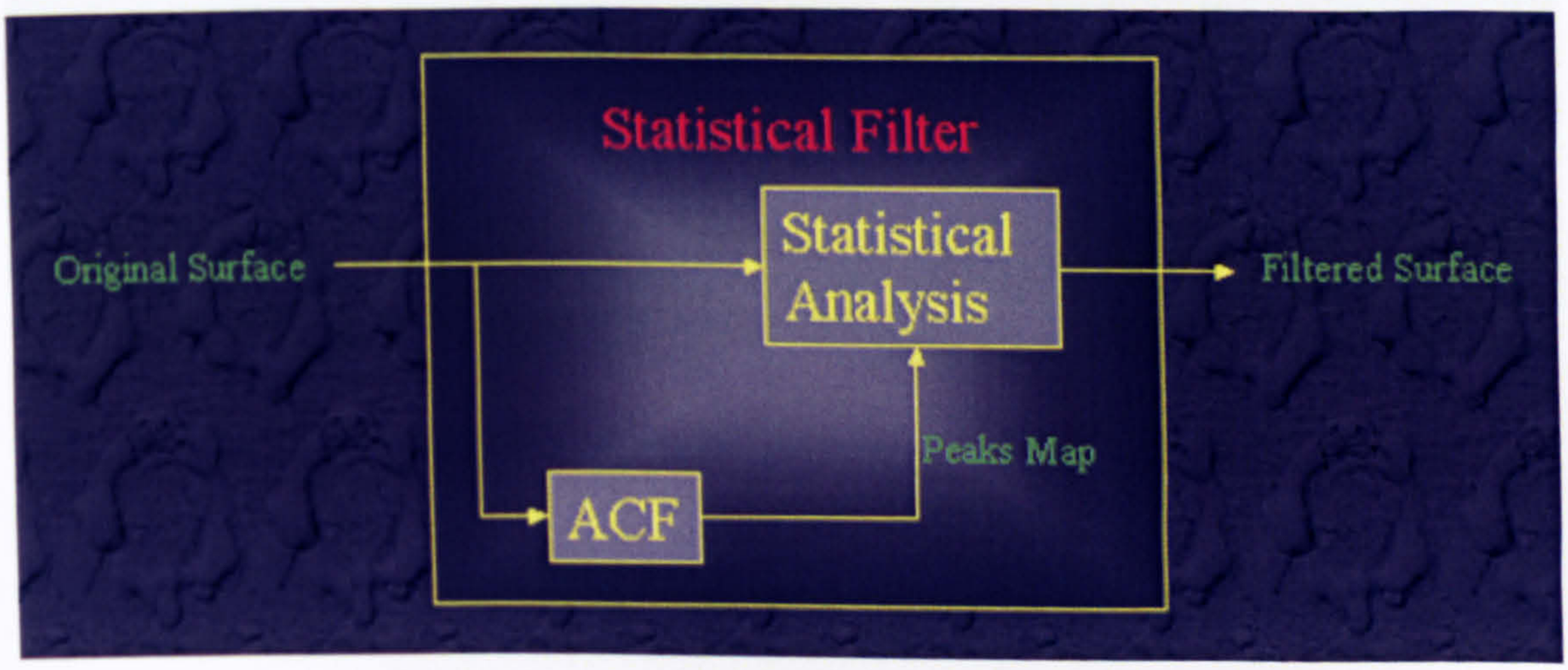

Figure 8-6 - Structure of the Statistical filter

Figure 8-7 shows an alternative scheme that could be used to improve the filter's performances. The shape of the EBT rings (or any deterministic feature) can be predicted through the expected parameters of the pattern. The simulated ring, cross correlated with the surface measurement, allows the creation of a peaks map that is statistically equivalent to the ACF peaks map for surface decomposition and reconstruction.

The great advantage is that the ACF gives information on the *relative* position of the rings, while the XCF shows their *absolute* position, so that every point of the peaks map corresponds to the centre of each ring. This greatly improves the operations of geometrical parameters extraction. Furthermore:

- The rings are not sensitive to the surface orientation due to their circular symmetry

- The XCF returns a map of points where the predicted feature matches the real ones, with no need for a periodic pattern anymore.

The predicted feature to be correlated with the surface can be either produced analytically (as an semi-torus of elliptic section for example, as in section 6) or extracted from a database of "ideal features" previously optimised in laboratory and stored in the computer memory.

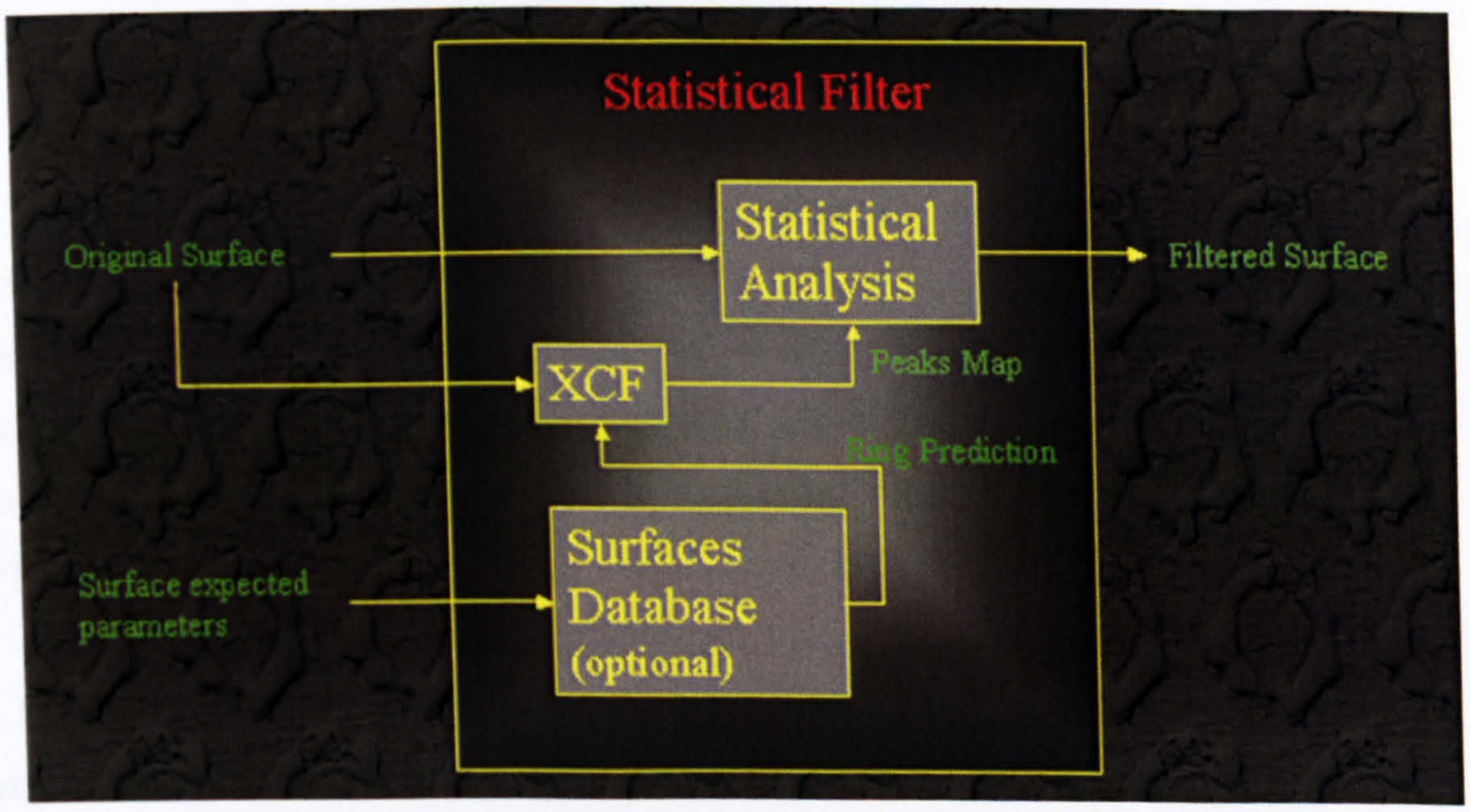

Figure 8-7 - Alternative filter structure for industrial application

The application to Process Control of the alternative structure is evident if used in conjunction with the simulated pictures described in section 5.3. The Original Surface that the filter will receive as input once implemented will be a greyscale picture taken on-line during production, while the Ring Prediction will be the simulation of a greyscale picture of the ideal ring.

The simulations of this process on all the available samples have been satisfactory and in accordance with the expected outcomes.

9. Conclusions

"An expert is a man who has made all the mistakes which can be made in a very narrow field."

— *Niels Bohr (1885-1962)*

The study of textured sheet surfaces has gradually moved throughout the years from 2D to 3D characterisation, forcing a progressive adaptation of the existing techniques, parameters and standards to the new approach. Filtering is a fundamental aspect of Surface Characterisation, and since the adoption of three-dimensional analysis there has been a constant effort of the research community to define filters for surface data that would allow the assessment of the desired surface characteristics.

Deterministic surfaces are textured with a deterministic pattern of features that confers to the sheet desired functional characteristics, and they are rapidly becoming a standard of the steel sheet production industry. Filters specifically designed for this kind of surfaces are not available at present, and the existing techniques are inadequate for their complete characterisation. It is hoped that this thesis will provide the research community with a useful innovative tool specifically designed for filtering deterministic patterns.

9.1 Achievements

The primary objective of this research was the definition of a filtering technique based on Statistical Analysis of highly correlated portions of surface, and the objective has been reached with the achievements summarised in the next sections.

9.1.1 Development of Grahm-Schmidt filter

The filter was created at Brunel University, and it has been immediately considered a good candidate for the characterization of surfaces with deterministic patterns, where statistics clearly represents the most suitable approach to the analysis. The technique has been inspected thoroughly from a theoretical viewpoint and proved to represent a stable method for the isolation of useful information in the presence of noise.

9.1.2 Development of a complete filtering package

The first implementation of the Statistical Filter was concerned only with the separation of deterministic patterns from surfaces as a way to estimate stochastic noise and access the average shape of the features. The technique has been inspected during the course of this research for wider applications, leading to numerous improvements and new options for the use of the filter. At present the package is complete with cross-correlation capabilities, multiple patterns extraction, features analysis tools, and other minor tools, and has been made completely automatic.

9.1.3 Adaptation to on-line Control

The filtering technique has been applied to on-line process control, in conjunction with an innovative optical measurement system developed in parallel during the project by a partner research centre.

Although still in a preliminary testing phase, the application of the Filter to the production line has been implemented and given satisfactory initial results; if the expected complete results are confirmed by future research, this technique could become a fundamental component of the first surface texture process control system for on-line production of steel sheets to be successfully developed.

9.1.4 SCOUT and the Statistical Filter GUI

Two software packages were created: one, SCOUT, during the Autosurf project in order to provide the research Consortium with a common tool for

surface filtering and parameters extraction, rapidly became a large Matlab toolbox with a wide range of features for surface analysis; the other one is the software that implements the Statistical Filter and its side-functions, including the ones for on-line process control.

SCOUT is currently circulating in the research community as an open-source code that is being constantly updated and improved, whilst the Statistical Filter GUI will undergo a final stage of debugging and fine tuning for industrial implementation.

9.2 Future work

The research currently performed on the filter is seen only as the first stage of its implementation: the direction that further research will follow is summarised in the following sections:

9.2.1 Filter Tuning

The filtering technique at the present is fully automated and can adapt to single or double textures, on both sheets and rolls; despite this, work is still required for fine-tuning of some parameters of the technique, in order to give the most stable possible result. Moreover, many aspects of the filtering, in particular regarding the on-line control system, still require to be validated on a properly designed set of data.

9.2.2 Design of Experiments

In order to confirm the capability of the Statistical Filter in assessing product quality during production a proper Design of Experiments procedure has been planned and started at Brunel University and OCAS; the samples will be associated with:

- their target values, for verification of accuracy
- different stages of production
- different stages of wearing

The application of the Statistical filter is expected to improve the knowledge of the roll wearing process, of the different contributions of different stages of production, and in general of EBT surfaces as a whole.

9.2.3 On-line implementation

The filter can be applied to the images coming from a sheet on the production line in order to monitor the quality of the product in real-time, which would represent a great improvement compared with the statistical control presently used. The success of this task is subordinated to the quality reached by the on-line camera and microscope system developed by CRM, but the results on the early tests have confirmed the potentiality of the Statistical Filter approach to the analysis of the data acquired on-line. Research is continuing both at Brunel University and OCAS for the fulfilment of this task in the shortest possible time, given the great industrial impact that this could have.

9.3 Contributions to knowledge

Although much work remains to be done, it is hoped that the research conducted in the past three years under the Statistical Filter Project will provide the research community with an innovative tool for surface characterisation. Although the applications of the filter are limited to surfaces that present a certain degree of determinism, the potential uses of the technique are numerous, considering the growth of EBT and analogue texturing methods.

The Filter will also be applied to on-line production in the very near future, and it is hoped to confirm the preliminary results, which suggest it has the potential to represent the solution for real-time Process Control on deterministic textured surfaces.

References

- Aspinwall D.K., Wise M.L.H., Stout K.J., Goh T.H., Zhao, F.L., El-Menshawy, M.F., 1992, Electrical discharge texturing, Int. J. Mach. Tools Manufact., Vol. 32, 183-193
- Aurenhammer F., 1991, Voronoi diagrams—a survey of a fundamental geometric data structure, ACM Computing Surveys (CSUR), v.23 n.3, p.345-405
- Autosurf Report N. 3 – Private Report of the Consortium – Feb 1998
- Barber C.B., Dobkin D.P., Huhdanpaa H.T., 1996, "The Quickhull Algorithm for Convex Hulls," ACM Transactions on Mathematical Software, Vol. 22, No. 4, Dec. 1996, p. 469-483. Available in HTML format at http://www.acm.org/pubs/citations/journals/toms/1996-22-4/p469-barber/ and in PostScript format at ftp://geom.umn.edu/pub/software/qhull-96.ps.
- Bergstrom T., Hamel R., Kummailil J., Gray A., Brown C., 2004, Comparison of surface texture measurement systems, Proceedings of the XI International Colloquium on Surfaces, Chemnitz, pp 13-21.
- Blunt L.,Jiang X., Scott P., Xiao S., 2004, Surface Metrology of MST devices, Proceedings of the XI International Colloquium on Surfaces, Chemnitz, pp 22-32
- Breitmeier U., 2004, White light interferometer for Engine Cylinder Topography Measurement, Proceedings of the XI International Colloquium on Surfaces, Chemnitz, pp 135-144.
- Crahay J., Renauld Y., Monfort G., Bragard, A., 1985, Present state of development of the lasertex process; Fachberichte Hüttenpraxis Metallweiterverarbeitung Vol. 23, No. 10, 968-975
- Coifman R.R., 1994, Wickerhauser M.V., Entropy-based algorithms for best basis selection, IEEE transaction on Information Theory, Vol. 38, pp 713-718
- Damir M. 1973, Error in measurement due tto stylus kinematics, Wear nr.26
- Dietzsch M., Frenzel C., Gerlach M., Groger S, Hamann D., 2004, Consequences of the GPS standards to the assessment of surface topography, Proceedings of the XI International Colloquium on Surfaces, Chemnitz, pp 1-12
- Dong W.P., Sullivan P.J., Stout K.J., 1994(a), Comprehensive Study of Parameters for Characterising Three-dimensional Surface Topography. III: Parameters for Characterising Amplitude and some Functional Properties, Wear No. 178
- Dong W.P., Sullivan P.J., Stout K.J., 1994(b), Comprehensive Study of Parameters for Characterising Three-dimensional Surface Topography. IV: Parameters for Characterising Spatial and Hybrid Properties, Wear No.178

- El-Menshawy F., Snaith B., 1991, Advances in electro-discharge texturing (EDT) for cold mill works, Iron and Steel Engineer, 57-59
- Hamilton DK., Wilson T., 1982, Three-dimensional surface measurement using the confocal scanning microscope, Applied Physics B, Vol. 27, pp. 211-213
- Hariharan P., 1985, Optical Interferometry, Academic Press, Australia
- Heberer K.H. 1987, Funkenerodiermaschine zur Oberflächenbearbeitung von Kaltwalzen, Stahl und Eisen 107 Nr. 3, 35-36
- Hedziora H., Parsons F., Tabenkin A., 2004, Industrial problems with proliferation and expansion of surface finish parameters, Proceedings of the XI International Colloquium on Surfaces, Chemnitz, pp. 93-100
- Horowitz J., Mattieren S., 1982, Von Skin-pass-Walzen in Kaltwalzwerken, Bänder Bleche Rohre 5, 121-125
- Huifen L., Xiangqian J., Zhu L., 2002, Robust processing for Gaussian regression filtering of engineering surfaces, Proceedings of the Second International Symposium on Instrumentation Science and Technology, v 3, p 3/659-3/663
- ISO Surface Texture, 1996: Profile method – Motif Parameters, ISO Standard 12085, International Standards Organisation
- ISODTS 16619-1, 2000: Geometrical Product Specification (GPS) – Data extraction techniques by sampling and filtration – Part 1: Basic Terminology,
- Jiang X.Q., Blunt L., Stout K.J., 1998, Wavelet framework representation for surface analysis (keynote paper), Proceedings of the IV Int. Symposium on Measurement Technology and Intelligent Instruments, Miskolc, pp 165-172
- Kay S, Nagesha V, 1994, Maximum likelihood estimation of signals in autoregressive noise, IEEE transaction of signal processing, Vol. 42
- Krystek M., 2004, Morphological filters in surface texture analysis, Proceedings of the XI International Colloquium on Surfaces, Chemnitz , pp 43-55
- Jonasson M., Wihlborg A., Gunnarsson L., 1998, Analysis of Surface Topography Changes in Sheet Steel Strips during Bending under Tension Friction Test, Int. J. .Mach. Tools & Manufacture, Volume 38, Nos. 5 & 6, pp 459-467
- Leach RK., Harris PM., 2002, Ambiguities in the definition of spacing parameters for surface-texture characterisation, Meas. Sci. Technol., N.13, pp. 1924-1930
- Lee S-H,, Zahouani H., Caterini R., Mathia T.G., 1998, Morphological Characterisation of Engineered Surfaces By Wavelet Transform, Int. Journal of Tools Manufacture, Vol. 38, Nos 5-6, pp 581-589
- McCool JI. 1984, Assessing the effect of stylus tip radius and flight on surface topography measurement, Transaction of the ASME Journal of Tribology n.106 pp 202-210

- Meyers DG., 1990, Digital Signal Processing Efficient Convolution and Fourier Transform Techniques, Prentice-Hall, New York
- Mignot J., Gorecky C., 1983, Measurement of surface roughness: comparison between a defect-of-focus optical technique and the classical stylus technique, Wear, Vol. 87, pp. 39-49
- Moreas, H., Uijtdebroeks, 2002, On-line roughness measurement of hot rolled strips, Publication CD European Communities, ISBN 92-894-3671-9
- Orfanidis, S.J. 1996, Introduction to Signal Processing. Upper Saddle River, NJ: Prentice Hall.
- Pawlus P., Smieszek M., 2004, The effect of stylus flight on surface topography measurement, Proceedings of the XI International Colloquium on Surfaces, Chemnitz, pp 65-74
- Pfestorf M, Engel U, Geiger M, 1998, 3D Surface Parameters and their Application on Deterministic Textured Metal Sheets, Machine Tools and manufacture, vol. 38, n. 5 & 6, page 607 – 614
- Porrino A., Sacerdotti F., Visintin M., Benati, F., 2000, Application of Gram-Schmidt decomposition for filtering of electron-beam-textured surfaces, Proceedings of the 17th IEEE Instrumentation and Measurement Technology Conference, pt. 1, p 442-6 vol.1
- Porrino A., Sacerdotti F., Vermeulen M., Butler C., 2003, Application of Statistical Filtering Technique to Single and Double Electron Beam Textured Surfaces, International Journal of Machine Tools and Manufacture n.43, pp. 1151 - 1156
- Porrino A., Vermeulen M., Butler C., Sacerdotti F., Clarysse F., 2004, On the Statistical Manipulation of Engineered Surfaces for Pattern Recognition in On-line Process Control Environment, Proceedings of the XI International Colloquium on Surfaces, Chemnitz, pp 33-42
- Proakis J.G., 1995, Digital Communications, McGraw-Hill
- Proakis, J.G., D.G. Manolakis., 1996 Digital Signal Processing: Principles, Algorithms, and Applications. Englewood Cliffs, NJ: Prentice Hall
- Raja J., Radhakrishnan V., 1978, Waviness separation in surface profiles using digital filters, Eng. Prod (New Dheli), vol. 2
- Ritterbach, B., 1997, Pretex - Ein neues Verfahren zur Erzeugung texturierter Feinbleche für höchste Ansprüche, Congress Stahl'97, Düsseldorf, Germany
- Rosén BG, 1998, Task 1.1 - Surface Topography Characterisation – A state of the art, Internal Report for Autosurf Project
- Rousseeuw PJ., Leroy AM., 1987, Robust Regression and Outlier Detection, John Wiley and Sons, New York.

- Sacerdotti F, Autosurf Consortium, 2000(a), Task 1.6 - Formulate 3D parameters, Internal Report for Autosurf Project.
- Sacerdotti F, Griffiths B, Benati F, Butler C, Autosurf Consortium, 2000(b), Software Variability in the Three-Dimensional Measurement of Autobody Steel Panel Surfaces, Proceedings of Chemnitz Conference, Feb 2000
- Sacerdotti F, Griffiths BJ, Benati F, 2000(c), Closed Regions: A proposal for spacing parameters for areal surface measurements, Submitted to Measurement Science and Technology
- Sacerdotti F, Griffiths BJ, Benati F, Butler C, 2000(d), Mathematical Modelling of three-dimensional surface topography in autobody manufacture - The State of the Art, Proceedings of the Institution of Mechanical Engineers, Vol 214 (2000), Part B, B03499
- Sacerdotti F, Griffiths BJ, Benati F, Butler C, 2000(e), The variability of Functional and Amplitude three-dimensional roughness parameters for Electron-Beam and Electro-Discharged textured Surfaces, Measurement Science and Technology, 11 No 3 (March 2000) P171-177
- Sacerdotti F, Griffiths BJ, Benati F, Butler C, Autosurf Consortium, 2000(f), Hardware Variability in the Three-Dimensional Measurement of Autobody Steel Panel Surfaces, Proceedings of the 8th international Conference on Metrology and Properties of Engineering Surfaces
- Sacerdotti, F., Porrino, A.; Butler, C.; Brinkmann, S.; Vermeulen, M., 2002, SCOUT - Surface Characterization Open-Source Universal Toolbox, Measurement Science and Technology, vol 13, n 2, pp N21-N26
- Sacerdotti F. 2000, Surface Topography Characterisation of Autobody Panels, Doctorate Thesis, Brunel University
- Scheers J., Vermeulen M., De Mare C., 1996, The Influence of Surface Texturing on the Tribological Behaviour of Sheet Steel, Third Seminar on the Influence of Surface Roughness on the Application of Sheet Steel
- Sheers J., De Marè C., 1998, The use of 'fine deterministic' steel sheet textures to improve the drawability and paint quality of high strength body panels, Proceeding of the 40th Mechanical Working and Steel Processing Conference, vol 36, Pittsburgh, Pensylvania, pp 93-99.
- Scheers J., 1998, Task 1.2 - Potential Equipment Requirements, Internal Report for Autosurf Project.
- Sherrington I., Smith EH., 1988 (a), Modern measurement techniques in surface metrology. Part I: Stylus Instruments, electron microscopy and non-optical comparators, Wear, Vol 125, pp. 271-288

- Sherrington I., Smith EH., 1988 (b), Modern measurement techniques in surface metrology. Part II: Optical Instruments, Wear, Vol 125, pp. 289-308
- Sherrington I., Smith EH., 1986, A quantitative study of the influence of stylus shape and load on the fidelity of data recorded by stylus measurements, Proceedings of the 2nd National Conference on Production Research, Edinburgh
- Scott PJ, 1997, Foundations for Topological Characterisation of Surface Texture, Proceedings of the 7th International Conference on Metrology and Properties of Engineering Surfaces, Goteborg, Sweden
- Scott PJ, 2000, An Algorithm to Extract Critical Points from Lattice Height Data, Proceedings of the 8th international Conference on Metrology and Properties of Engineering Surfaces
- Staeves J., Filzek J., Schmoeckel D., 1998, Surface qualification n the sheet metal domain, Proceedings of the 6th Int. Conf. Sheet Metal, pp 277-294
- Stout KJ, Sullivan PJ, Dong W P, Mainsah E, Luo N, Mathia T and Zahouani H. 1993, The Development of Methods for the Characterisation of Roughness in Three Dimensions, Report EUR 15178EN. Published by Kogan Page.
- Stout KJ, Blunt L., 2000, Three Dimensional Surface Topography, Penton Press
- Stout KJ., Blunt L., 2001, A contribution to the debate on surface classifications - Random, systematic, unstructured, structured and engineered, International Journal of Machine Tools and Manufacture, vol 41, n 13-14, p 2039-2044
- Swelden W., 1994(a), Construction and application of Wavelets in Numerical Analysis, PhD thesis
- Swelden W., 1994(b), The lifting scheme: a construction of second generation wavelets, University of South Carolina
- Takahashi S, Ikeda T, Shinagawa Y, Kunii TL, Ueda M., 1995, Algorithms for Extracting Correct Critical Points and Constructing Topological Graphs from Discrete Geographical Elevation Data, Dept. of Information Science, Faculty of Science, The University of Tokio. EUROGRAPHICS '95 Vol 14, Num 3
- "The Primary Set", Parameters for 3D surface characterisation, 1998 , ver. 2.0, Computer Software by Ultra-precision engineering centre, Huddersfield University.
- Thomas TR. 1978, Some examples of versatility of stylus instruments, Mécanique, Matériaux, Electricité, Vol. 337, pp. 17-25
- Thomas TR. 1982, Rough Surfaces, Longman Press, London
- Vermeulen M., Scheers J., De Mare C., De Cooman B., 1995, 3D Characterisation of EBT Steel Sheet Surfaces, Int. J. Mach. Tools & Manufacture, Volume 35, No. 2, pp 273-280

- Vermeulen M., Scheers J., 1996, 2D and 3D Characterisation of Sibetex textures, Third Seminar on the Influence of Surface Roughness on the Application of Sheet Steel
- Whitehouse DJ, 1982, Parameter Rash, Is There A Cure?, Wear, Vol 83,pps 75-78.
- Whitehouse DJ, 1994, Handbook of Surface Metrology, IOP publishing, pps376-531
- Whitehouse DJ, 1975, Some ultimate limits on the measurement of surfaces using stylus techniques, Measurement and Control, Vol. 8, pp. 147-151

Websites

- "Autosurf", Surface Topography Optimisation for the Automotive Industry - European Project - www.autosurf.org
- "CRM", Centre for Research in Metallurgy, www.crm-eur.com.
- "Darmstadt", J. Staeves, J. Filzek, D. Schmoeckel, Surface qualification in the sheet metal domain, http://www.ptu.tu-darmstadt.de/forschung/tribologie/shemet/shemet.htm.
- "Matlab" Release 5.4 - Computer Matrix Laboratory - www.mathworks.com
    - (a) Signal processing toolbox reference, available online at www.mathworks.com/access/helpdesk/help/pdf_doc/signal/signal_tb.pdf
    - (b) Image processing toolbox reference, available online at www.mathworks.com/access/helpdesk/help/pdf_doc/images/images_tb.pdf
- "Minitab", Statistical Software Website, www.minitab.com.
- "OCAS" Research centre for the application of steel (OnderzoeksCentrum voor Aanwending van Staal), www.ocas.be.
- "SCOUT" - Surface Characterisation Open-Source Universal Toolbox, www.euscout.org.
- "SurfStand", Development of a basis for 3D Surface Roughness Standards - European Project - www.hud.ac.uk/schools/engineering/research/ultrap/surface/project_open.html.

Appendix: Publications

- Porrino A., Sacerdotti F., Visintin M., Benati, F., 2000, Application of Gram-Schmidt decomposition for filtering of electron-beam-textured surfaces, Proceedings of the 17th IEEE Instrumentation and Measurement Technology Conference, pt. 1, p 442-6 vol.1
- Porrino A., Sacerdotti F., Vermeulen M., Butler C., 2003, Application of Statistical Filtering Technique to Single and Double Electron Beam Textured Surfaces, International Journal of Machine Tools and Manufacture n.43, pp. 1151 - 1156
- Porrino A., Vermeulen M., Butler C., Sacerdotti F., Clarysse F., 2004, On the Statistical Manipulation of Engineered Surfaces for Pattern Recognition in On-line Process Control Environment, Proceedings of the XI International Colloquium on Surfaces, Chemnitz, pp 33-42
- Sacerdotti, F., Porrino, A.; Butler, C.; Brinkmann, S.; Vermeulen, M., 2002, SCOUT - Surface Characterization Open-Source Universal Toolbox, Measurement Science and Technology, vol 13, n 2, pp N21-N26